DOE/ID/12779--T1

Development of Novel Active Transport Membrane Devices

Phase I Final Report

by

Daniel V. Laciak
Robert Quinn
George S. Choe
Philip J. Cook
Fu-Jya Tsai

August 1994

Work Performed Between 31 October 1988 and 31 January 1994
Under Cooperative Agreement No. DE-FC36-89ID12779

Prepared for

United States Department of Energy
Golden Field Office, Golden Colorado
Sponsored by the Office of the Assistant Secretary
for Energy Efficiency and Renewable Energy

Office of Industrial Technology
Washington, D.C.

Submitted by

Air Products and Chemicals
7201 Hamilton Boulevard
Allentown, PA 18195-1501

Development of Novel Active Transport Membrane Devices

Phase I Final Report

by

Daniel V. Laciak
Robert Quinn
George S. Choe
Philip J. Cook
Fu-Jya Tsai

August 1994

Work Performed Between 31 October 1988 and 31 January 1994
Under Cooperative Agreement No. DE-FC36-89ID12779

Prepared for

United States Department of Energy
Golden Field Office, Golden Colorado
Sponsored by the Office of the Assistant Secretary
for Energy Efficiency and Renewable Energy

Office of Industrial Technology
Washington, D.C.

Submitted by

Air Products and Chemicals
7201 Hamilton Boulevard
Allentown, PA 18195-1501

Foreword

In 1988 Air Products and Chemicals entered into a Cooperative Agreement with the United States Department of Energy to develop "Active Transport" (AT) gas separation membranes recently discovered in our Corporate laboratories. Active Transport systems exploit chemical complexation reactions between the membrane and specific contaminant gases and thus are significantly more selective than commercial (i.e. solution-diffusion) polymer membranes. Air Products has identified Active Transport materials which selectively permeate carbon dioxide from mixtures with methane and hydrogen, hydrogen sulfide from mixtures with carbon dioxide and methane, and ammonia from mixtures with nitrogen and hydrogen.

Two significant advances in ATM technology were made during Phase IA of this Cooperative Agreement. APCI successfully translated the gas-reactive chemistry of molten salts and molten salt hydrate liquid membranes into the solid state by synthesizing new polyelectrolyte compositions. Second, APCI demonstrated that polyelectrolytes could be fabricated as thin film composite membranes in which the ATM component is stabilized on a microporous support fiber. Such composites were operated at pressures up to 1000 psi and were stable over 3 weeks of continuous testing. In Phase IA Air Products fabricated and evaluated spiral-wound thin film composite lab scale modules of NH_3 and CO_2 selective ATMs. These prototype modules displayed high permselectivity at low pressures, however, significant concentration polarization effects were observed under laboratory simulated process conditions. The major objective of this, the final segment of Phase I (Phase IB), was to demonstrate that ATMs could be fabricated in the commercially viable form of a hollow fiber device exhibiting permselectivity for separating carbon dioxide from mixtures with methane. Such membranes could be used for:

- permeating CO_2 from natural gas
- permeating CO_2 from landfill gas
- permeating CO_2 from wastewater treatment offgas

The task schedule for the Phase IB contract period is shown in Figure i. Major accomplishments for this contract period included:

- Established substrate polymer selection criteria and identified a candidate material.

- Established the effect of fiber spinning variables on substrate fiber properties and produced a hydrocarbon-resistant fiber with tunable surface porosity in the range 100 - 1000Å.

- Demonstrated concept feasibility by fabricating lab-scale, ATM composite hollow fiber membrane modules incorporating non-optimized substrates that were stable to 1000 psi and for at least 50 days of continuous operation.

- Estimated that an optimized ATM system (i.e., one which meets all performance and cost targets) could upgrade subquality natural gas (6% CO_2) for approximately 20% less than the cost of conventional (DEA) acid gas scrubbing technology.

- Identified technical hurdles that require resolution prior to further developing and commercializing Active Transport membranes.

These accomplishments are discussed in detail in Chapters III-VII. A general summary and recommendations for additional work are contained in Chapter VIII.

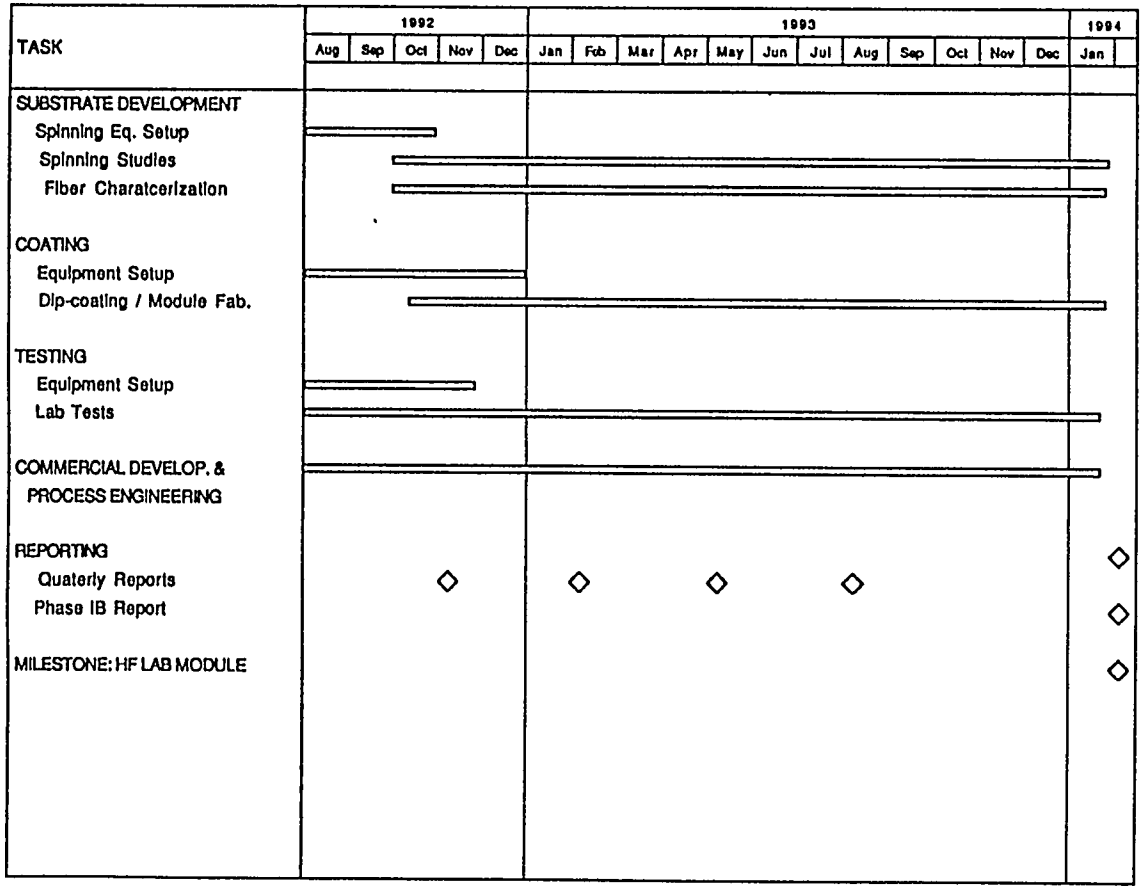

Figure i: Program Schedule

Figure iA

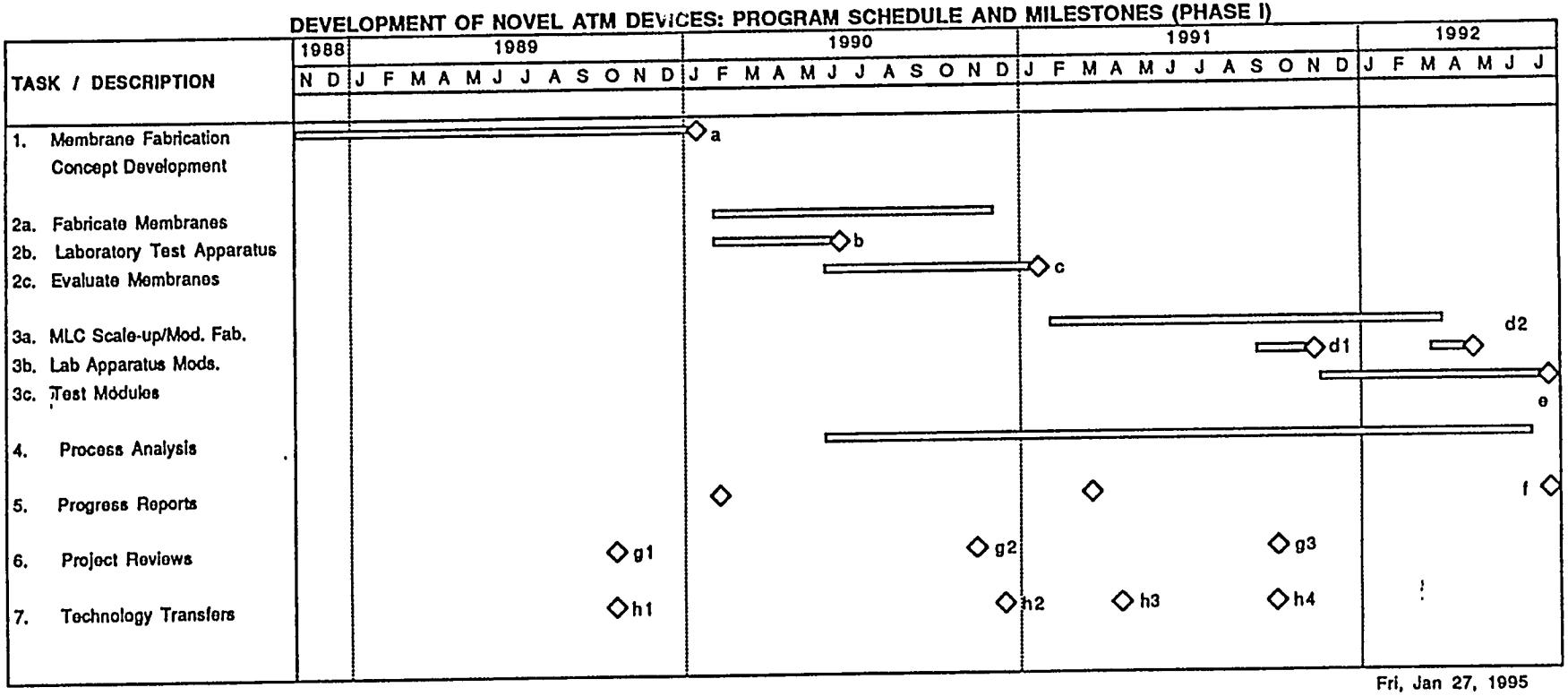
DEVELOPMENT OF NOVEL ATM DEVICES: PROGRAM SCHEDULE AND MILESTONES (PHASE I)
TASK / DESCRIPTION
1988
1989
1990
1991
1992
N D J F M A M J J A S O N D J F M A M J J A S O N D J F M A M J J A S O N D J F M A M J J
1. Membrane Fabrication Concept Development
2a. Fabricate Membranes
2b. Laboratory Test Apparatus
2c. Evaluate Membranes
3a. MLC Scale-up/Mod. Fab.
3b. Lab Apparatus Mods.
3c. Test Modules
4. Process Analysis
5. Progress Reports
6. Project Reviews
7. Technology Transfers
a
b
c
d1
d2
e
f
g1
g2
g3
h1
h2
h3
h4
Fri, Jan 27, 1995

TABLE OF CONTENTS

List of Figures

List of Tables

List of Abbreviations and Acronyms

AGR	Acid gas removal
ATM	Active Transport Membrane
l	Membrane thickness
P	Permeability
P/l	Permeance
P/Po	Actual H_2O vapor pressure/saturated H_2O vapor pressure
PAI	Polyamideimide
PAN	Polyacrylonitrile
PSA	Pressure swing adsorption
PVBTAF	Poly(vinylbenzyltrimethylammonium fluoride)
PDMS	Poly (dimethylsiloxane)
TMAF	Tetramethylammonium fluoride
α	Selectivity
UDEL	Polysulfur
Ultem	Polyetherimide

I. Executive Summary

The main objective of this program was to identify and develop through proof of concept, a technique for fabricating Active Transport Materials* (ATM) into lab-scale membrane devices. Air Products met this objective by applying thin film, multilayer fabrication techniques to support the AT material on a substrate membrane. In Phase IA, spiral-wound and later in Phase IB, hollow fiber membrane modules were fabricated and evaluated. These nonoptimized devices were used to demonstrate the AT-based separation of carbon dioxide from methane, hydrogen sulfide from methane, and ammonia from hydrogen. During this period, Air Products determined that a need exists for a more cost efficient and less energy intensive process for upgrading subquality natural gas. Air Products estimated the effectiveness of ATM for this application and concluded that an optimized ATM system could compete effectively with both conventional acid gas scrubbing technology and current membrane technology. In addition, the optimized ATM system would have lower methane loss and consume less energy than current alternative processes. Detailed results were communicated to DOE through a series of interim reports.

During the last budget period, Air Products made significant progress toward the ultimate goal of commercializing an advanced membrane for upgrading subquality natural gas. The laboratory program focused on developing a high performance hollow fiber substrate and fabricating and evaluating ATM-coated lab-scale hollow fiber membrane modules. Selection criteria for hollow fiber composite membrane supports were developed and used to evaluate candidate polymer compositions. A poly(amide-imide), PAI, was identified for further study. A research spinning line was constructed and used to establish the effect of spinning process variables on fiber performance. Conditions were identified which produced microporous PAI support membrane with tunable surface porosity in the range 100-1000Å. The support fibers exhibited good hydrocarbon resistance and acceptable tensile strength though a higher elongation may ultimately be desirable. ATM materials were coated onto commercial and PAI substrate fiber. Modules containing 1-50 fibers were evaluated for permselectivity, pressure stability, and lifetime. Several nonoptimized modules exhibited permselectivity comparable to planar thin film composite membranes supported on polysulfone. In general, higher flux modules would be needed to achieve commercially attractive economics.

Concurrent with but separate from this Cooperative Agreement, Air Products has maintained an active program to further develop the chemistry of its ATM materials. Results from this program

*Active Transport materials are Air Products' proprietary advanced facilitated transport gas separation polymers.

were incorporated into a semi-empirical computer model of the ATM permeation mechanism which was used to determine process economics for the natural gas application. Several technical issues related to the ultimate commercialization of ATM technology were identified. These issues include an apparent reactivity with hydrogen sulfide and, most importantly, a strong dependence of the carbon dioxide permselectivity on the concentration of water vapor in the feed gas stream. New ATM compositions which exhibited a 10-fold improvement in carbon dioxide flux while maintaining high carbon dioxide/methane selectivity were identified. Planar composite coupons of these compositions meet preliminary carbon dioxide flux and selectivity targets, however, initial indications are that they will be subject to the same commercialization challenges identified previously.

Phase IA also assessed the potential for ammonia separation membranes and modules. While excellent permselectivity was achieved for laboratory devices and it is believed that laboratory properties could eventually be scaled to a commercial system, the market potential for such membranes does not appear large enough to warrant the substantial development investment to commercialize these membranes.

Based on the results of this program, Air Products recommends a follow-on program with the task elements listed below.

- Continued efforts to assess the commerciality of ATM as related to the issues of (a) the water dependence of the carbon dioxide flux and selectivity and (b) hydrogen sulfide reactivity of the ATM component.
- Continued computer modeling of the ATM permeation mechanism, especially in regard to adequately incorporating into the model the water vapor dependence of the permselectivity.
- Continued process engineering and economic analysis to (a) further quantitate the benefits of an ATM-based natural gas purification process and (b) set performance targets for the ATM.
- Address issues related to scale-up and optimization of substrate fiber.
- Field testing of substrate and composite membranes.
- Continued commercial development activities to coordinate field testing and maintain industry contacts.

II. Program Overview

1.0 Introduction

In a recent research needs assessment performed for the U.S. Department of Energy,[1] the membrane based separation of acid gases from hydrocarbons and H_2 was ranked "high" in importance (8 out of a possible 10) and with "good" prospects for success. The study further pointed out that high selectivity materials, $\alpha(H_2S/CH_4) > 45$ and $\alpha(CO_2/H_2) > 20$, are needed to compete effectively with alternative technologies. Since 1983, Air Products has pioneered the development of active transport (AT) membranes (referred to in the literature as "facilitated" transport membranes) for the removal of acid gases from process streams. AT membranes, unlike polymeric membranes, selectively permeate acid gases by exploiting two properties:

(1) the membranes exhibit a specific and reversible chemical reactivity with acid gases, and
(2) the solubility of non-acid gases in the membranes is very low.

The reversible reactivity of the membranes result in enhanced permeation of acid gas while the membranes exhibit barrier properties to non-acid gases due to their low solubilities.

The AT materials under development through this Cooperative Agreement are polyelectrolytes. Polyelectrolytes are ionic polymers which have a high ionic content, up to one ionic unit per polymer repeat unit. Air Products has demonstrated that certain polyelectrolytes exhibit reversible reactivity with respect to gases and possess absorption capacities in excess of 1 mol gas / mol polyelectrolyte. In addition, we have shown that acid gas permeabilities increase with decreasing feed pressure, an observation which is consistent with active transport of the gas. In contrast, H_2 and CH_4 permeabilities are independent of feed pressure and are low. These gases cannot react with the polyelectrolyte membrane and, due to the ionic character of polyelectrolytes, H_2 and CH_4 are almost insoluble in the membrane. The performance of small planar sheet membranes was favorable. Acid gas

[1] "Membrane Separation Systems - A Research & Development Needs Assessment" by the Department of Energy Membrane Separation Systems Research Needs Assessment Group; Volume II, March 1990.

permeances (CO_2 and H_2S) were relatively high: 1.0 - 0.7x10^{-6} $cm^3/cm^2 \cdot s \cdot cmHg$ for CO_2 and 3.0 - 30x10^{-6} $cm^3/cm^2 \cdot s \cdot cmHg$ for H_2S. The selectivity of acid gas to H_2 and CH_4 selectivities were exceptional: $\alpha(CO_2/H_2)$ = 10 - 60; $\alpha(CO_2/CH_4)$ = 50 - 700; $\alpha(H_2S/CH_4)$ = 260 to >2000. These properties are not observed for conventional polymeric materials and may have considerable practical value in processing streams containing CO_2 and/or H_2S such as subquality natural gas.

2.0 Background

Gas transport in conventional polymeric membranes occurs by a "passive" solution-diffusion mechanism; that is, gases dissolve in the polymer membrane at the high pressure (feed) side and diffuse in a concentration gradient to the low pressure side where they are liberated to the permeate stream. The intrinsic measure of a material's resistance to gas transport is termed the standard permeability, P. It is the flow rate of gas (Q) permeating a membrane of unit cross-sectional area (A), unit thickness (ℓ), and unit partial pressure driving force (ΔP):

$$P = \frac{Q \cdot \ell}{A \cdot \Delta P} = \frac{cc(STP) \cdot cm}{cm^2 \cdot s \cdot cmHg}$$

It has become customary to represent permeability in Barrer units where
1 Barrer = 10^{-10} $cc \cdot cm/cm^2 \cdot s \cdot cmHg$.

When the membrane thickness is unknown or ill-defined (such as in an asymmetric membrane), it is useful to refer to the permeance, P_0/ℓ of the membrane

$$\text{permeance} = P/\ell = cc/cm^2 \cdot s \cdot cmHg$$

From a practical point of view, permeance is the property which predominantly controls the amount of membrane area required to effect the separation of a given amount of gas and is related to the system capital investment.

Selectivity of a polymer for two species, A and B, is defined as the ratio of the standard permeabilities of the two species through the polymer.

$$\text{selectivity (A/B)} = \alpha(A/B) = P(A)/P(B) = [P/\ell](A) / [P/\ell](B)$$

The membrane selectivity controls the amount of product lost to the permeate. Higher selectivities result in lower product losses and usually improved economics. Low selectivity can sometimes be compensated for by staged processes (multiple membranes connected through interstage compression) but these are more complicated and usually more energy and capital intensive than single stage processes.

Active or facilitated transport gas separation membranes capitalize on chemical reactions or interactions between a species in the membrane and the gaseous component of interest. This provides an additional transport pathway for that gas as shown in Figure 2-1. Both gases A and B permeate the facilitated transport membrane via a solution-diffusion mechanism. However, gas A can react with a species in the membrane and thus has a second mechanism for permeation. As a result, active transport membranes can have permeability and selectivity considerably greater than polymeric membranes.

Several types of active transport membranes have been previously investigated. The most widely studied have been immobilized-liquid, mobile carrier facilitated membranes (ILMs). These membranes consist of a solution of a chemically reactive "carrier" and a solvent immobilized in a microporous polymer matrix. This mode of facilitated transport is shown in Figure 2-2. At the feed side of the membrane, gas A reacts reversibly with carrier molecule C (which is dissolved in a solvent) to form a carrier-gas complex AC:

$$A + C \leftrightarrow AC$$

This complex diffuses in a concentration gradient to the permeate side of the membrane where it dissociates. Uncomplexed carrier C diffuses back to the feed side of the membrane to complete the cycle while gas A is liberated to the permeate stream. Nonreactive component B still permeates the membrane by a conventional solution-diffusion mechanism (as does A); however, under conditions favorable to the facilitation reaction, (which depend on the thermodynamics and kinetics of the A+C reaction), a very high flux of A relative to B can be obtained and hence, a very high selectivity, $\alpha(A/B)$. Examples of this type of active transport are the selective removal of CO_2 from streams containing O_2, N_2,and CH_4,[2,3] the

[2] W.J. Ward and W.L. Robb, ***Science***, 1981 (1967).
[3] J.D. Way, R.D. Noble, D.L. Reed, and G.M. Ginley, ***AIChE Journal, 33(3),*** 480 (1987).

Figure 2-1
Passive vs. Active Mechanisms

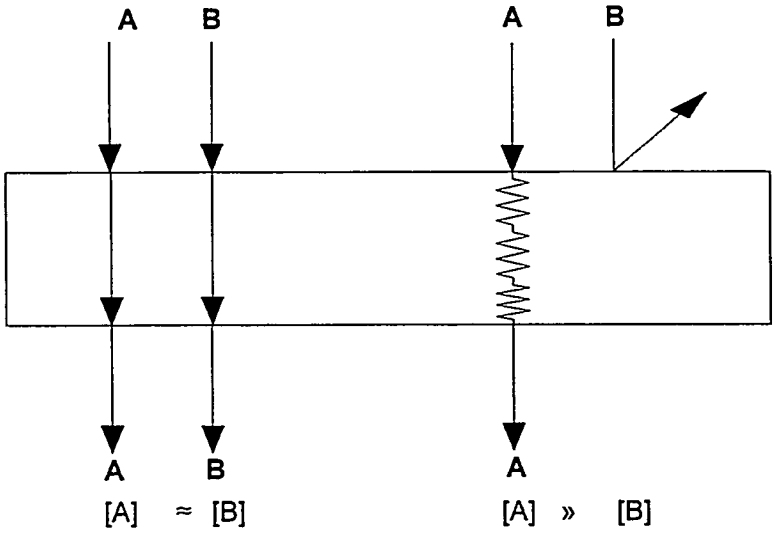

Passive Pathway (Solution-Diffusion)

Reactive Pathway (Active-Transport)

Figure 2-2
Cross Section Of An Immobilized Liquid,
Facilitated-Transport Membrane
Containing A Mobile Carrier Species

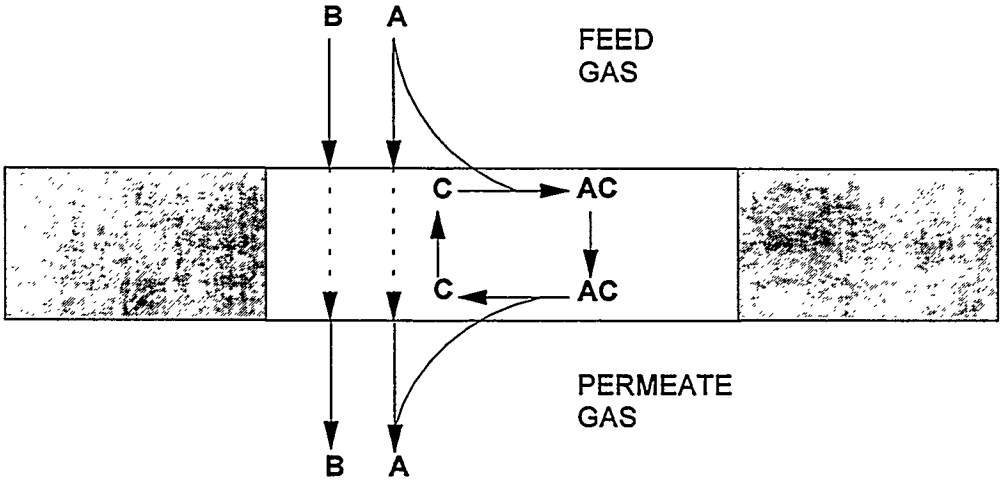

selective removal of H_2S, CO and NO from various streams,[4,5] and the separation of oxygen from air.[6] While ILMs have been investigated since the 1960's and are reported in the literature to have shown impressive selectivities, there are a number of technical hurdles which have prevented such membranes from gaining commercial acceptance. Some of these are:

- **Fabrication of immobilized liquid membranes which are dimensionally stable to the high process pressures.** Many commercial processes operate at pressures greater than 300 psi and often in the range of 1000 to 2000 psi. Immobilized liquid membranes (ILMs) depend on capillary forces to maintain integrity. All other factors being equal, the pore size of the support membrane determines the maximum operating pressure of the ILM. The unavailability of inexpensive, defect-free, high porosity matrices with a narrow distribution of very small pores has hindered the commercialization of ILMs.

- **Identification of stable carrier species.** Facilitated transport membranes contain chemically reactive species which can either degrade over time or undergo side reactions with other components; the latter is especially true if the membrane is contacted with commercial process streams.

- **Identification of suitable nonvolatile solvents..** Membrane life can be limited by the rate of solvent evaporation. Solvent recovery and replenishment systems have been designed into immobilized liquid facilitated transport membrane modules,[7,8,9] but apparently have not been practical. Solvent loss from the membrane is not only a membrane performance and cost issue, but also leads to contamination of product and vent streams.

- **Saturation of the chemical pathway.** Facilitated transport membranes rely on chemical reactions for their permselectivity. For many active transport systems the

---

[4] J.D. Way, R.D. Noble, T.M. Flynn, and E. Dendy Sloan, ***J. Membrane Sci., 12***, 239 (1982).
[5] C.A. Koval, R.D. Noble, J.D. Way, B. Louie, Z.E. Reyers, B.R. Bateman, G.M. Honn and D.L. Reed, ***Inorg. Chem., 24***, 147 (1985).
[6] J.A.T. Norman, G.P. Pez and D.A. Roberts, in "Oxygen Complexes and Oxygen Activation by Transition Metals", A. E. Martell and D. T. Sawyer, eds., Plenum Publ. Corp. 1988 and references therein.
[7] S.L. Matson, U.S. Pat. No. 4,119,408 (1978).
[8] G.E. Walmut and S.L. Matson, U.S. Pat. No. 4,187,086 (1980).
[9] S.L. Matson, U.S. Pat. No. 4,174,374 (1979).

chemical pathway is saturated at relatively low pressure and consequently the permselectivity at commercial conditions may often be no better than conventional (passive transport) polymer membranes.

These areas are the focus of current research in several laboratories. Some efforts involve synthesis of more robust carriers for acid gases[10] and oxygen[11]. Other research centers on the development of new devices, such as Hollow Fiber Contained Liquid Membranes, designed to minimize the negative features of traditional facilitated membranes.[12] Interest has also focused on facilitated transport of gases through solid membranes which contain immobilized reactive sites. Figure 2-3 shows two transport mechanisms which have received attention. In pathway 1, gas molecules bind directly to specific fixed sites, O, within the membrane matrix. A bound gas molecule can then exchange or "hop" to a nearby empty site. As this process is repeated, the gas is effectively transported across the membrane with a concurrent "flux" of empty sites in the opposite direction. The second pathway (2) consists of solubilization of a gas within a nonspecific matrix site, (□), diffusion to and binding at a reaction specific site, (O), and dissolution back into the matrix. Note that transport in conventional polymeric membranes is simply transport between non-specific sites. Barrer[13] has published a mathematical analysis of transport in such "fixed-site" membranes. Nishide[14] *et al.* have published evidence that active transport of O_2 may occur in polymeric membranes that contain fixed oxygen complexes, most likely by the second mechanism. It is only recently that evidence for a direct site-to-site transport mechanism has appeared.[15]

In addition to suffering some of the limitations of the immobilized liquid membranes, solid state active transport membranes face the following additional hurdle:

- **Fixed site membranes with a high concentration of sites.** Current fixed site facilitated transport membranes have a relatively low concentration of reactive sites. Performance could be improved if the site density were significantly increased.

---

[10] C. Koval, M. Rakowski-Dubois, and R.D. Noble, "Sulfur Resistant Complexing Agents for Olefin Separations", presented at the 5th Annual Meeting of the North American Membrane Society, Lexington, KY, May 1992.
[11] D. Ramprasad et al., in "5th Symposium on Activation of Dioxygen and Homogeneous Catalytic Oxidation", in press.
[12] S. Majumdart, A. Guha, and K.K. Sircar, ***AIChE Journal, 34,*** 1135 (1988).
[13] R.M. Barrer, ***J. Membrane Sci., 18,*** 25 (1984).
[14] M. Nishide, O. Ohyanagi, O. Okadra, and E. Tsuchida, ***Macromolecules, 20,*** 417 (1987).
[15] S. Skinkai, K. Tarigoe, O. Manabe, and T. Kajiyama, ***J. Am. Chem. Soc., 109,*** 4458 (1987).

Figure 2-3
Schematic Of Possible Transport
Pathways For A Solid-State Membrane Containing
Immobilized Active Sites

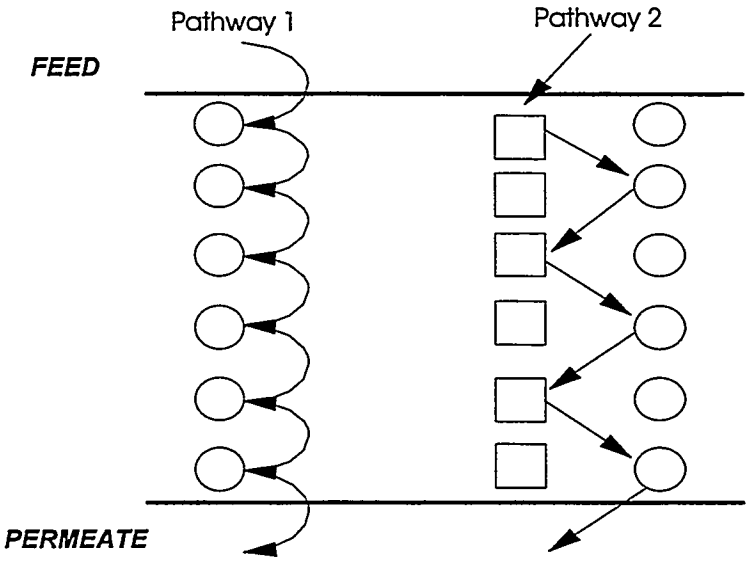

An important point to note about active transport systems in general, both of the immobilized liquid and solid types, is that, because they rely on chemical reactions between the permeant gas and a carrier species in the membrane, the permeability and permeance of such membranes will be a function of the kinetics and equilibrium constant expression for the carrier-gas reaction. Because the equilibrium expression for the carrier-gas complex includes a term for the gas partial pressure, active transport membranes often exhibit a pressure dependent permeability (and permeance). This behavior is shown in Figure 2-4. The permeability is greatest at low pressures where the reactive pathway is used to full advantage. As the pressure is increased, the reactive pathway becomes saturated and the permeability, which is normalized for the partial pressure driving force, decreases proportionately. Because the permeability of non-interacting gases does not depend on the pressure, the selectivity of active transport membranes also exhibits this pressure dependence, and may be no better than conventional membranes under high pressure operating conditions.

Membrane processes normally favor the highest possible operating pressures in order to maximize the amount of gas that can be processed with the minimum amount of membrane area. In contrast, the properties of AT membranes discussed above, i.e., an inverse relationship of permeance and selectivity with pressure, may tend to favor lower operating pressures for AT membrane-based processes. These somewhat conflicting properties of active transport systems gives rise to the notion of an optimum operating pressure window for AT membrane-based systems.[16,17] They also suggest that a detailed understanding of membrane operating characteristics as a function of process conditions will be required in order to design engineered systems which make optimum use of the AT membranes.

[16] L.L. Kemena, R.D. Noble, and N.J. Kemp, ***J. Membrane Sci., 15,*** 259 (1983).
[17] E.L. Cussler, A. Aris and A. Bhown, ***J. Membrane Sci., 43,*** 149 (1989).

Figure 2-4
Pressure Dependence Of Permeance And Selectivity
Of An Active Transport Membrane

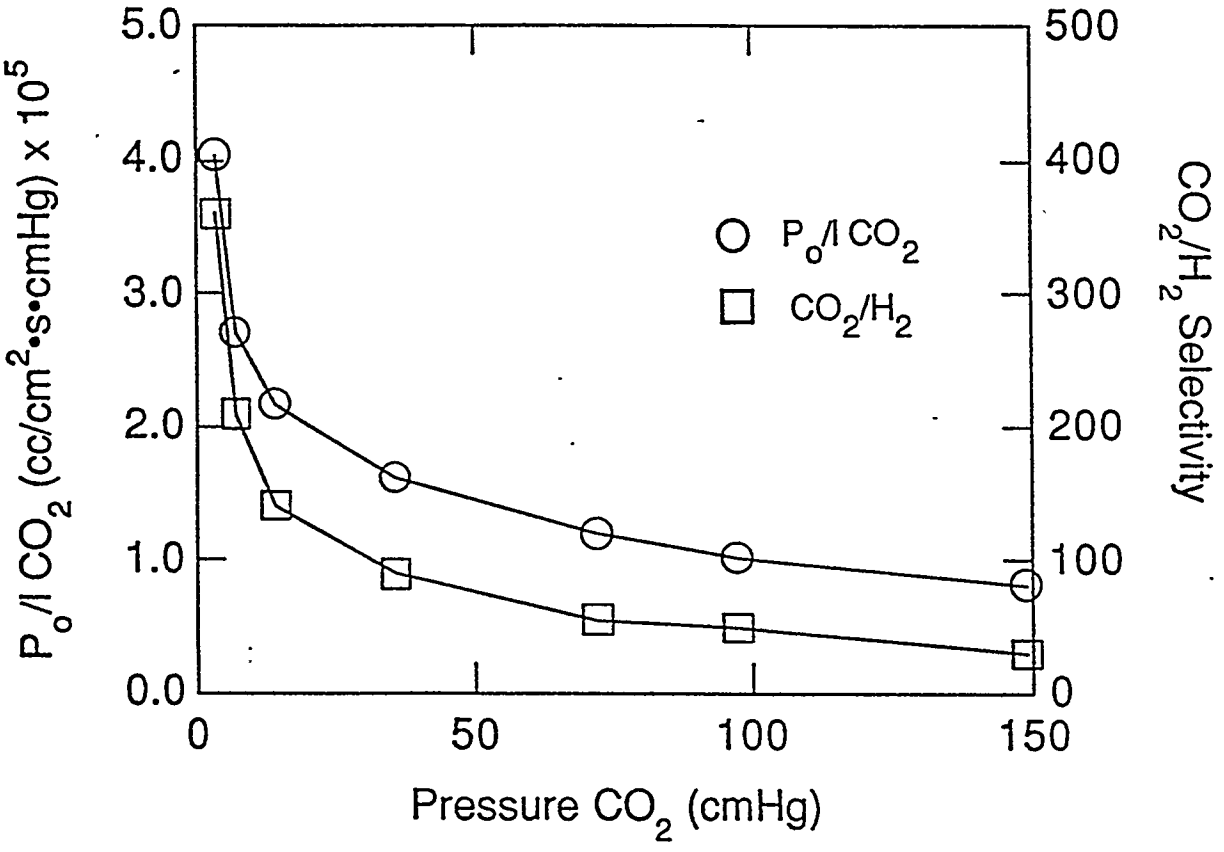

3.0 Historical Perspective - Air Products Work in AT Membranes

Recognizing the potential impact of membranes in general and active transport membranes in particular, Air Products in 1983 initiated a research and development program in this technology area within its Corporate Research group. This program focused on addressing many of the technical hurdles which have thus far kept gas facilitated transport systems a laboratory curiosity. Air Products initially sought to develop stable, low volatility materials which reacted reversibly with oxygen and ammonia. The program was later expanded to include the development of materials for reaction with carbon dioxide, carbon monoxide, hydrogen sulfide and water vapor.

Molten salts were the first active transport media investigated. The concept of using molten salts as active transport media brought several novel and unique features to facilitated transport. First, since molten salts are inherently liquid, no solvent was necessary. As a result, the concentration of carrier species was extremely high and there were no solvent evaporation issues. Furthermore, since molten salts are ionic, they have very low vapor pressures. The ionic nature of the molten salt media also acts to minimize the permeation of non-interacting gases by a solution-diffusion mechanism via the "salting-out effect."[18] Immobilized molten salt membranes were fabricated which exhibited exceptional active transport of oxygen[19] and ammonia[20] at 300°C. This was the first example of facilitated transport membranes which functioned at such high temperatures. Air Products was awarded patent coverage on the use of molten salt membranes for gas separation.[21, 22]

Further work expanded the scope of molten salt facilitated membranes to include selective permeation of CO_2 and CO at near-ambient temperatures by using molten salts which contained large organic cations to lower their melting points.[22] These large organic cations, however, also increased the solution-diffusion permeation of the non-interacting gases, resulting in a lower selectivity. To circumvent this problem, Air Products developed molten salt hydrate membranes. Lab tests showed immobilized liquid membranes fabricated from molten salt hydrates were extremely selective for CO_2 and H_2S over CH_4 and exhibited the

---

[18] D.A. Palmer and R. Van Eldik, ***Chem. Rev., 83,*** 651 (1983).
[19] G.P. Pez and R.T. Carlin, ***J. Membrane Sci., 65,*** 21 (1992).
[20] D.V. Laciak, G.P. Pez and P.M. Burban, ***J. Membrane Sci., 65,*** 31 (1992).
[21] G.P. Pez and R.T. Carlin, U.S. Pat. No. 4,617,029 (1986).
[22] G.P. Pez, R.T. Carlin, D.V. Laciak and J.C. Sorensen, U.S. Pat. No. 4,761,164 (1988).

highest reported selectivity for CO_2 over H_2.[23] The unique nature of these membranes was recognized in two U.S. Patents.[24, 25]

By the mid 1980s Air Products had developed a variety of inherently liquid active transport materials with potential in a number of commercial applications including ammonia synthesis, merchant hydrogen production, acid gas scrubbing, and gas dehydration. Continued development of this technology required active transport materials in a form suitable for fabrication into practical membranes and separation devices. In 1985, Air Products began to synthesize "polymeric analogs" of molten salts and molten salt hydrates; namely, polyelectrolytes. Active transport polyelectrolytes consist of a polymeric backbone containing pendant cationic functionality and their associated counter ions--a polymeric salt. New compositions which showed unprecedented selectivity for ammonia over nitrogen and hydrogen were developed.[23] In 1988, Air Products was awarded two patents on these materials.[26, 27]

In October of 1988, Air Products entered into this Cooperative Agreement with the U.S. Department of Energy, Office of Industrial Programs (DE-FC07-89ID12779). The goal of this Phase I project was to demonstrate that Air Products' proprietary Active Transport membrane materials could be fabricated into commercially practical membranes and devices. Thus far, Air Products identified, developed and evaluated composite ATM membranes, fabricated and evaluated lab-scale spiral-wound modules and refined ATM-based separation schemes for commercial processes.[28,29]

Meanwhile, Air Products continued its independently funded active transport materials development program. In 1990, polyelectrolytes were synthesized for separating carbon dioxide and hydrogen sulfide from hydrogen and methane. The effectiveness of these materials was demonstrated as part of the Phase I program.[28, 29] Moreover, these active transport compositions possessed high selectivity for hydrogen sulfide over carbon dioxide.

---

[23] D.V. Laciak, R. Quinn, G.P. Pez, J.B. Appleby and P.S. Puri, ***Sep. Sci. and Tech., 25*** 1295 (1990).
[24] R. Quinn, G.P. Pez and J.B. Appleby, U.S. Pat. No. 4,780,114 (1988).
[25] R. Quinn and G.P. Pez, U.S. Pat. No. 4,973,456 (1990).
[26] D. V. Laciak and G.P. Pez, U.S. Pat. No. 4,758,250 (1988).
[27] G.P. Pez and D.V. Laciak, U.S. Pat. No. 4,762,535 (1988).
[28] (a) D.V. Laciak, "Development of Novel Active Transport Membranes Devices", DE-FC07-89ID12779, interim report February 1990. (b) ibid. March 1991.
[29] J.S. Choe, L.J. Kellogg, D.V. Laciak, T.A. Shenoy, and S.C. Weiner, "Development of Novel Active Transport Membranes Devices", DE-FC07-89ID12779, interim report January 1993.

These materials are the subject of two patent applications. In 1994 Air Products received a patent on the use of polyelectrolyte membranes for the separation of acid gases.[30]

4.0 Phase IA Accomplishments

Since November 1988 Air Products has pursued a cooperative research program with the U.S. Department of Energy-Office of Industrial Technology aimed at assessing the feasibility of commercializing ATM technology. This program included various laboratory tasks, and process and commercial development activities. Detailed results have been reported to DOE.[28,29] Specific accomplishments from that program include:

- **Identified a composite membrane fabrication concept.** A technique whereby the active transport polyelectrolyte was supported on a microporous substrate and coated with a relatively permeable but nonselective polymer (e.g. silicone rubber) was identified and developed. Figure 2-5 shows a schematic cross-section of such a composite and an image taken by a scanning electron microscope. Fabrication of composite coupons (4 cm^2) were scaled to planar sheets (1 ft^2).

- **Demonstrated high pressure operation of CO_2 and NH_3-selective composite ATM coupons.** Composite AT coupons were evaluated in mixed gas streams at Air Products' laboratories as a function of gas pressure (to 1000 psi), composition, and flowrate, temperature, and, in some cases, water vapor content of the gas stream. Membrane stability was demonstrated for 30+ days of continuous operation.

- **Fabricated and evaluated lab-scale spiral wound ATM modules.** Planar composite membranes were wound into spiral elements (200 cm^2) and their performance was evaluated at conditions approaching those of commercial processes. Lab tests suggested that concentration polarization effects reduced the effectiveness of the membrane module at the flow rates tested by introducing a significant gas phase resistance to permeation. This might be less of an issue in high flow rate commercial installations where the feed gas streams are better mixed.

---

[30] R. Quinn, D.V. Laciak, J.B. Appleby and G.P. Pez, Polyelectrolyte Membranes for the Separation of Acid Gases", U.S. Pat. No. 5,336,298 (1994).

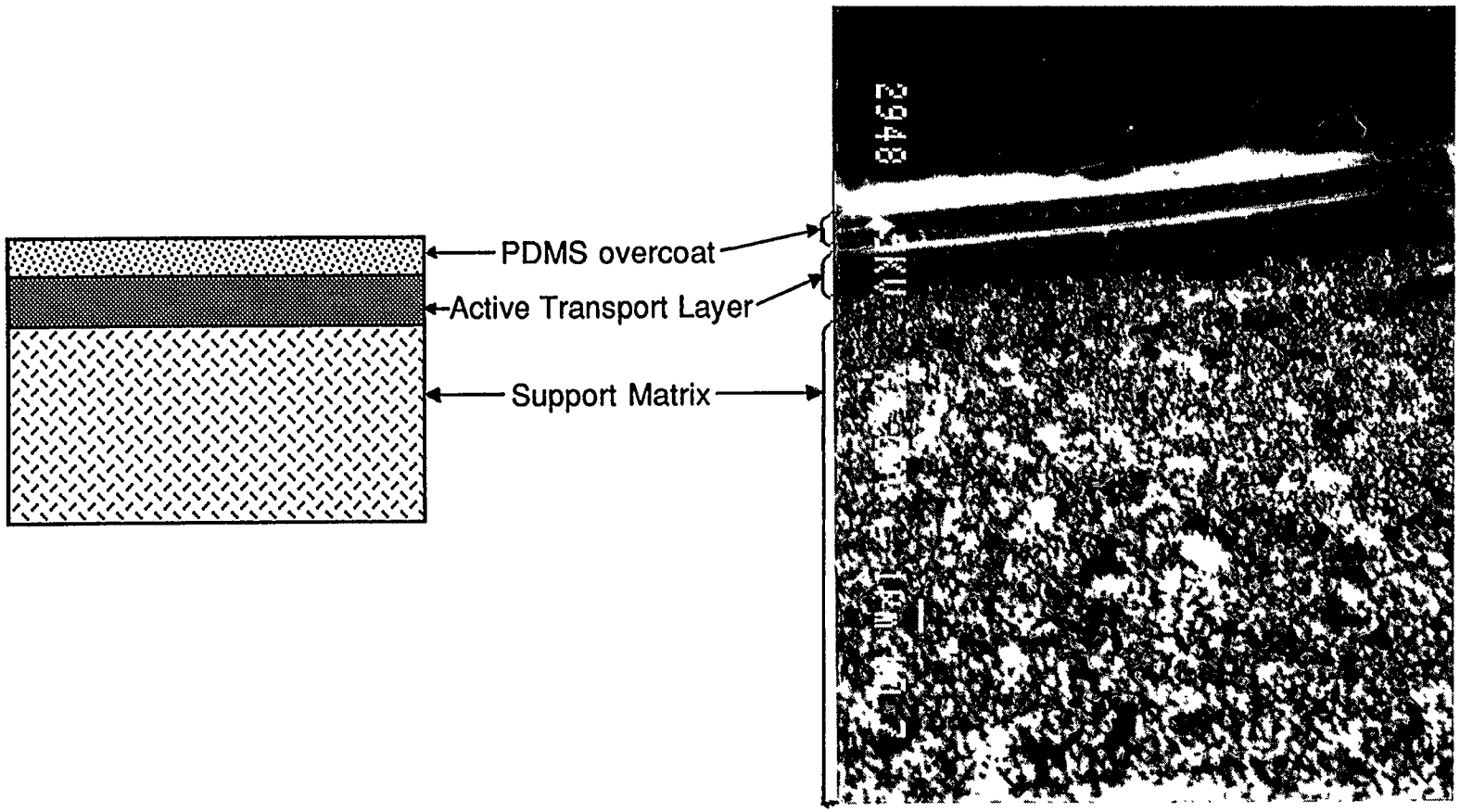

Figure 2-5
Cross-section of a Multilayer Composite Membrane

- **Developed detailed flow sheets for incorporating ATMs into selected commercial processes.** Process schemes were developed for utilizing ATMs and ATM-hybrids in hydrogen production via steam-methane reforming. Estimated membrane performance was used to predict mass and energy balances. Bottom-line economics showed that ATMs can be cost competitive with conventional acid gas scrubbing systems by providing an energy savings to offset the cost of capital. Several potential process schemes were identified for incorporating ATMs into ammonia synthesis plants. The ATM-based systems had both lower capital and energy costs.

- **Identified natural gas processing as a market with high potential for ATM technology.** Several markets including ammonia and urea synthesis, merchant hydrogen and syngas production, and natural gas processing were analyzed. Sizable growth is projected for natural gas production. ATM-Pressure Swing Absorption hybrids are expected to offer opportunities in the strong hydrogen market. Slow growth is forecast for domestic ammonia capacity. Energy savings was found to be an important but not a key factor in choosing among competing technologies.

- **Identified areas for further experimental work.** The permselectivity of ATMs was found to be highly sensitive to the water vapor content of the feed gas stream. The implication of this observation to projected module performance and economics will need to be assessed in any follow-on program. ATM material modifications to moderate this effort should also be sought. In addition, follow-on work should focus on increasing the CO_2 flux of the ATM composite either by thinning the ATM layer, by identifying and incorporating catalysts or both.

5.0 Technical Focus

As indicated in Section 2.2, of Chapter II, the objective of this phase of the program was to demonstrate ATM technology in a commercially feasible form. For simplicity and due to its ready accessibility, the initial demonstration of membrane and module fabrication was accomplished in flat sheet and spiral wound module form. Hollow fiber configurations, however, offer the following inherent advantages relative to flat sheet and spiral configurations:

- A hollow fiber module is inherently simpler than a spiral since it does not require the spiral's spacer components.

- Hollow fiber modules are less labor intensive and, hence, cheaper to produce.

- Hollow fiber modules provide a higher membrane packing density than spirals (often by as much as a factor of 10 or more). The higher packing density permits the design of smaller, less costly systems.

Overall, the combination of fewer components, an inherently cheaper manufacturing technology, and a lower system cost are expected to provide significantly improved economics for the membranes in hollow fiber form. While the primary focus of DOE must be on energy savings and on bringing new energy sources to the market, acceptance of this technology by the ultimate users will depend heavily on the economics of this technology. The favorable economics of hollow fibers and the strong focus of Air Products as well as DOE on technology commercialization mandated that we translate the early work conducted on flat sheets to hollow fibers.

Many years of research at Air Products (both with DOE and in our independently funded programs) have been devoted to the fabrication of composite membranes. This experience has taught us about the critical inter-relationship of the properties of the support membrane, the coating polymer properties, and the process variables of the coating process on the overall properties of a composite membrane. With the decision to fabricate the ATM in hollow fiber form, a fresh look was taken at the nature of the membrane structure, and we set out to separately optimize each of the membrane's individual components in order to maximize the

overall membrane properties for its intended end use application. Therefore, the technical program for this, the last segment of Phase I included:

- **Hollow Fiber Substrate Fiber Spinning**

  The demanding process conditions of natural gas processing operations require that the composite membrane be support on a robust support membrane. It was not apparent that commercial microporous membranes possessed acceptable properties. Therefore, this task included defining the chemical and physical characteristics for a high performance substrate, screening candidate materials, and finally formulating a spin dope and spinning fiber samples for physical and coating evaluations.

- **Composite Membrane Development**

  The primary focus of this task was to translate the planar and spiral-wound composite membrane fabrication technology to the commercially viable form of a multilayer composite hollow fiber membrane. For this purpose, laboratory modules were to be fabricated and evaluated as a function of several process variables including total gas pressure, acid gas partial pressure, temperature, and feed and permeate gas water vapor content. A second aspect of this task was to provide (a) feedback to substrate development efforts to help define support fiber parameters such as base permeance, pore size, and porosity, etc. and (b) feedback to process application development efforts to gauge the effectiveness of ATMs in natural gas applications.

- **Process Application Development and Economic Analysis**

  Efforts were to focus on defining new gas processing schemes centered on ATMs and/or on hybrids of ATM and current acid gas removal (AGR) technology. Optimization of the process would define the bottom line economic and energy savings benefits of the ATM process as compared to other membrane systems and other stand-alone gas processing technologies. Results from these studies would guide laboratory work in both substrate development and composite membrane development.

The results of this program are described in the following chapters.

III. Substrate Fiber Development

The goal of this task is to develop a high performance hollow fiber substrate to accept the active transport membrane coating and involves two major objectives: 1) identifying a polymer that fulfills the requirements of a "high performance" substrate and 2) developing spinning technology; that is, both the fiber spinning process and the polymer formulation needed to fabricate the identified polymer into a microporous hollow fiber substrate for suitable coating.

1.0 Introduction

Membrane devices can be fabricated as flat disks, plate and frame assemblies, spiral-wound elements and as hollow fibers. It is generally accepted that the hollow fiber module configuration has several advantages over other fabrication geometries including 1) hollow fibers are self supporting within a permeator thus allowing for a much simpler module fabrication process, and 2) hollow fibers generate higher surface area to permeator volume ratios than other configurations. These two factors suggest that the hollow fiber configuration should result in a significant reduction in cost over competing membrane technology.

Hollow fibers have been manufactured in the textile industry for the past several decades, mainly for use in thermal insulation applications. These fibers are typically produced by a melt-spinning process which involves heating a polymer above its melting point. The molten polymer is extruded through a spinneret to produce a fine filament which cools and solidifies into a fiber. The fiber produced through this method is dense across the entire wall of the fiber; that is, it contains no porosity. However, to produce the kind of the porous structure suitable for gas separation, a dry jet-wet spinning process (solution spinning) is commonly practiced. The dry jet-wet spinning process involves a phase inversion mechanism in which polymer solution is extruded as a fine tubular casting. The process can best be understood by considering the four steps of membrane formation: 1) extrusion, 2) air exposure/partial phase separation, 3) coagulation, and 4) washing/annealing. The reader is also referred to Figure 3-1.

1) Extrusion: A hollow fiber membrane is formed by extruding a concentrated polymer solution downward through a tube-in-orifice die (spinneret). The lumen (bore) of the fiber is created by delivering a coagulant fluid to the concentrically aligned capillary tube within the orifice. The extrusion results in a self supporting nascent hollow fiber.

2) Air exposure/partial phase separation: After extrusion, the nascent fiber travels through a short conditioning zone ("air gap") before entering a coagulation bath. In this stage, the polymer solution often undergoes a partial phase separation due to partial evaporation of the solvent, penetration of the ambient moisture into the extrudate, and/or temperature gradients established during the journey. Conditions in this critical zone can significantly influence membrane structure, especially the surface of the fiber, and were examined as part of this program.

3) Coagulation/phase separation*: Solidification of the fiber occurs by phase inversion (non-solvent induced phase separation) in the coagulation bath. In this stage, the polymer solution undergoes a more complete phase separation which results in a polymer-rich phase and a solvent-rich phase. This step plays an important role in determining the overall membrane structure especially that just under the surface layer. The effect of coagulation bath temperature on fiber properties was examined as part of this project.

4) Washing/Annealing: A water-wash step is employed to remove traces of residual solvent so that the pore structure created during the previous steps can be preserved. By this stage, morphology of the fiber has been determined, however, minor tuning in the pore structure may be achieved by warm-water annealing. The warm water washing can also enhance the rate of solvent exchange.

In the Phase I of this project, hollow fiber substrates were developed via the dry jet-wet spinning technique in the Corporate Science & Technology Center of APCI. The major task elements included setting support fiber criteria, identifying and evaluating candidate polymers against these criteria, studying candidate polymer processability for spinning, and initiating optimization of the spinning process and dope formulation for the polymer. Phase I goals included:

*A detailed description of the phase separation process can be found in J.M.Sci. (8), p. 41-57 (1993).

- to set-up a spinning line with controllable spinning parameters.
- to identify a spinnable polymer that fulfills the requirements for a composite membrane support for the targeted application.
- to gain an understanding of the operation variables-fiber property relationship.
- to develop reliable techniques to characterize the spun fibers.

2.0 Experimental

2.1 Hollow Fiber Spinning

A state-of-the-art hollow fiber spinning line was set up for this project. A schematic of the spinning line is shown in Figure 3-1. The major components of the line include: an in-line mixing system, a dope delivery system, a bore-fluid injection system, a coagulation bath, two duo-godet-wash bath assemblies, and a take-up winder.

1) *In-line mixing system:* The polymer solution (referred to as the "dope") was prepared in a customized Ross mixing system. The mixed dope can be transferred directly into the dope reservoir by a gear pump. In addition, degassing could be conducted inside the mixer by means of house vacuum. A condenser (heat exchanger) was attached to prevent solvent loss and maintain initial dope concentration.

2) *Dope Delivery System*: The resulting degassed dope solution was transferred from the reservoir to the spinneret via the gear pump. Before arrival at the spinneret the polymer solution was forced through a filter (mesh size: 60 μm) to remove particulates. The temperature of the entire delivery system was controlled using silicone rubber encased resistance heaters.

3) *Bore Fluid Injection System*: The internal coagulant (bore fluid) was supplied to the injection capillary of the spinneret via a bore fluid injection system. This set-up was designed to pump a small volume of fluid with a minimum of pulsing. The typical dope delivery pressure was about 3 psig.

4) *Coagulation Bath & Duo-godet-Wash Bath Assembly:* After extrusion, the partially solidified fiber was guided through a coagulation bath by a pair of

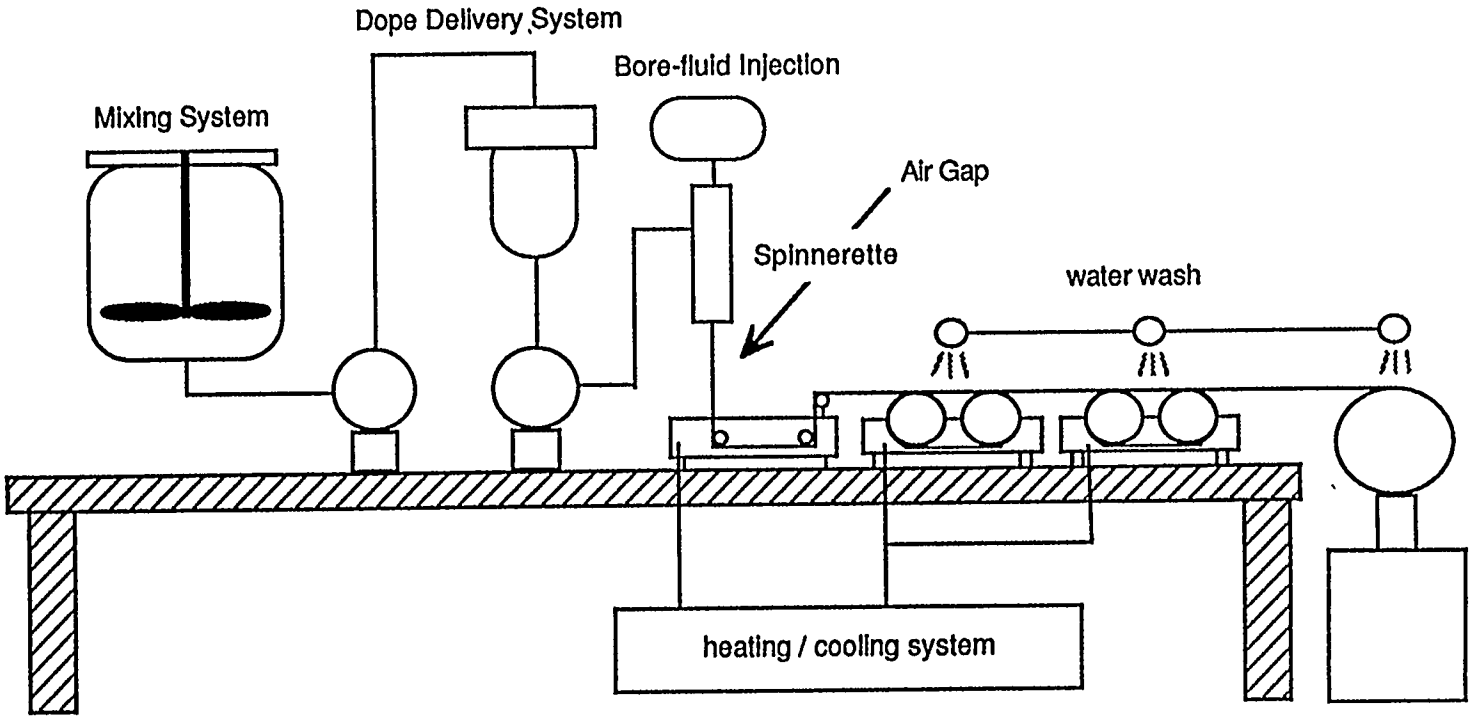

Figure 3-1
Fiber Spin Line Schematic

non-slip rollers (a duo-godet). On leaving the coagulation bath, the fiber was washed by entering a series of duo-godet-wash bath assemblies. The temperatures of the coagulation bath and wash baths, depending on experimental needs, were controlled by a circulating water bath.

5) *Take-up Winder and Fiber Storage:* After washing the fiber was wound onto a spool by an automatic, tension controlled take-up winder. Additional washing was provided at the winder by employing a water sprayer. The spooled fiber was stored in a water tank for at least 72 hours to remove the residual solvent which might be trapped in the fiber.

2.2 Hollow fiber Characterization

A typical spin run produced 1000-2000 linear feet of hollow fiber support membrane. Five foot lengths of fiber were cut from the spool and hung to dry at room temperature. Characterization of hollow fiber support membranes included determining the overall fiber appearance, fiber dimension (outer diameter OD and inner diameter ID), average surface pore and defect size by optical and electron microscopy; quantifying the defect rate by bubble point measurements; measuring tensile strength by dynamic mechanical analysis; and measurements of gas permeance.

3.0 Result and Discussions

3.1 Polymer Selection Criteria and Candidate Polymer Screening

In order to qualify as a high performance acid gas substrate the candidate polymer should meet the following criteria: 1) good hydrocarbon resistance, 2) stable at end use temperature, 3) easily processable, and 4) commercially available. Polyimide-based polymers including PYLE-ML (polyimide), AI-10 (polyamide-imide), and PAI (polyamide-imide) were identified from the literature as potential support polymers.

The candidate polymers were first screened for processability, i.e. how easily could they be spun into hollow fibers. Table 3-1 summarizes the results of this investigation. High molecular weight (MW) PAI had the best processability among the polymers studied.

Table 3-1
Comparison in Spinning Processability

Material	Source	Processability
PYLE-ML	DuPont	fair
AI-10	Amoco	poor
AI-10	Air Products	poor
PAI (low MW)	Amoco	poor
PAI (high MW)	Amoco	good

Other critical properties were also examined. Table 3-2 lists physical properties of four commercially available polymers. Of the candidate polymers, PAI has the advantage of high temperature endurance as manifested by its high glass transition temperature (Tg) and superior mechanical strength as manifested by its high tensile strength. In addition, PAI shows the best hydrocarbon resistance. Table 3-3 shows the % tensile strength retained after 24 hour solvent exposure at 93°F. Commercial polymers such as polysulfone are degraded in, e.g., xylene and toluene. These investigations indicate that high molecular weight PAI is the most promising candidate among the polymers studied .

Table 3-2
Physical Properties of Candidate Polymers

Properties	**Udel (3500)** *Amoco*	**PAN (PAN-X)** *Bayer*	**Ultem (1000)** *GE*	**PAI (4000)** *Amoco*
MW	80,000	57,000	30,000	30,000
Tg (°C)	185	85	215	**279**
Tensile Strength (MPa)	70.3	118	105	**135**

Table 3-3
Hydrocarbon Resistance of PAI

Chemical	% Tensile Strength Retained*
Cyclohexane	100
Diesel Fuel	99
Gasoline (120 °F)	100
Heptane	100
Mineral Oil	100
Motor Oil	100
Xylene	100
Toluene	100

*After 24 hour exposure at 93 °C

Of the polymers investigated, PAI is clearly the leading candidate for further development. In addition to the general polymer criteria discussed above, other targets imposed on substrate fiber include:

- *good hydrocarbon/solvent resistance:* Screening studies measured hydrocarbon resistance of the bulk polymer. It is critical that this resistance be maintained after the polymer is spun into a fiber, especially in regard to those compounds present in natural gas streams.

- *good tensile strength:* The mechanical strength of the spun fiber should be strong enough for routine handling. The targeted tensile strength is comparable to that of commercial polysulfone fiber.

- *high gas permeance:* The initial base permeance for the support fiber is targeted at ≈ 1,000 x10 $^{-6}$ $cm^3/cm^2 \bullet sec \bullet cmHg$. However, the final flux target will be modified when it is integrated with the overall ATM performance targets set during composite optimization.

- *small and uniform surface pores:* Based on the molecular weight and radius of gyration of the ATM coating polymers, the target surface pore size is 100-200 μm.

However, the final target may vary with the chosen coating process and the coating material used.

- *compatibility with the ATM material.* The support fiber should be stable to ATM coating solvents (methanol and water). It should be wet by the ATM material and the resulting ATM-coated fiber should exhibit permselectivity close to intrinsic values.

The following sections of this chapter describe progress against these targets. It should be noted that these PAI fibers were developed throughout Phase I of this project and only limited work was performed to optimize substrate properties. Nonetheless, the results to date are encouraging. Support fiber optimization will continue as part of Phase II.

3.2 Solvent Resistance of PAI Support Fiber

In this study, the solvent resistance of polysulfone, Ultem, and polyacrylonitrile fiber was compared to PAI fiber. All fiber was produced by Air Products for this study.

The solvent resistance tests were performed by immersing small sections (5 cm) of fibers into five different solvents for a period of 2 weeks. The changes in fiber appearance were then observed and recorded. The solvents studied included 1,4 dioxane, 1,2 dichlorethane (DCE), tetrahydrofuran (THF), toluene, and hexane. These solvents are either common contaminants in streams or used for dissolving traditional coating polymers. Hexane is often a solvent used for dissolving polydimethylsiloxane (PDMS); the formulation is used to repair defective or leaky fibers.[31] Table 3-4 summarizes the experimental results. All the fibers had good solvent resistance against the hexane. However, only the PAI fiber remained opaque in the other solvents studied. PAN fiber turned translucent and the others dissolved completely. The translucence of the fiber may indicate that solvent penetrates into the fiber wall, which may result in swelling. This study demonstrated that PAI fiber has the best solvent resistance among the examined hollow fibers . The order of solvent resistance of the fibers is: PAI > PAN > Ultem > polysulfone.

[31] J.M. Henis and M.K. tripodi, Multicomonent Membranes for Gas Separations", U.S. Pat. No. 4,230,463 (1980).

Table 3-4
*Chemical Resistances of Candidate Fibers**

Solvent	PSN	Ultem	PAN	PAI
Toluene	-	-	+	+
Dioxane	-	-	+	+
1,2 DCE	-	-	+	+
THF	-	-	+	+
Hexane	+	+	+	+

+ = stable; - = unstable
*After 2 week immersion at room temperature.

A more intensive test of PAI solvent resistance was also performed. The N_2 permanence of the support fiber was measured before and after exposure to the various solvents. Permeance loss (or gain) would indicate fiber degradation or changes to the micropore structure brought about by solvent exposure. The fiber used in this study had an initial permeance of 10,000 $x10^{-6}$ $cm^3/cm^2 \cdot s \cdot cmHg$. Small sections of fiber were immersed in the various solvents for 5 seconds. The permeance of the fibers was then remeasured and compared to the original values. Table 3-5 lists the percent permeance loss after solvent exposure. The permeance of PAI fiber is affected only by 1,2 DCE and methanol (40 % loss).

We have found that PAI solvent resistance can be improved by heat-treating the fiber at high temperature (over 200 °C) for several hours in an inert gas environment. This effect is also shown in Table 3-5. After thermal treatment PAI fiber had good solvent resistance even to DCE and methanol.

Table 3-5
Effect of Solvent Exposure on PAI Fiber Permeance

Solvent	Permeance loss*	
	non-heat-treated	heat treated
1,2 DCE	~ 40%	0%
MeOH	~ 40%	0%
Toluene	0%	0%
Hexane	0%	0%
Freon	0%	0%
Water	0%	0%

* after 5 sec solvent exposure

The necessity of the thermal-treatment process will be evaluated as part of Phase II. If this process is indeed needed, optimal curing time and temperature will be determined.

3.3 Tensile Strength of PAI Fiber

Tensile strength tests were performed to compare the PAI fibers with polysulfone, Ultem, and polyacrylonitrile (PAN) fibers. In addition, two types, microporous and asymmetric, of PAI fibers were compared. The results are shown in Table 3-6. PAI fiber has tensile strength comparable to other available fibers. In addition, the tensile strength of the PAI fiber depends on the fiber microstructure (asymmetric vs. microporous). The strongest PAI fiber produced so far has a tensile strength of 43% greater than polysulfone, and 150% greater than PAN. Overall, the PAI fiber has better mechanical strength (higher tensile strength) but less elasticity (lower elongation %) than the polysulfone and PAN fibers.

Table 3-6
Tensile Strength Tests of Fibers

Hollow Fiber	Structure	Tensile Strength at Break*	Elongation at Break*
Polysulfone	asymmetric	1.0	1.0
PAN	microporous	0.56	0.83
Ultem	microporous	0.92	0.29
PAI	microporous	**1.43**	**0.39**
PAI	asymmetric	**1.12**	**0.88**

* polysulfone = 1.0

The tensile strength of the fiber may depend not only on the material itself but also on the fabrication process and the dope composition. These factors could result in significant variations in fiber porosity, pore size, pore size distribution, phase separation mechanism (e.g. spinodal decomposition vs. nucleation and growth), and the existence of macrovoids. It should be noted here that the polysulfone fibers were spun from a higher polymer content dope than PAI and this may influence the results. Nonetheless, microporous PAI fibers were found to have the highest tensile strength among all the fibers investigated. Further improvement in fiber tensile strength and elongation % may be achieved through substrate optimization.

3.4 Pore Size/Permeance Control of PAI Substrate

Two important issues in developing the hollow fiber substrate are matching the support fiber properties to the needs of the coating polymer and ensuring that fiber manufacturing techniques will consistently produce uniform, high performance substrate. The ability to control the surface characteristics (e.g. pore size, porosity, and permeance) of the fiber is critical in matching the support fiber to the properties of the coating polymer. In addition, the ability to understand the effect of process variables on fiber properties is vital to ensuring fiber reproducibility not just within a given spinning run but also between spinning runs.

Fiber spinning is a complex process involving many interdependent parameters. Our efforts focused on the effect of three process variables on fiber permeance and surface pore size. The air gap length, coagulation bath temperature, and the environment within the air gap, on fiber properties (permeance and surface pore size) were investigated. Details of the study are described in the following sections.

3.4.1 Effect of Air Gap Length on PAI Fiber

The air gap is the distance from the bottom of the spinneret to the surface of coagulation bath. Two processes can occur as the fiber traverses this distance: 1) thermal phase separation induced by the difference between spin dope temperature and ambient temperature and 2) solvent induced phase separation resulting from ambient humidity and/or vapors given off from the coagulation bath. The degree to which each process occurs (or whether it will occur at all) is in part determined by air gap length. Therefore, the effect of the air gap was measured while all other spin variables were held constant. In addition, since water was used in the coagulation bath, two coagulation bath temperatures, 70 and 10 °C were chosen in the study to provide some indication of the effect of "uncontrolled" humidity on fiber performance. The results, summarized in Table 3-7, indicate that both the gas permeance and surface pore size increase with decreasing air gap for a 70°C bath but that these parameters are not sensitive to air gap length at the lower bath temperature. Additionally, a dense skin was observed on the fibers for all three air gap lengths investigated at using a 10°C bath. This last result was confirmed by the very low (2-50 $10^{-6}cm^3/cm^2 \bullet s \bullet cmHg$) gas permeance of the fibers.

Table 3-7
Effect of Air Gap on Fiber Permeance

	70 °C Bath Temperature		10°C Bath Temperature	
Air Gap	Permeance*	Pore Size	Permeance*	Pore Size
30 cm	1500	200 Å	2	<40 Å
20 cm	6500	400 Å	52	<40 Å
10 cm	15000	1000 Å	33	40 Å

* 10^{-6} $cm^3/cm^2 \bullet s \bullet cmHg$; average of at least 5 modules.

3.4.2 Effect of Coagulation Bath Temperature on PAI Fiber

Coagulation bath temperature was varied from 10 °C to 70 °C while the other spinning parameters, including air gap length were held constant. Figure 3-2 shows the effect of coagulation bath temperature on fiber permeance. Higher coagulation bath temperatures resulted in a higher permeance substrate. As expected, the surface pore size of the fibers (~100 Å to ~1000 Å) increased with increasing coagulation bath temperature. The most permeable fiber was produced in a 70°C coagulation bath temperature of 70 °C and exhibited a permeance of 15,000 X $10^{-6}cm^3/cm^2 \bullet s \bullet cmHg$ with a surface pore size of ~ 1000 Å.

3.4.3 Effect of Environment Within the Air Gap on PAI Fiber

As suggested in Table 3-7, the environment within the air gap can have a profound effect on the fiber properties. The aim of this study was to examine the extent to which the surface pore size and morphology could be controlled by maintaining a specific set of conditions within the air gap. The influence of the coagulation bath temperature (coagulation bath media vapor pressure) on the environmental effect within the air gap was also studied. Two coagulation bath temperatures, 51°C and 60 °C, were used in this investigation.

A "chimney" enclosing the spun nascent fiber within the air gap area was designed and installed to better control the environment within the air gap. An opening at the bottom of the chimney served as the inlet for the flowing gas which was vented at the top of the chimney. The experiments were conducted to compare the difference in fiber properties

Figure 3-2

Effect of Coagulation Bath Temperature on Permeance

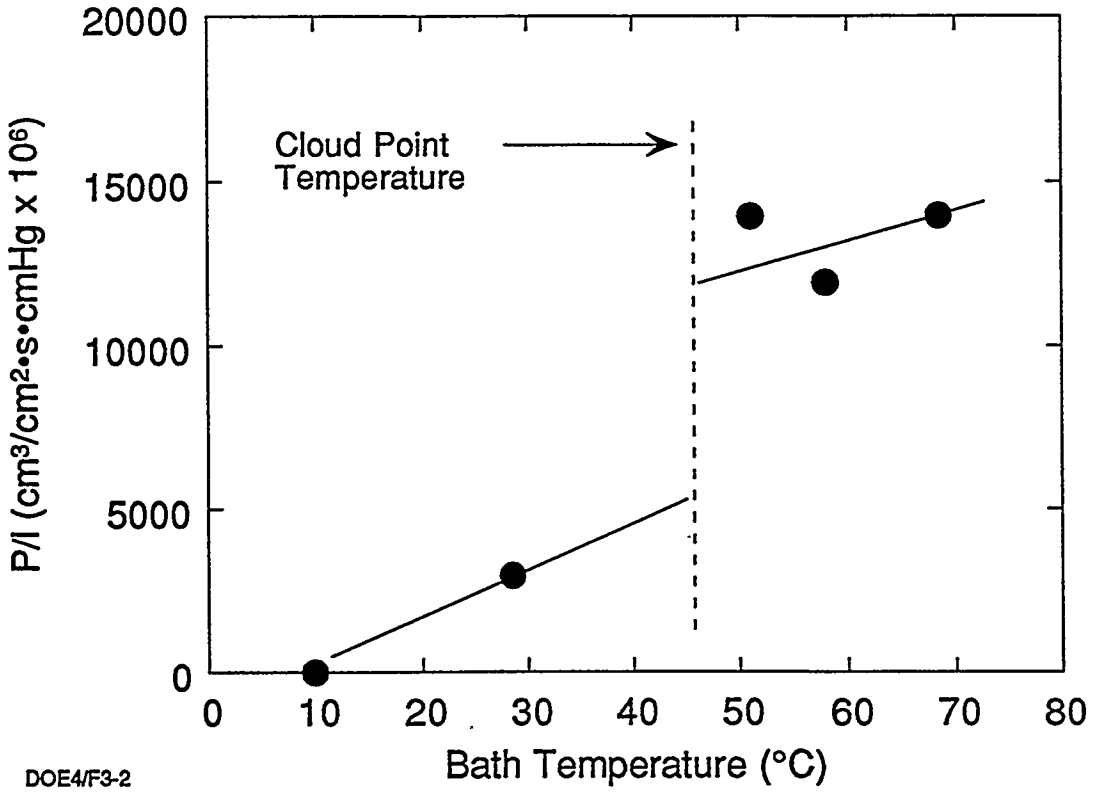

between environmental and non-environmental control of the air gap. The air gap environment was changed by flowing, countercurrent to the fiber, dry nitrogen at 400bsccm. In the "no control" case, the chimney was in place but no gas was flowing.

Table 3-8 lists the resulting fiber permeances and surface pore sizes for the fibers. Interestingly, significant differences in both the permeance and the surface pore size between the fibers produced with and without the environmental control were observed. It should be noted that a more porous structure was produced in the non-environmental control condition.

Table 3-8
Environmental Effect in Air Gap on Fiber Property
(Coagulation Bath Temperature 51 °C)

condition	$P/\ell\ N_2$*	surface pore size
dry N_2	5	dense (< 40 Å)
no control (56%)	4910	~100Å

* 10^{-6} $cm^3/cm^2 \bullet s \bullet cmHg$

In the second set of experiments, the coagulation bath temperature was set at 60 °C. In the first data set, the air gap contained flowing dry N_2. In the second, the air gap contained nitrogen humidified to a dew point of 70C. In the last set, no gas was flowing. Table 3-9 compares the results for fibers spun under these conditions. A low permeance fiber was obtained with dry nitrogen circulating through the chimney. The general trend of this result is consistent with that obtained in the lower coagulation bath temperature. It is believed that dry N_2 both lowers the effective water (bath) vapor pressure and accelerates the rate of evaporation, leading to a less porous surface. A fiber with an extremely high permeance, moderate surface pore size, and high porosity (20%) was produced when warm, moist N_2 filled the air gap. It is believed that this condition should enhance a uniform phase separation through the cross-section of the nascent spun fiber (the fiber just extruded from the spinneret). Fiber produced without environmental control has a high permeance and large surface pores but a low porosity (7%). In addition, no macrovoids* were observed for the fibers produced with the environmental control while some macrovoids were observed in the non-environmental control condition.

*Large areas of free volume within the fiber wall

Table 3-9
Environmental Effect in Air Gap on Fiber Property
(Coagulation Bath Temperature 60 °C)

control condition	P/ℓ*	macrovoid	pore size
dry N_2	129	no	~ 100 Å
warm wet N_2	97300	no	~ 800 Å
no control**	67080	yes	~ 500 Å

* 10^{-6} $cm^3/cm^2 \bullet s \bullet cmHg$
** ≈60% relative humidity

4.0 Summary and Recommendations

In Phase I of this project, a state-of-the-art spinning line was designed, installed and used to examine the relationship between various parameters in the spinning process. This line was set up to simulate a continuous manufacturing process from polymer formulation to fiber formation and winding. A set of routine characterization methods were developed to examine the quality of the spun fibers including permselectivity measurements, surface pore size, defect pore size and rate, solvent resistance, and tensile strength.

A polymer fulfilling the substrate requirements was identified. A dope formulation and spinning process for this material were demonstrated. A parametric study identified key parameters for controlling surface pore size and fiber permeance. Fiber permeance and surface pore size were found to be strong functions of the air gap length, coagulation bath temperature, and the environment within the air gap. Circulating dry nitrogen through the air gap produces fiber with smaller surface pores while warm and wet nitrogen within the air gap produces fiber with large surface pores and high porosities. The nonoptimized fiber has met the preliminary targets set for a high performance substrate and shows promise as a coatable substrate for the ATM material. The current status of fiber development is summarized in Table 3-10.

Table 3-10
Current Status of Development

Parameter	Status
High Gas Permeance	up to 100,000 $10^{-6}cm^3/cm^2 \bullet s \bullet cmHg$
Small Surface Pores	tunable from < 40 to 1000 Å
Tensile Strength	comparable to commercial fiber
Hydrocarbon Resistance	Good

A follow-on program should focus on optimizing the PAI hollow fiber by incorporating results from ATM coating studies. The spinning process is complex and its variables are often interdependent. Therefore, a forward program should include the completion of a process variables / fiber property relationship matrix. An optimal dope composition and process conditions for scale-up should be determined. Finally, fibers with the desired properties should be produced in large quantity to support laboratory module fabrication and field testing efforts. The necessity of the post-spinning thermal treatment should also be examined during that segment.

IV. Composite Membrane Development

The objective of this task was to demonstrate the separation of CO_2 from CH_4 using hollow fiber active transport membranes. This objective was met by forming thin film composite membranes of the AT polyelectrolyte PVBTAF and polysulfone or PAI hollow fiber substrates. Lab-scale modules were evaluated at pressures up to 900 psi and for periods as long as 1 month. This chapter is divided into three sections. The first describes the characterization of the candidate coating solutions in terms of their solubility, viscosity, molecular weights, etc. The second reports on the coatability of potential substrate materials with PVBTAF by fabricating and evaluating planar thin film composite membranes. The last describes the fabrication and evaluation of lab-scale hollow fiber modules.

1.0 Physical Properties of Coating Solutions

1.1 Molecular Weight and Distribution of ATM Polymers

Most coating work employed the AT polymer poly(vinylbenzyltrimethylammonium fluoride), PVBTAF. This polymer is derived from either of two batches (batch 1 and batch 2) of poly(vinylbenzyltrimethylammonium chloride), PVBTACl[32] which differed in molecular weight. Molecular weight, molecular weight distribution and estimated molecular size were determined using Gel Permeation Chromatography/Magic Angle Laser Light Scattering (GPC-MALLS). Results are shown in Table 4-1. The molecular weight of all samples were sufficiently high (Mw > 500,000) to be film forming. The radius of gyration, an estimate of the volume occupied by a polymer chain in solution, is 400-500 Å suggesting that a substrate fiber with surface pores smaller than 1000 Å diameter will be required. Other work focused on coating substrates with poly(diallyldimethylammonium fluoride), DADMAF, and proprietary blends based on high molecular weight poly(vinylalcohol), PVOH (Mw > 100,000). These polymers were also film forming and of similar radius of gyration.

[32]Details of the synthesis of AT polyelectrolytes can be found in U.S. Pat. No. 5,336,298

Table 4-1:
GPC MALLS Molecular Weight Determination of Poly(vinylbenzyltrimethylammonium) and Poly(diallyldimethylammonium) AT Polymers

Reference	Sample	Batch No.	Mw	Mw/Mn	Rg (Å)
13100-17-1	PVBTACl	1	739,000	2.5	463
13371-4A	PVBTAF	1	822,000	3.0	445
13771-4B	PVBTAF	1	841,000	3.0	444
13649-14A	PVBTACl	2	1,270,000	2.5	486
13391-34-2	PVBTAF	2	1,129,000	2.1	461
13100-12-1	DADMACl	1	239,000	4.6	312
13100-13-1	DADMAF	1	343,000	6.8	343

1.2 Solubility of AT Polymers

All the Active Transport polymers are soluble in water to at least 15 wt% polymer. PVBTAF and DADMAF are also soluble in methanol (MeOH) to at least 5 wt% polymer.

1.3 Viscosity of ATM Solutions

The room temperature viscosity of the primary ATM coating solutions (PVBATF/H_2O and PVBTAF/MeOH) was determined using a Brookfield Digital Viscometer. Viscosity was measured for polymer concentrations between 1-35 wt%. Solution viscosity is plotted in Figure 4-1. The measured viscosity is the same for the two solvents indicating that water and methanol are equally good solvents for PVBTAF.

1.4 Wetting Behavior of AT Systems

Wettability can be estimated by measuring the contact angle between the coating solution / solvent and the substrate. Wettability can be inferred if the contact angle is less than 90°.

Figure 4-1
Viscosity of ATM Coating Solutions

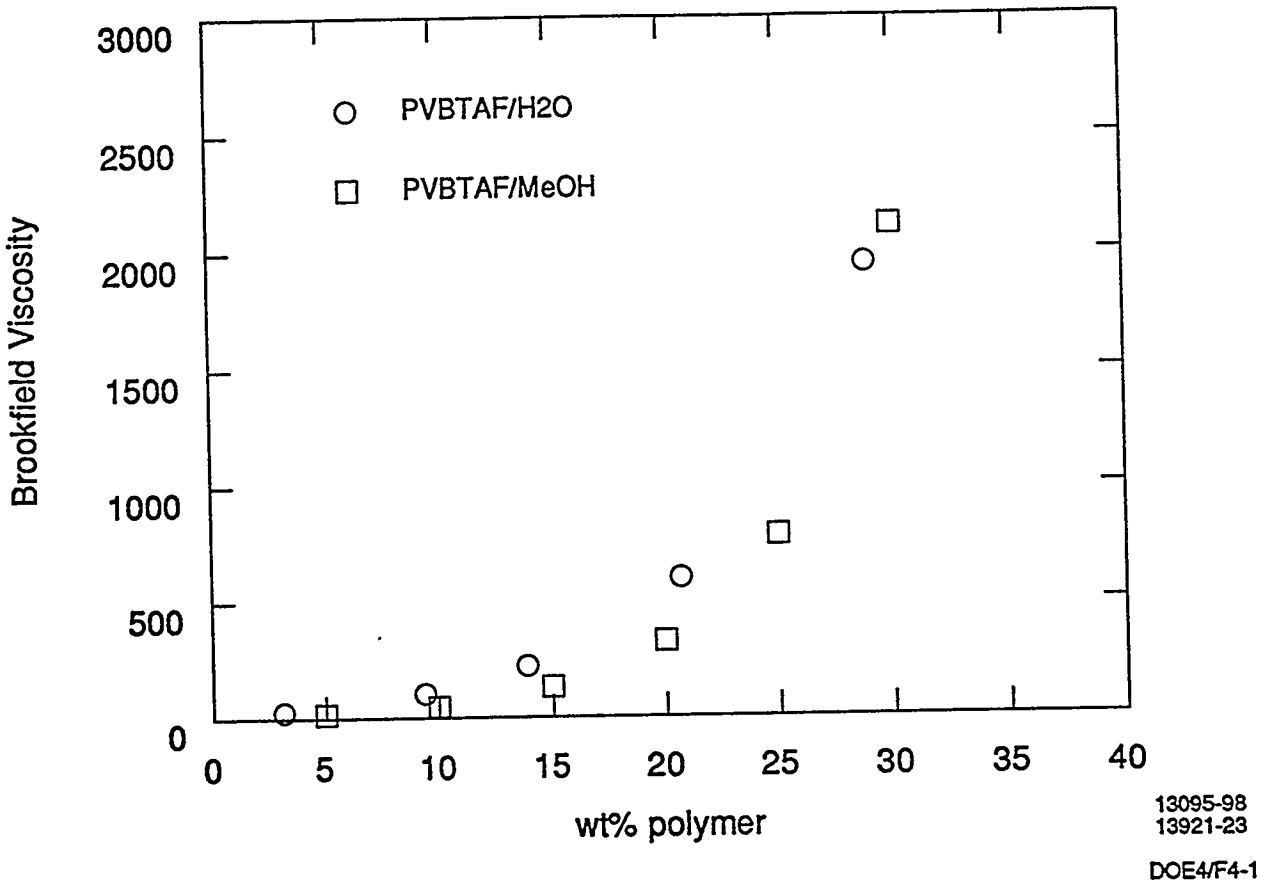

Conversely, the materials are nonwetting if the contact angle is substantially greater than 90°. Several methods for measuring contact angles are given in reference[33]. This work employed two methods to measure the contact angles. In one, the contact angle between coating solvents and dense planar coupon of substrate was measured by the sessile drop technique. The results (Table 4-2) indicate that both solvents wet the substrate.

Table 4-2
Contact Angle of ATM Solvents with Substrate Polymers

	Contact Angle	
Substrate Polymer	**Water**	**Methanol**
polysulfone	≈ 60°	≈55°
PAI	≈50°	≈40°

The *dynamic* contact angle between PAI fibers and ATM solutions was examined by hanging a small section of the dense substrate fiber from a Cahn micro-balance and monitoring the weight change as a function of time while either dipping the fiber into the test solution (advancing angle) or pulling the fiber out of the solution(receding angle). A dense rather than microporous substrate was used to prevent wicking of the solution into the pore wall. The fiber end contacting the polymer solution was sealed in an epoxy resin to prevent capillary rise of the solution into the fiber bore. In this study, the solutions were 1 wt% PVBTAF in water or in methanol. The surface tension of the ATM solutions was 70 and 23 dynes/cm, respectively - slightly lower from the pure solvent values of 72.6 and 24.0 dynes/cm. The dynamic contact angles were calculated from the surface tension of the solution, the surface area of the fiber, and the weight change upon contact with the solution.

Results are summarized in Table 4-3. Contact angles are less than 90 degree suggesting that PVBATF should coat PAI fiber. In reality a porous PAI substrate will be used. In that case the surface porosity of the substrate fiber should reduce the contact angle and therefore enhance the coatability.

[33]A.W. Adamson, "Physical Chemistry of Surfaces"3rd ed., J. Wiley & Sons, New York (1976).

Table 4-3

Dynamic Contact Angle Between ATM Coating Solutions and PAI Fiber

Contact angle	PVBTAF/H_2O	PVBTAF/MeOH
Advancing	65.0°	50.0°
Receding	50.7°	44.5°

2.0 Coatability of Planar Substrate Coupons

The coatability of polysulfone and PAI with PVBTAF was investigated by fabricating small laboratory test coupons (flat sheet membranes about 2 inches in diameter) for screening studies. The microporous polysulfone support membrane was made by a proprietary process. Microporous PAI support membranes were produced via phase inversion technology using the spin dope formulations described in Chapter 3. Membranes were examined using optical or electron microscopy and were also evaluated for permselectivity. The surface pores of the uncoated PAI support ranged from 300Å to 1000Å in diameter; its N_2 permeance was ≥70 x 10^{-6} $cm^3/cm^2 \cdot s \cdot cmHg$. The N_2 permeance of the planar polysulfone membrane was ≥ 100 x 10^{-6} $cm^3/cm^2 \cdot s \cdot cmHg$. PVBTAF composite membranes were fabricated and evaluated as described previously[29]. In general, adhesion between PVBTAF and the substrates was good, however, some delamination occurred at extremely low humidity (P/Po<0.05). Representative screening results are shown in Tables 4-4 and 4-5.

Table 4-4 : Permselectivity of a PVBTAF/Polysulfone Flat Sheet Composite Membrane as a Function of CO_2 Pressure (12484-76B)

Feed Pressure (psig)#	P_{CO_2} (cmHg)	P/l CO_2(x 10^6)*	$\alpha CO_2/H_2$	$\alpha CO_2/CH_4$
5.3	31.7	6.02	87	1024**
20.0	55.0	4.51	82	765**
40.0	86.7	3.78	71	640**
61.1	120.1	3.19	48	540**
75.6	143.1	2.88	43	490

# feed mix: 30% CO_2/34% CH_4/36%H_2
Temp=23°C; P/Po=0.31
* units of $cm^3/cm^2 \cdot s \cdot cmHg$
** no CH_4 detected in permeate; selectivity estimated from observed CH_4 permeance at 75.6 psig

Table 4-5: Permselectivity of a PVBTAF/PAI Planar Coupon as a Function of CO_2 Pressure (12484-82)

Reference	Feed Pressure (psig)#	P_{CO_2} (cmHg)	P/l CO_2 (x 10^6) *	$\alpha CO_2/H_2$	$\alpha CO_2/CH_4$
uncoated PAI #1	15	51	1030	1.2	1.0
PVBTAF-coated	39.7	93.2	1.38	48	>150**
	102.5	201	0.915	33	>100**
uncoated PAI #2	39.0	92.3	70	0.63	0.91
PVBTAF-coated	39.0	92.3	3.05	50	>300**
	99.0	196	0.804	10	>85**

# feed mix: 33% CO_2/33% H_2/34%CH_4
Temp=23°c;P/Po=0.31
* units of $cm^3/cm^2 \cdot s \cdot cmHg$
**no CH_4 detected in permeate; selectivity estimated from detection limits of gas chromatograph

These results demonstrate that it is possible to coat both polysulfone and PAI flat sheets with PVBTAF and that good permselectivity can be achieved. The facilitated transport aspect of the membranes is maintained as evidenced by the pressure dependent nature of the permselectivity.

3.0 Hollow Fiber Module Fabrication and Evaluation

3.1 Dip Coating Procedures

Microporous and dense hollow fiber substrates were coated with ATM polyelectrolytes by dip coating techniques. Dip coating is a batch process which simulates the elementary steps of a continuous meniscus coating operation. The elements of the dip coating process are shown schematically in Figure 4-3. First, the bottom of the fiber was either heat sealed or pinched closed to prevent penetration of the coating solution into the bore and the fiber was immersed into the coating bath containing 0.5-10 wt% ATM polymer for ≈15 sec. Coating solution was deposited on the fiber as it was withdrawn from the bath at a constant rate. An equilibrium liquid film thickness was established which depended on the viscosity of the coating solution, the contact angle between the coating solution and the fiber, the surface tension of the liquid, the rate at which the fiber is drawn from the solution, and the fiber diameter. The coated fiber was hung to complete solvent evaporation and a dry coating was formed. Next an overcoat of a silicone rubber-like material (e.g. 1 wt% Sylgard 184 in isopentane or 1 wt% Petrarch PS254 in methylene chloride) was deposited by the same procedure. For comparison, a continuous coating process is shown in Figure 4-4. The coated fibers were stored at room temperature in a relative humidity of 20-40%.

The Deryaguin coating model, i.e. mathematical relationship between the various coating parameters described above, is shown in equation 1. This relationship is valid for nonporous substrates when the capillary number (Un/S) is in the range 10^{-5} - 10^{-2} .[34,35]

Equation 1: $$h/R = 1.33\ (Un/S)^{2/3}$$

where h = liquid film coating thickness
R = fiber radius
U = fiber velocity
n = coating solution viscosity
S = surface tension of the coating liquid

Recently, Tsai et. al. have accounted for deviations from the Deryaguin model when microporous substrates are used. They postulated that capillary suction of solvent into the

[34]B.V. Deryaguin, ***Acta Physicochim***, 20, 349 (1945).
[35]D. Quere, J-M. Di Meglio and F. Brochard-Wyart, ***Science***, 249, 1256 (1990).

Figure 4-3
Schematic Representation of a Dip Coating Process

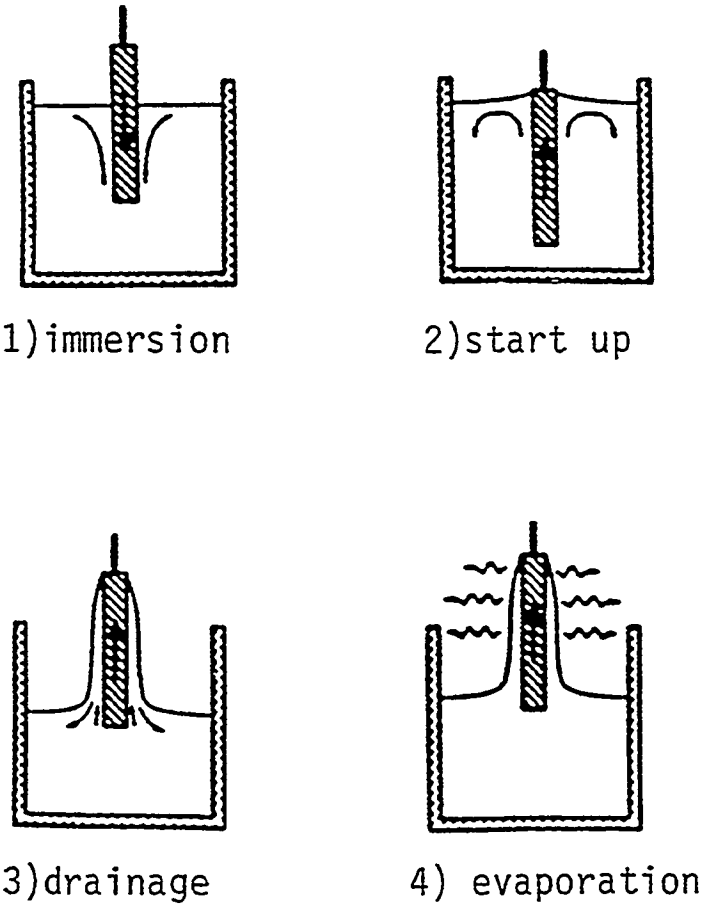

Figure 4-4

Schematic representation of a Continuous Meniscus Coating Process

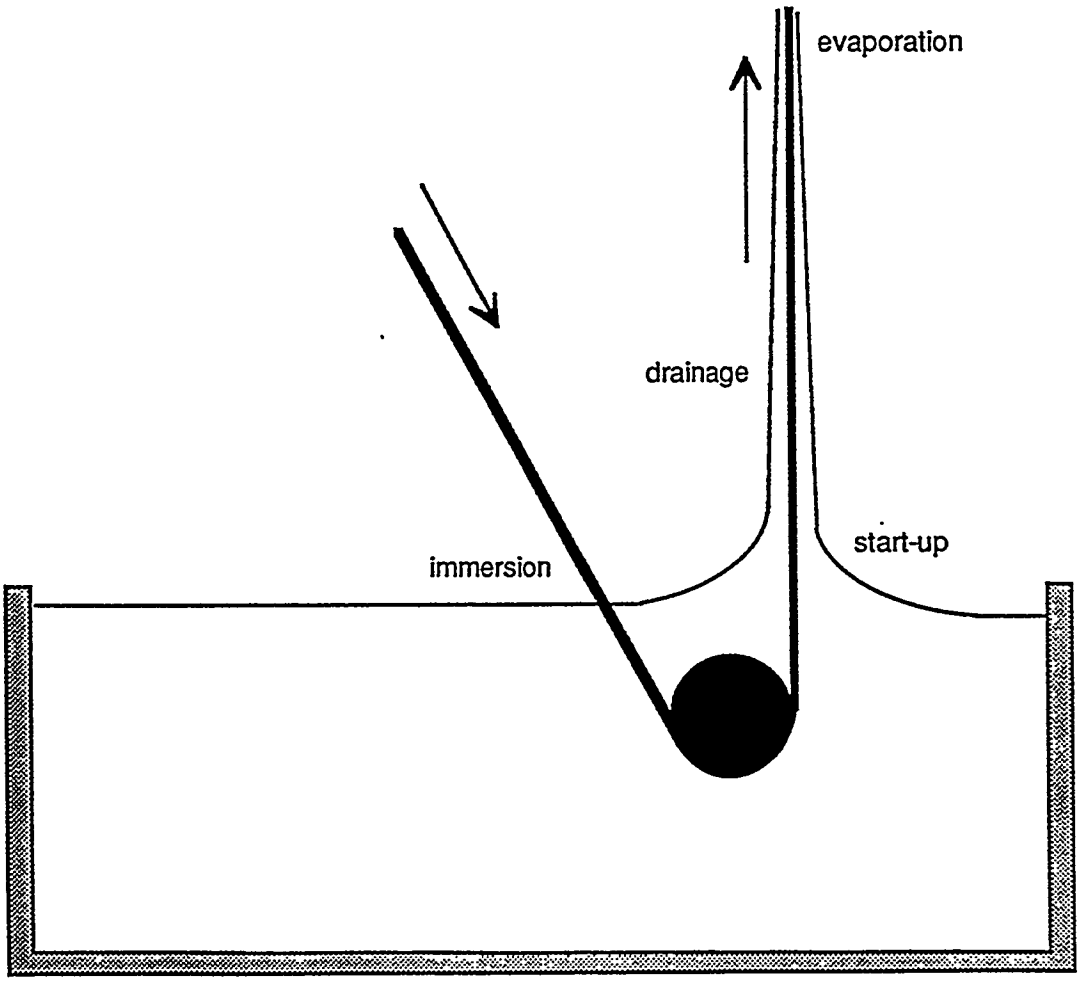

pores of substrates results in a localized viscosity increase near the fiber surface. Thus, the wet film thickness on microporous substrates is greater than if a nonporous substrate is used. This refined Deryaguin model requires knowledge of the equilibrium capacity and the kinetics of solvent absorption by the fiber.

The various support fibers used in this work were coated from aqueous or methanolic solutions containing 0.5 - 10 wt% Active Transport polymer. The ratio of wet film thickness to fiber radius (h/R), estimated from the Deryaguin model, ranged from 0.004 to 0.02. (There is currently insufficient information to apply the refined Deryaguin model.) Lab-scale modules, containing between 1 and 50 nine inch long fibers, were fabricated by potting a fiber bundle into a stainless steel housing as shown in Figure 4-5. Feed gas was circulated on the shell side. The active fiber length was nominally taken as 9" in all modules although small variations between modules were likely. In most experiments the bore, or fiber lumen, was swept with an inert gas (helium or nitrogen) in order to facilitate detection of the permeating species by a gas chromatograph. Details of the experimental procedures can be found in previous reports.[28,29]

3.2 Results and Discussion - PVBTAF Coated Commercial Substrates

3.2.1 Membrane Characterization

Substrate Characterization

This phase of the work used two types of commercial polysulfone hollow fiber substrates which are here designated SUB1 and SUB2 (substrate 1 and substrate 2). Both fibers were asymmetric with a very thin dense skin on the shell-side of the fiber. The fibers differed in their wall and skin thickness. For example, the wall of SUB1 was approximately twice that of SUB2. It is important to note that neither fiber was optimized for use as a thin film composite substrate. In addition, the fibers were found to contain manufacturing flaws or defects which include small amounts of surface debris and gouges in the skin (Figures 4-6).

Characterization of the Composite Hollow Fiber Membrane

Scanning Electron Microscopy (SEM) was the primary characterization tool. The only procedure which produced a sharp cross-section was one in which the sample was frozen in liquid nitrogen and then gently fractured. However, the coatings of samples prepared even by this method often delaminated making it difficult to consistently obtain meaningful cross-

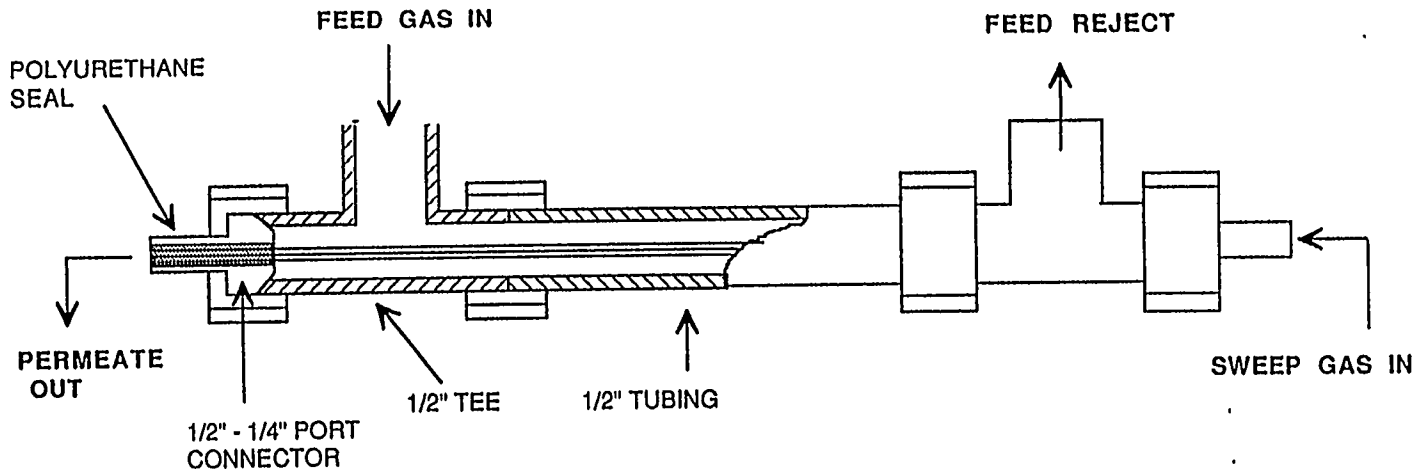

Figure 4-5
Lab-Module Potting Arrangement

Figure 4-6

Apparent Manufacturing Defects of SUB1 and SUB2 Substrates

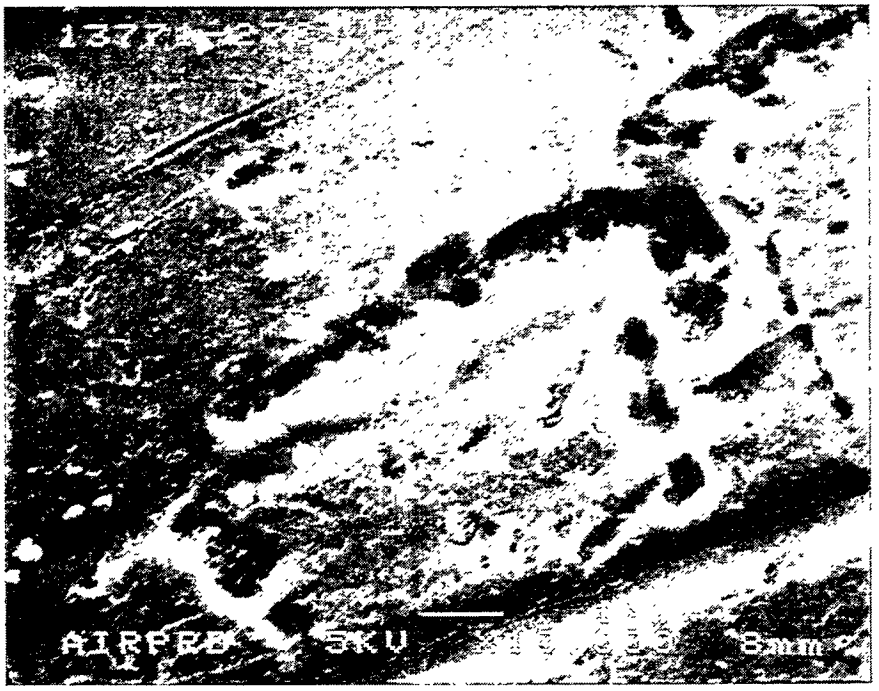

Figure 4-7

Representative Cross-section of ATM-coated SUB1

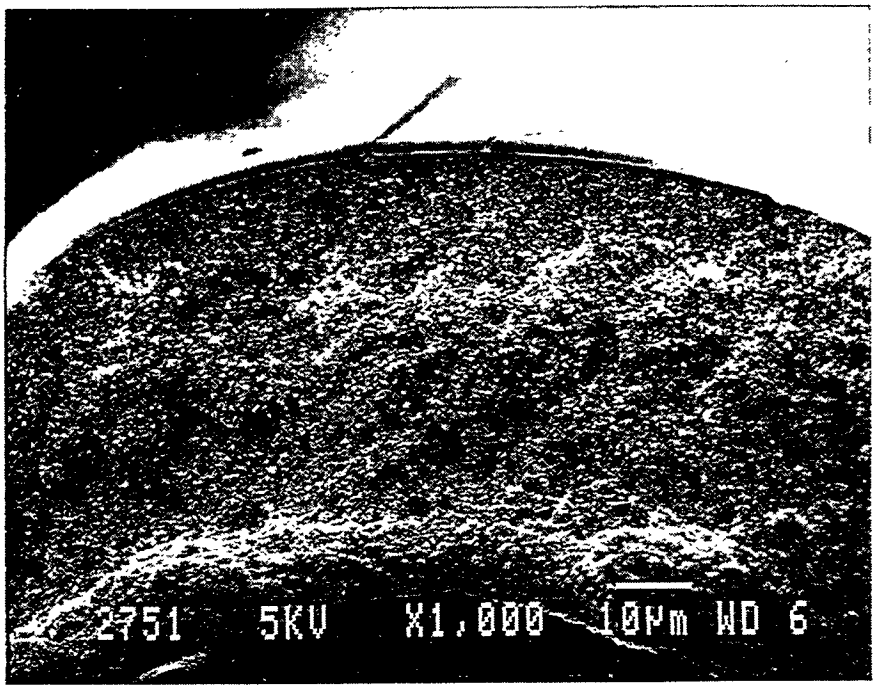

section analysis. The ATM layer was usually found to be between 2 and 10 μm thick (Figure 4-7).

3.2.2 Permselectivity Evaluation

Modules were evaluated for CO_2, CH_4 and, in some cases, H_2 permselectivity in a mixed gas, flowing test system similar to those described earlier.[29] The water content of the feed and sweep gases as a critical experimental parameter[36]. Therefore, the test system incorporated a means to vary the hydration level of the feed and sweep streams from P/Po≈ 0.2 to P/Po≈0.8 where, P is the H_2O vapor pressure at the hydrating bubbler temperature and Po is the vapor pressure of H_2O in equilibrium with liquid water at the temperature of the membrane. Chilled mirror hygrometers (General Eastern Corp.) were used to measure the dew point of the gas feed and permeate but it was not possible to obtain an accurate mass balance of H_2O by this method.

The permeance (P/ℓ) of the various components was calculated using the known or experimentally determined parameters from the equation:

$$(P/\ell)_i = F_i / A \bullet \Delta P_i$$

and the set of simultaneous linear equations:

$$[i] = F_i / \Sigma F_i$$

where

Fi = flow rate of permeating species i
A = membrane area, based on the OD of the uncoated substrate fiber
ΔP_i = partial pressure driving force of species i = P_i (feed source) - P_i (bulk permeate)
[i] = concentration of species i as determined by gas chromatography
ΣF_i = total species flow rate in the N_2-swept permeate stream

[36]For a full discussion of this effect see Section V.1.0 of this report.

The calculated permeance is that of the module under the given set of experimental conditions. A model which would (1) derive the composite membrane properties from the experimentally determined module properties and also (2) derive the intrinsic AT layer properties from the composite properties does not exist at this time. This treatment of the data penalizes the module to some degree since experimental data was often taken under non-zero recovery of CO_2; that is, only 1-15% of the CO_2 in the feed gas was allowed to permeate the membrane. In most cases however, the membranes were operated under zero recovery of H_2O.

More than 40 PVBTAF-coated SUB1 and SUB2-based modules were fabricated and evaluated. A summary of results is provided in Table 4-6. Early attempts at fiber coating and module fabrication used SUB2 fiber and were not very successful. Eventually, modules utilizing both Sub1 and Sub2 were successfully fabricated and evaluated. Specific examples illustrating important concepts or results are detailed below.

• P/l CO_2 and $\alpha CO_2/CH_4$ as a function of CO_2 Partial Pressure [13074-67C]

A commercial ATM will have to operate near natural gas well-head pressures (about 1000 psi). These conditions were simulated in the test equipment. The SUB1-based hollow fiber ATM was evaluated as a function of total feed gas pressure up to about 800 psig while the permeate pressure was maintained at approximately 15 psia. The results are shown in Figure 4-8. Because CO_2 is transported via a chemically-assisted pathway, its permeance is pressure dependent and is highest at low CO_2 feed partial pressures. Its value depends not solely on the partial pressure difference but on the specific value of the partial pressures[3,28]. Methane is transported via a Henry's Law solution-diffusion pathway and hence, its permeance is independent of pressure. Thus, the $\alpha(CO_2/CH_4)$ also varies with CO_2 feed pressure. The most important conclusion from this study is that the composite hollow fiber module is dimensionally stable at high pressure. In the extreme, the transmembrane pressure was almost 800 psi. At high CO_2 partial pressure, where the chemically-assisted pathway is saturated, $\alpha(CO_2/CH_4)$ was ≈ 75 which is 3-4 times higher than the pure component selectivity of most polymer membranes at < 100 psig.

PVBTAF-coated SUB1 Fibers
25% CO_2, 25% CH_4, 50% H_2 @ 75 sccm

Reference #	P/Po	cmHg CO2	P/l CO2	CO2/CH4	T on Stream	Comments
13074-67C	0.27	69	2.98	366	13 days	
	0.27	156	1.87	200		
	0.27	291	1.12	147		
	0.27	416	0.929	126		
	0.27	544	0.757	111		
	0.27	681	0.629	91.5		
	0.27	806	0.549	84.5		
	0.27	949	0.463	76.1		
	0.27	1072	0.399	71.3		
	0.27	1105	0.480	73.3		no sweep
	0.27	699	0.609	87.6		no sweep
	0.27	348	1.111	146		no sweep
	0.27	153	1.60	201		no sweep
	0.27	70	1.69	265		no sweep
	0.27	68	2.54	364		
	0.27	71	1.65	216		no sweep
	0.27	84	0.424	1.8		after H2S testing
13074-88A	0.28	79	2.00	221	8 days	20 sccm feed
	0.28	143	1.55	135		20 sccm feed
	0.28	147	1.60	151		
	0.28	541	0.669	48.2		
	0.28	815	0.505	32.9		
13399-40	0.34	96	3.493	108	4.5 days	
	0.24	93	2.702	134		
	0.49	93	4.445	57.6		
13399-41	0.34	96	3.829	134	5 days	
	0.24	96	2.735	202		
	0.17	92	1.871	252		
	0.23	92	2.300	257		

Table 4-6

Summary: Permselectivity of PVBTAF-coated SUB1 and SUB2 Modules

Reference #	P/Po	cmHg CO2	P/l CO2	CO2/CH4	T on Stream	Comments
13921-24	0.27	100	0.98	300	48 days	H2S -free (25% CO2 in CH4)
lifetime test	0.27	100	0.87	280		0.3& H2S, unstable
	0.27	114	0.49	150		3% H2S
	0.27	100	0.50	260		H2S-free
13921-25	0.27	100	2.20	250	48 days	H2S -free (25% CO2 in CH4)
	0.27	100	1.75	245		0.3& H2S, unstable
	0.27	114	0.92	150		3% H2S
	0.27	100	1.05	210		H2S-free
13921-45	0.27	52	0.47	144		
	0.20	53	0.27	111		
	0.15	52	0.19	72		
13921-54	0.27	53	1.80	316	12 days	feed : 10% CO2 in CH4
	0.39	53	2.68	164		
	0.53	53	3.83	75		
	0.72	53	5.75	43		
	0.27	53	2.08	273		
	0.19	53	1.49	351		
	0.15	53	1.04	356		
	0.09	53	0.64	134		
	0.27	53	2.04	212		

Table 4-6 (cont'd)

PVBTAF-Coated SUB2 Fibers
(coatings are PDMS/PVBTAF onless otherwise stated)
feed gas is generally 25%CO2/, 25%CH4, 50% H2

Reference #	P/Po	cmHg CO2	P/l CO2	CO2/CH4	T on Stream	Comments
12577-97B	0.16	55	1237	0.9	1 day	no coating
	0.16	58	85.0	1.0		no PDMS
MOD I	0.18	61	809	0.9	1.5 days	no coating
	0.38	59	8.03	28.3		2 PVBTAF dips/no PDMS
MOD III					0.5 days	potted in septa
MOD IV	0.34	57	6.89	22.5	1 day	potted in septa; PVBTAF only
	0.34	58	6.29	18.2		PVBTAF+PDMS
13074-1	0.36	59	18.3	1.7	2 days	
	0.36	59	5.91	22.3		PVBTAF repair
13074-3B	0.38	63	5.56	60.5	1.5 days	
	0.38	59	4.27	55.3		
	0.38	57	4.21	57.0		195 sccm feed
13074-3C	0.38	66	4.58	42.3	1.5 days	
	0.38	62	7.34	57.9		195 sccm feed
	0.38	62	4.92	37.6		
	0.38	71	4.24	11.6		
13074-13G	0.38	65	4.46	32.9	1 day	
	0.38	67	2.17	19.7		20 sccm feed
13074-17B	0.38	65	3.77	44.8	3.5 days	
	0.38	65	3.26	39.5		20 sccm feed
	0.38	65	3.31	41.5		
13074-23B	0.38	63	4.50	44.0	0.5 days	

Table 4-6 (cont'd)

Reference #	P/Po	cmHg CO2	P/l CO2	CO2/CH4	T on Stream	Comments
13074-23C	0.38	62	13.76	1.6	0.5 days	
13074-23D	0.38	62	206	1.0	0.5 days	
13074-23E	0.38	62	4.79	7.0	0.5 days	
	0.38	62	3.85	2.0		
13074-26B	0.38	62	3.37	14.3	0.5 days	13074-23D recoat
13074-29B	0.38	62	5.36	10.2	0.5 days	
13074-29C	0.38	65	4.78	200	2 days	
	0.38	65	4.29	315		20 sccm feed
	0.38	65	4.63	226		
	0.27	65	3.45	78.4		
	0.27	65	3.27	276		20 sccm feed
13074-31B	0.38	62	4.23	3.4	0.5 days	13074-29C recoat
	0.38	62	14.0	1.5		
13074-35A	0.38	62	4.08	10.0	0.5 days	
	0.38	65	6.23	8.9		13074-35A recoat
13074-35C	0.38	62	3.74	235	6 days	
	0.38	62	3.41	238		20 sccm feed
	0.52	62	5.88	60.4		20 sccm fedd
	0.38	62	3.55	223		20 sccm feed
	0.27	62	2.75	289		20 sccm feed
	0.27	95	2.30	366		20 sccm feed
	0.38	97	3.13	179		
	0.38	98	2.72	210		20 sccm feed
13074-35C-2	0.27	67	0.0239	---	1 day	retest after H2S exposure
	0.27	150	0.0103	----		
13074-40C	0.38	63	2.37	37.3	1 day	5" fiber
	0.38	65	2.15	36.7		5" fiber; 20 sccm feed
13074-42C	0.38	65	1.78	98.0	0.5 days	
			4.40	86.7		

Table 4-6 (cont'd)

Reference #	P/Po	cmHg CO2	P/l CO2	CO2/CH4	T on Stream	Comments
13074-42D	0.38	65	1.22	30.9	0.5 days	
13074-43C	0.38	65	4.35	37.3	2 days	
	0.38	65	3.33	60.9		polyurethane fill to ends
	0.27	65	2.08	78.0		
13074-49D	0.38	63	5.96	194	15 days	
	0.27	63	4.43	512		
	0.27	95	3.69	316		
	0.27	135	3.05	275		
	0.27	180	2.50	240		
	0.27	214	2.20	219		
	0.27	215	2.11	221		
	0.24	215	1.76	243		
	0.24	215	1.76	251		
	0.24	180	1.98	309		
	0.24	137	2.35	400		
	0.24	92	2.97	577		
	0.24	68	2.91	574		
	0.27	65	3.42	460		
	0.31	65	3.86	328		
	0.38	65	5.22	222		
13074-51C	0.27	71	2.05	195	13 days	
	0.38	70	3.25	142		
	0.24	71	1.77	171		
	0.27	152	1.44	124		
	0.27	217	1.14	80.7		
	0.27	286	0.895	58.8		
	0.27	418	0.773	47.0		180 sscm feed
	0.27	418	0.687	42.1		
	0.27	555	0.584	33.2		
	0.27	570	0.541	32		20 sccm feed
	0.27	689	0.463	27		
	0.27	822	0.404	9.5		

Table 4-6 (cont'd)

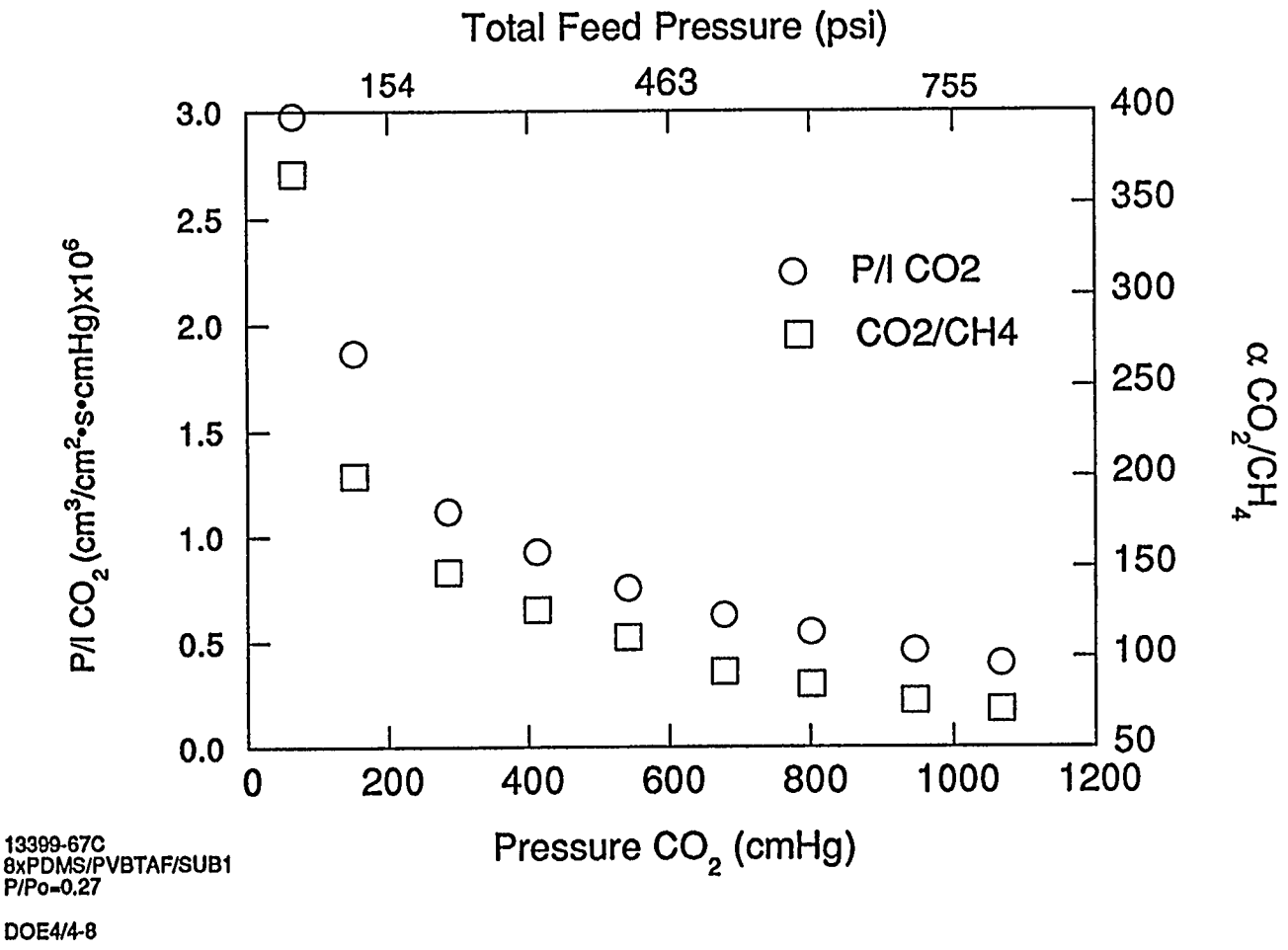

Figure 4-8
Effect of Feed Pressure on Performance

• Effect of Fiber Strength on Membrane Integrity [13074-51C]

The effect of support fiber strength is shown in Figure 4-9. In this experiment, a PDMS/PVBTAF ATM was supported on SUB2 fiber. The feed pressure was incrementally raised to about 800 psig. Permselectivity parallels that of a SUB1-based ATM at low feed pressures. However, at ≈ 600 psig, the support fiber begins to collapse and membrane integrity is compromised. The composite failed completely at feed pressures greater than 650 psig. As the wall thickness of SUB2 is only about 50% that of SUB1, it is not surprising that this failure occurred. This result indicates the need to maintain the proper support fiber wall thickness to fiber OD ratio for high pressure operation.

• Effect of Bore-side Sweep Gas on Performance [13074-67C]

In order to maintain the largest driving force, the preferred mode of operating an Active Transport membrane is to sweep the fiber lumen with a diluent. However, it may not always be either technically or economically feasible to provide this option. Therefore, the performance of the hollow fiber composite module was evaluated without a permeate sweep gas. In this test, the permeate gases were collected at 15 psia and, downstream of the membrane, diluted with helium and analyzed. As expected (Figure 4-10), the lack of sweep gas only affects permselectivity at low CO_2 partial pressures. The CO_2 permeance of the non-facilitated (Henry's Law) pathway depends only on the absolute value of the CO_2 pressure difference and is not affected in the high pressure regime, where the Henry's Law pathway dominates. On the other hand, the chemical (facilitated) transport pathway dominates at low CO_2 feed pressures. The CO_2 permeance in this regime depends on the absolute values of the CO_2 partial pressure in the feed and permeate streams. Therefore, this regime shows a deviation in performance.

• P/l CO_2 and $\alpha CO_2/CH_4$ as a function of P/Po [13921-54]

The ATM materials development program identified a strong dependence of performance on the water content of the gas streams. This dependence was evaluated for PDMS/PVBTAF/SUB1 hollow fiber lab modules by varying the water content, as defined by P/Po, of both the feed and sweep gas streams. The partial pressure of CO_2 in the feed stream was maintained at 53 cmHg. All other experimental parameters were held constant. Data was recorded at increasing P/Po from 0.27 to 0.72, then performance at the lower values of P/Po was investigated. Finally, the membrane was returned to the original conditions and

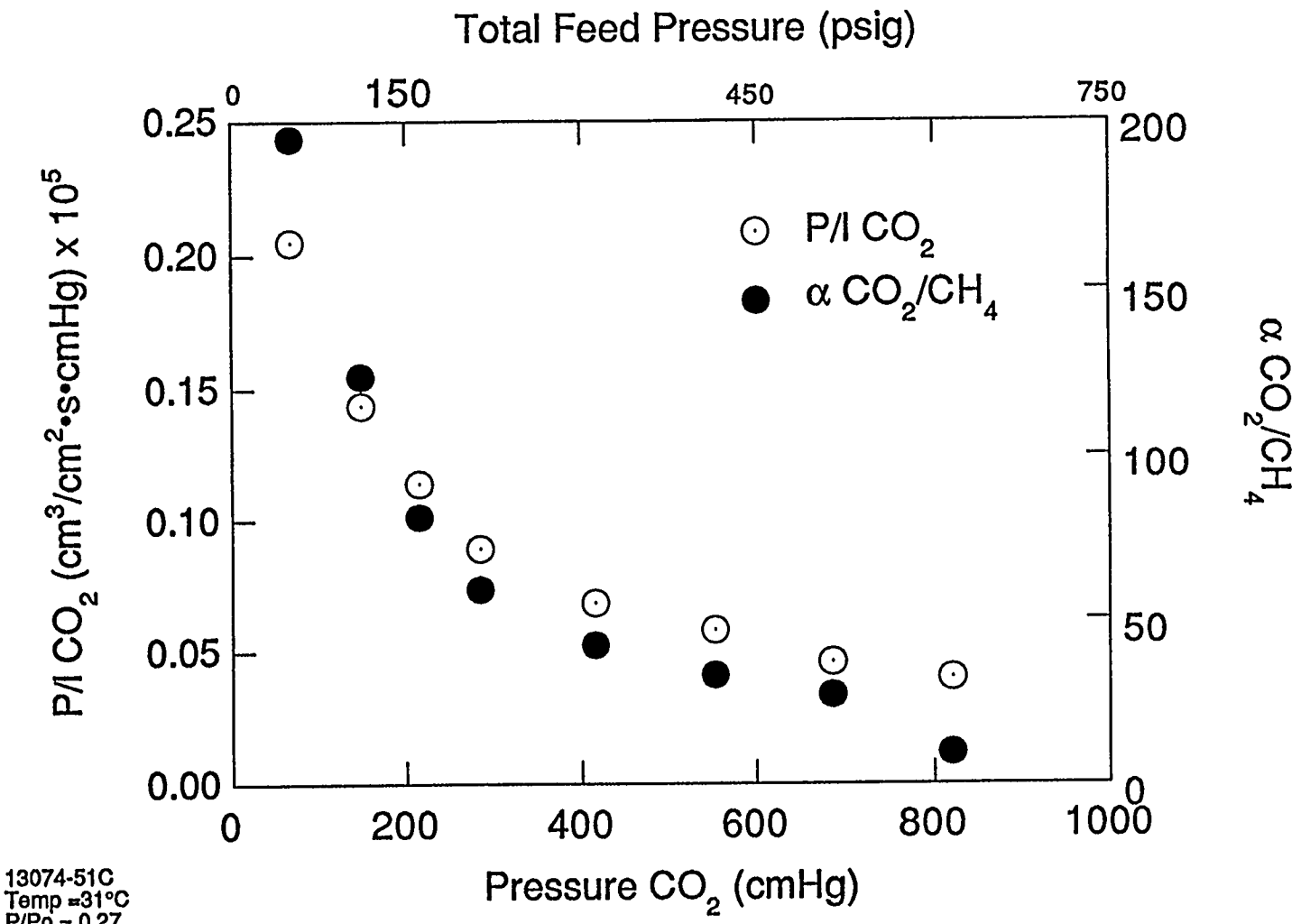

Figure 4-9
Performance on SUB2 Substrate

Figure 4-10

Performance Comparison: Bore-Side Sweep vs. No Sweep

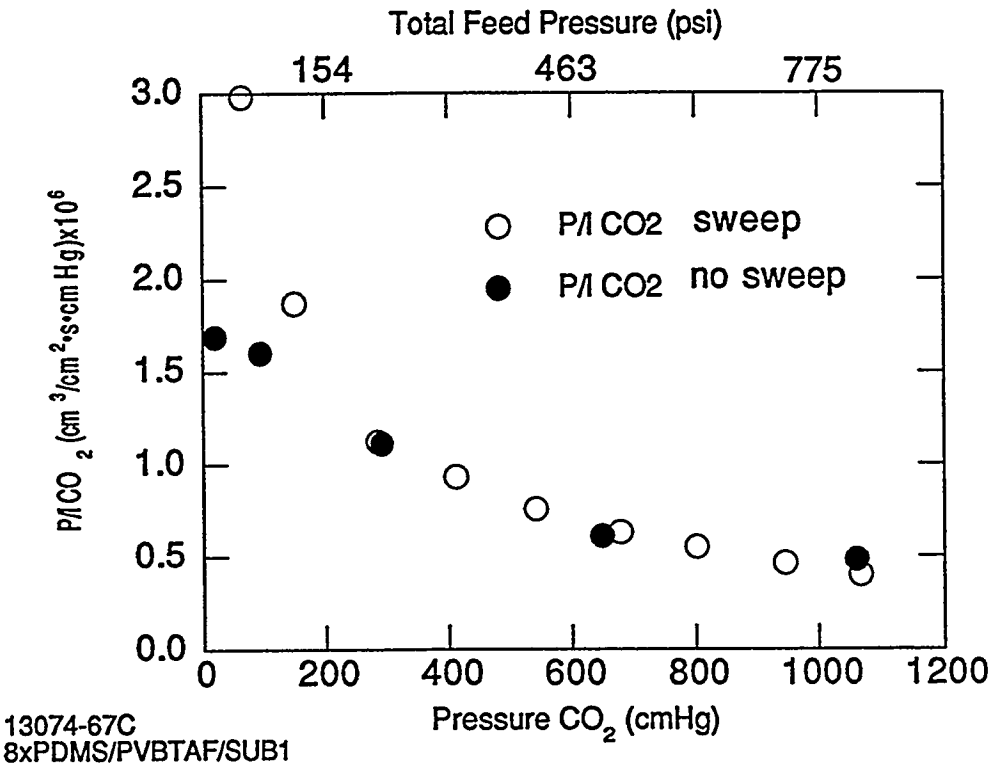

13074-67C
8xPDMS/PVBTAF/SUB1
P/Po=0.27

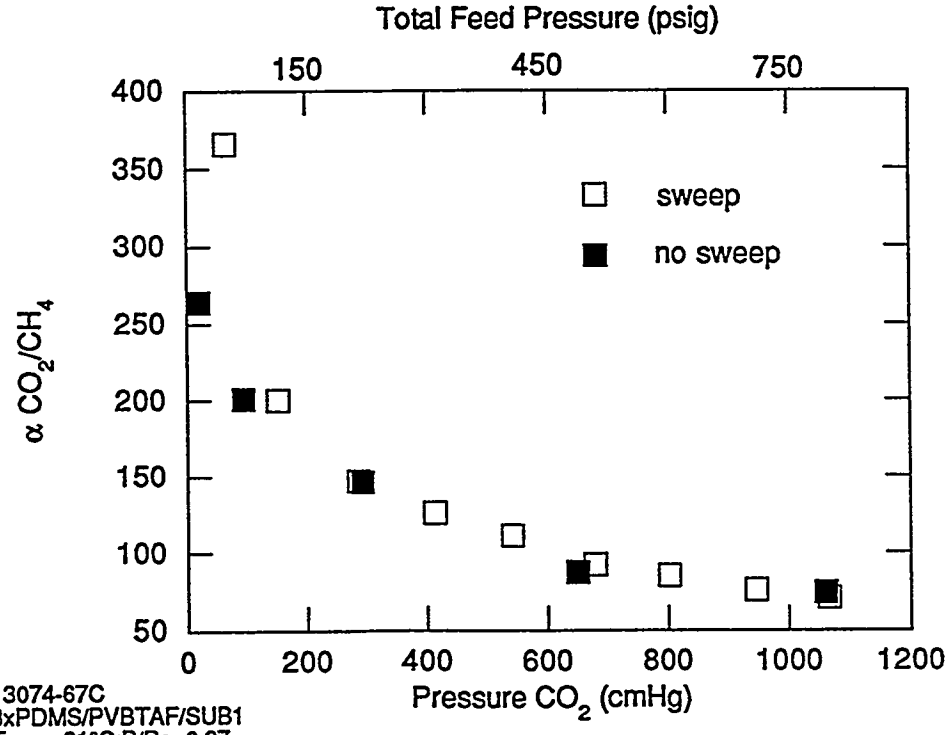

13074-67C
8xPDMS/PVBTAF/SUB1
Temp=31°C;P/Po=0.27
25%CO2/25%CH4/50%H2 @ 75sccm

the data (represented by the filled symbols) was recorded. Results are shown in Figure 4-11. The CO_2 permeance increases linearly with increasing P/Po in the range $0.1 < P/Po < 0.75$. The selectivity however, passes through a maximum. Figure 4-11 defines three regimes of membrane performance. At $P/Po \leq 0.1$ both the CO_2 permeance and the selectivity are low because strong ionic intermolecular forces maintain a "tight" polymer network which inhibits diffusion of all gases. Additionally, a low water content in essence "shuts down" the chemical transport pathway in which H_2O is a reactant. An optimal regime exists in the P/Po range of 0.15 - 0.35. The CO_2/CH_4 selectivity is maximized with a moderate CO_2 permeance. At higher P/Po, excess water retards the chemical pathway and plasticizes the membrane. Thus, the flux of all gases is high and the membrane is nonselective. This aspect of ATMs is discussed in greater detail in Chapter V.

• Effect of Higher Membrane Temperature on Performance at Constant P/Po

It was found that membrane temperature can have significant effect on performance. A PDMS/PVBTAF/SUB1 module was evaluated at two temperatures, 31°C and 50°C while all other experimental parameters, including P/Po were constant. A modest 20°C temperature rise increased the observed CO_2 permeance ≈185%. Moreover, the selectivity also increased. For comparison, conventional polymeric membranes (non ATMs) usually exhibit increased permeance but decreased selectivity at higher temperatures. The results (Table 4-7) suggest better economics might be achieved if the membrane could be operated at ≈50°C. Additional experimental work is needed to define the upper temperature limit.

Table 4-7: Temperature Dependence of Permselectivity

Membrane	P/Po	P/ℓ CO_2 ($cm^3/cm^2 \cdot s \cdot cmHg \times 10^6$)	$\alpha CO_2/CH_4$
31°C	0.23	3.41	185
50°C	0.23	6.27	254

conditions: 18 cmHg CO_2

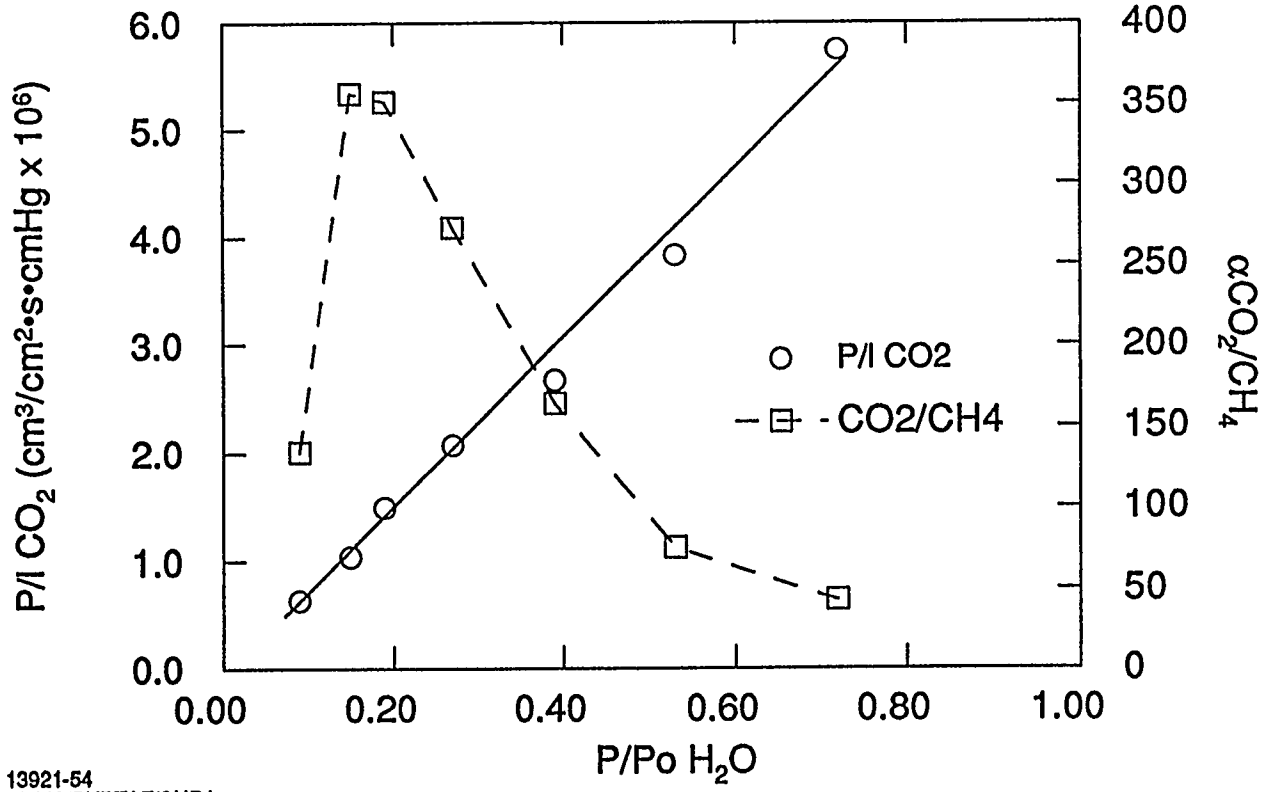

Figure 4-11
Effect of P/Po on Performance

• Lifetime / Stability Testing and Sensitivity to H_2S-containing Gas Streams

Two types of lifetime/stability testing were investigated. In the first, a module was evaluated over a set of conditions, usually increasing feed pressure, and then re-evaluated under conditions similar to those used early in the experiment. The results of such a study are shown in Figure 4-12. After evaluation at 800 psi, the module was retested at low pressure. The results from the retest are shown in solid symbols. The original results are reproduced and, hence, the module is stable to at least limited pressure cycling. In addition, this evaluation spanned 14 days of continuous operation.

The second type of evaluation comprised a lifetime study at constant conditions for a specified period of time in order to evaluate flux creep or degradation. Additionally, various levels of H_2S, a common co-contaminant in natural gas, was also added to the feed gas to evaluate its effect on performance. Results are shown in Figure 4-13. For the first 14 days, the feed gas contained only CO_2 and CH_4. After an induction period, a steady state is reached. For days 14 - 27, a feed gas containing 2900 ppm H_2S was used. The CO_2 permeance began to decline but appeared to stabilize at about 75% of the original value. For days 28 - 36, a feed gas containing 3% H_2S was used. Again, the CO_2 permanence decreased significantly and appeared to stabilize at about 45% of the original value. There are at least two reasons for this effect. First, like CO_2, H_2S is an acid gas and competes with CO_2 for the same acid-gas reactive sites in the ATM. This competition reduces the CO_2 flux and, as a result, the CO_2/CH_4 selectivity is also reduced. The H_2S/CO_2 selectivity at this point was 10. Second, H_2S, or trace contaminants in the H_2S may react with the membrane. This reaction may involve irreversible binding to the active sites or crosslinking of the polymer network. The data from days 38 - 45 suggest both mechanisms may be operative since a return to an H_2S-free stream did not restore the CO_2 flux but did restore some of the CO_2/CH_4 selectivity. The conclusion from this study is that H_2S (or H_2S contaminant) has some detrimental and irreversible or long-lived effect on permselectivity but that a meta-stable state is achieved, the permeance of which is dependent upon the H_2S concentration.

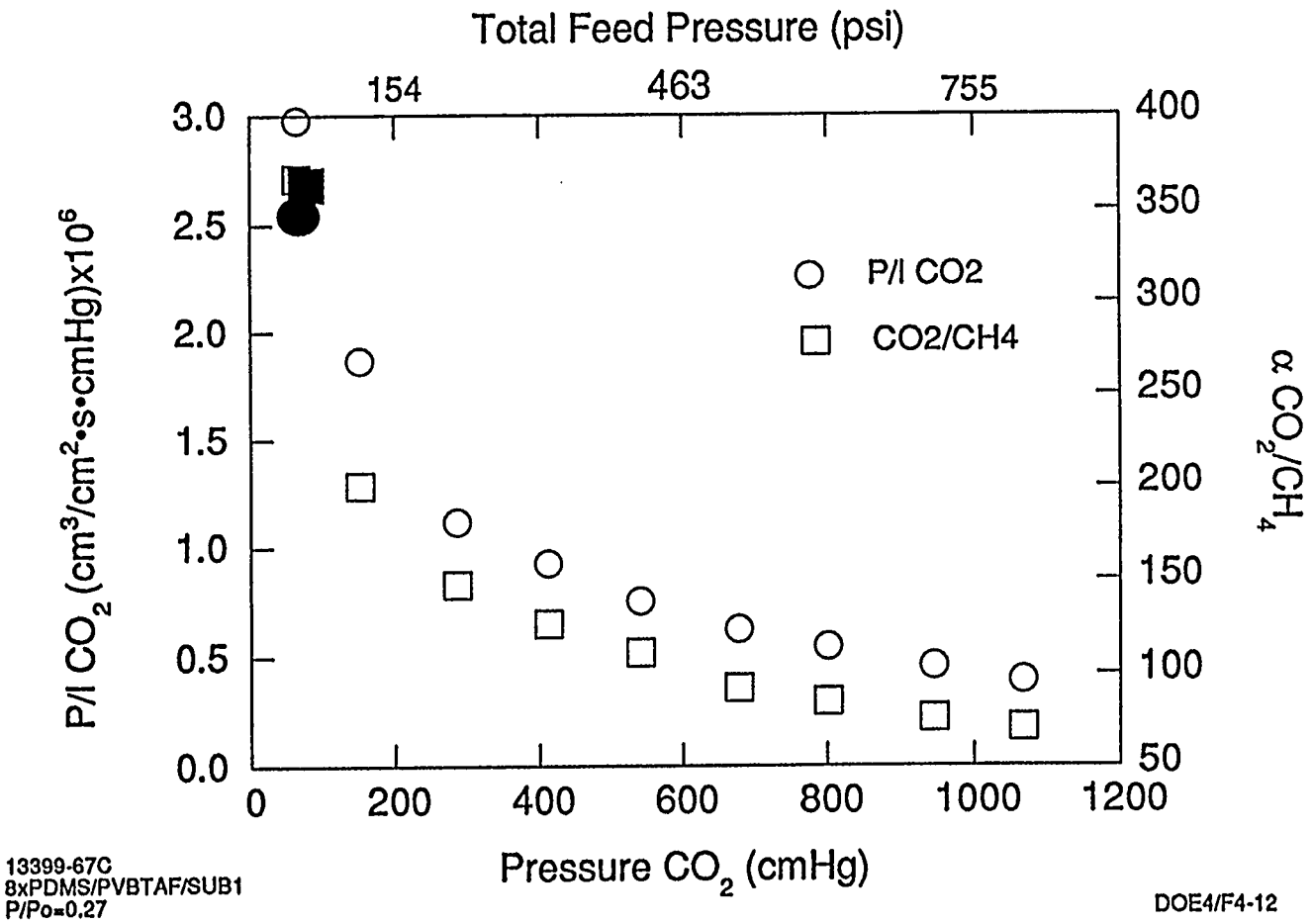

Figure 4-12:
Stability of Lab-Scale Hollow Fiber ATM Modules

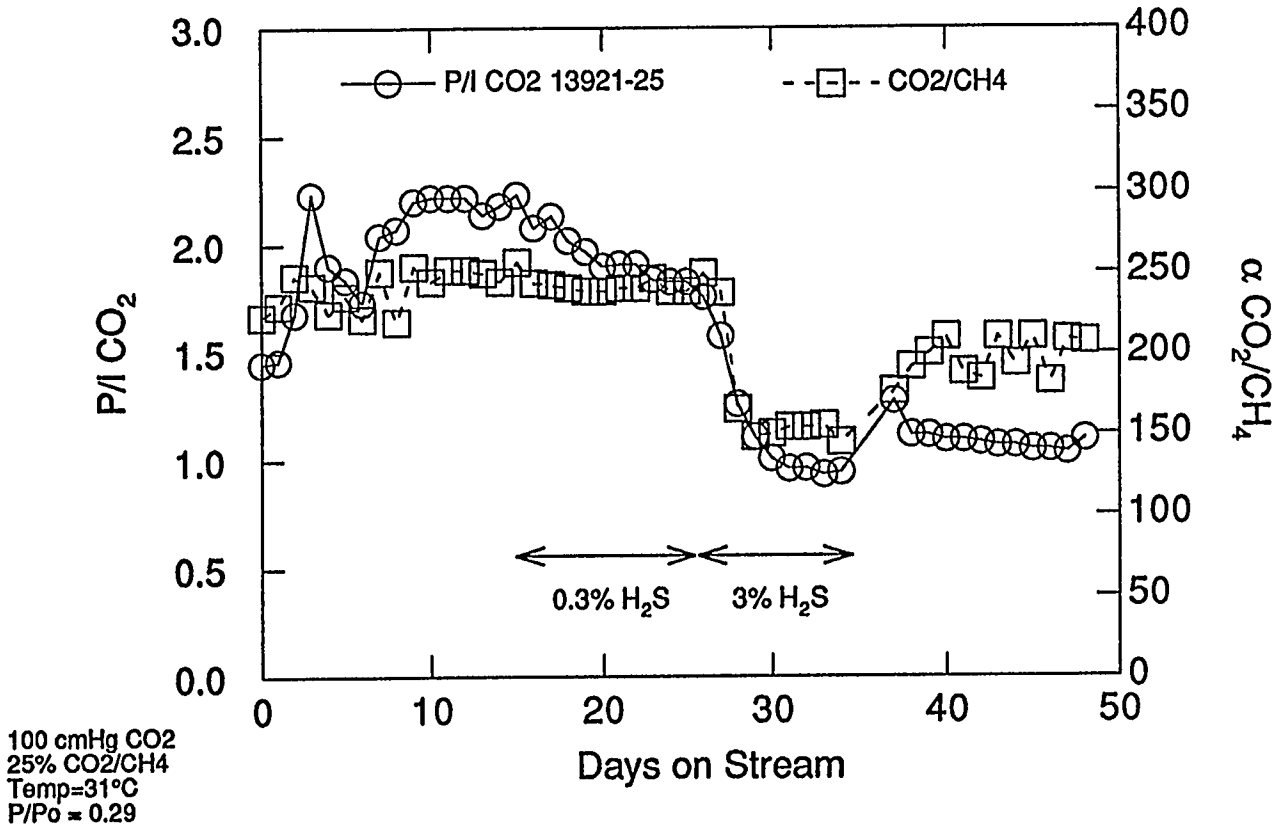

Figure 4-13
Lifetime/H_2S Stability of Hollow Fiber ATM

• Defect Modeling of Composite ATMs

A series resistance model can be applied to explain the differences between the permselectivity of planar ATM composite membranes and hollow fiber ATM composite membranes. Table 4-8 summarizes typical laboratory properties under comparable test conditions for PVBTAF composite ATMs.

Table 4-8
Comparison of Typical Planar and Hollow Fiber Membranes

	P/l CO_2 (x 10^6)*	$\alpha CO_2/H_2$	$\alpha CO_2/CH_4$
Planar Membrane	1-6	20-50	200-500
Hollow Fiber Membrane	1-5	2-10	100-300

* in units of $cm^3/cm^2 \cdot s \cdot cmHg$

Hollow fiber composite ATMs achieve CO_2 permeance and generally $\alpha CO_2/CH_4$ similar to the planar counterpart however, $\alpha CO_2/H_2$ is always significantly less than expected. To explain these results the following model is proposed. The model consists of the following components:

(1) A series resistance calculation to determine the intrinsic permselectivity of the PVBTAF layer from the experimentally determined properties of a planar multilayer composite membrane, the uncoated substrate (assumed to be nonporous) and the PDMS overcoat. The result is scaled to the same experimental conditions under which the hollow fiber ATM was evaluated.

(2) The defects are assumed to occur over a nonporous region of the support fiber as shown in Figure 4-14. The model then uses a two parameter fit to simultaneously solve for the ratio of the PVBTAF layer thicknesses between the planar coupon and the hollow fiber composite and the defective area. The total gas flux of any species (i) is then the sum of the flux through the coated composite of area, x, and the flux through the defect area, (1-x). These parameters are then used to predict the CH_4 permeance and $\alpha CO_2/CH_4$.

Figure 4-14: Schematic Representation of Defect Model

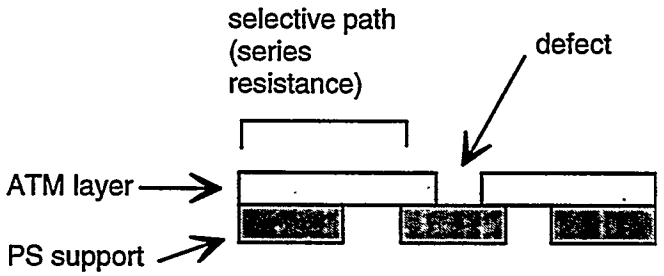

$$(P/l)_i \text{ [composite]} = L \bullet x \ (P/l)_i \text{ [series resistance]} + (1-x) \bullet (P/l)_i \text{ defect}$$

where L = PVBTAF thickness of fiber /PVBTAF thickness of coupon
x = defect-free area

The component permselectivities used in the calculations are given in Table 4-9.

Table 4-9
Permselectivity Basis for Defect Model

Component	Thickness	P/l CO_2 (x 10^6)*	P/l H_2	P/l CH_4
substrate	1000Å	57	108	2.2
PDMS	5 μm	194	42	14

* in units of $cm^3/cm^2 \bullet s \bullet cmHg$

An important result of the model is that neither the polysulfone (sheet or fiber) nor the PDMS overcoat provide significant mass transfer resistance to these membranes. Table 4-10 compares the experimental properties of the flat sheet ATM composite, the experimental permselectivity of a hollow fiber ATM composite and predicted (model) permselectivity for PVBTAF-coated onto SUB2 hollow fibers. The defective area was calculated at 0.17%.

Table 4-10: Comparison of Experimental and Model Predicted Permselectivity for an ATM Hollow Fiber Module (x = 0.9983)

Property	PVBTAF Intrinsic Properties	experimental flat sheet (12484-76B)**	experimental hollow fiber (13074-49D)***	predicted (defect model)****
P/l CO_2 (x 10^6)*	2.95	2.88	3.05	3.05
$\alpha CO_2/H_2$	44	43	12.1	12.1
$\alpha CO_2/CH_4$	500	490	275	316

* in units of $cm^3/cm^2 \cdot s \cdot cmHg$
** conditions: 143 cmHg CO_2, P/Po=0.31
***conditions: 135 cmHg CO_2, P/Po=0.27
****scaled to experimental conditions of 13074-49D

Although the model is limited and does not take into account the variation in effective permeation area as the PVBTAF layer is thinned, the agreement between model and experiment is good. It provides a semi-quantitative rationalization of the experimental results and can be used to guide future work.

3.3 Results and Discussion - ATM coated PAI Substrate

This work incorporated PAI substrate developed under task 1 (Section III of this report) and new high performance ATM compositions (e.g. EXTM6-4; see Section V of this report). Planar coupons of these ATM compositions exhibited a ten-fold increase in CO_2 permeance without loss of selectivity. The performance of hollow fiber composite lab modules is reported below.

- EXTM6-4-coated PAI Substrate

Screening results for EXTM6-4 coated PAI are summarized in Table 4-11. Early results were discouraging. Eventually a procedure was developed to make largely defect free EXTM6-4 and EXTM8 coatings on small pore PAI substrate. While $\alpha(CO_2/CH_4)$ is good, ranging from 100-400, CO_2 permeance values are approximately that observed for PVBTAF-coated SUB1 which suggests that optimization of the PAI substrate is needed to realize the potential of the high performance ATMs. For instance, a higher CO_2 permeance was achieved on

100A pore/1500 GPU PAI (13745-5Å) compared to the <40Å pore/150 GPU PAI (13745-15B). These results demonstrate that it is possible to coat PAI with the ATM. Additional work is necessary to evaluate permselectivity under more rigorous conditions.

Table 4-11
Performance of EXTM6-4 Coated PAI Hollow Fiber Modules

Reference	Fiber Ref	P/Po	P CO_2*	P/l CO_2**	α CO_2/CH_4
13921-83	90B	0.38	98	1.1	240
		0.52	106	1.4	153
		0.27	103	0.79	159
13921-85	13475-15B	0.28	50	1.4	227
		0.30	50	0.94	399
		0.40	124	0.65	133
		0.36	124	0.66	178
13921-94	13475-5A	0.29	125	2.1	274
		0.4	125	2.6	237

* cmHg

** units of 10^{-6} $cm^3/cm^2 \bullet s \bullet cmHg$

• EXTM8-Coated PAI Substrate

Table 4-12 summarizes results for EXTM8-coated PAI. Here too, EXTM8 based composites exhibit high selectivity but not the expected improved CO_2 permeance. These results re-emphasize the need to optimize the support fiber. It is worth noting that in some cases Rayleigh instability[37] was observed during the coating process and may be an issue in EXTM8 coating scale-up.

[37]D. Quere et. al., "Spreading of Liquids on Highly Curved Surfaces", ***Science***, 249, 1256 91990).

EXTM8-Coated PAI Fibers
Feed gas: 25% CO2,25%CH4,50%H2@75sccm

Fiber #	Ref #	P/Po	P CO2	P/l CO2	CO2/CH4	t on stream	Comment
69A	13074-93B	0.27	83	4.7	321	96 hrs	
		0.27	153	3.3	1325		
		0.27	272	2.2	637		
69A	13074-94E	0.27	88	3.4	485	64 hrs	
		0.21	88	2.0	22		
		0.27	98	3.3	50		
		0.38	98	3.8	292		
69A	13074-100	0.27	162	6.5	1.1	3 hrs	
69A	13074-101	0.27	162	2.4	22.3	5 hrs	
		0.27	162	21.9	0.8		
69A	13074-102	0.27	162	23.2	0.9	24 hrs	
		0.27	162	29.9	0.9		
69A	13074-103	0.38	92	4.0	1.1	4 hrs	
		0.38	124	0.41	7.5	4 hrs	recoated in housing
69A	13399-1	0.27	124	3.2	8.6	4 hrs	
		0.38	149	1.9	3.8		recoated in housing
		0.52	149	1.4	13.8	20 hrs	
38A	13399-2	0.27	124	60.3	1.0	4 hrs	
38A	13399-3	0.27	124	14.4	1.1	4 hrs	
69A	13399-4	0.27	147	10.7	1.1	4 hrs	
69A	13399-5	0.27	149	11.1	1.1	4 hrs	no sweep
69A	13399-10	0.27	89	1.2	1.1	4 hrs	

Table 4-12

Summary: Permselectivity of EXTM8-coated PAI Modules

Fiber #	Ref #	P/Po	P CO2	P/l CO2	CO2/CH4	T on stream	Comment
69A	13399-13	0.27	84	1.6	38.8	96 hrs	
		0.38	84	2.0	83.0		
		0.52	79	2.3	292		
		0.52	160	1.8	5.0		
69A	13399-14	0.27	91	1.7	11.2	148 hrs	
		0.52	91	1.9	117.2		
		0.52	156	1.8	38.4		
		0.38	92	2.1	82.1		
		0.52	96	2.0	129		
69A	13399-18	0.52	92	2.5	24	4 hrs	
69A	13399-19	0.52	87	3.5	199	72 hrs	
		0.52	88	3.5	270		
		0.52	157	2.9	53		
		0.38	157	2.8	21.2		
		0.52	157	3.0	48.9		
69A	13399-22	0.52	88	3.6	2.3	4 hrs	
69A	13399-23	0.52	88	3.0	9.1	4 hrs	
69A	13399-25	0.52	92	3.1	10.7	4 hrs	
69A	13399-26	0.52	91	2.9	140	14 hrs	
69A	13399-27	0.52	91	1.5	133	270 hrs	
		0.52	88	1.7	117		
		0.38	89	0.85	454		
		0.38	170	0.61	249		
		0.27	170	0.21	???		
		0.38	170	0.45	308		
		0.38	296	0.31	273		
		0.38	245	202	1.1		failure at 185 psig

Table 4-12 (cont'd)

Fiber #	Ref #	P/Po	P CO2	P/l CO2	CO2/CH4	T on stream	Comment
69B	13399-28	0.38	88	3.8	16.7	148 hrs	
		0.52	91	2.8	26.9		
		0.71	91	2.4	84.1		
		0.52	84	2.3	32.8		
68C	13399-45	0.34	95	4.1	2.4	4 hrs	wiped fiber
12932-68C	13399-48	0.34	92	20.0	1.5	4 hrs	
12932-68C	13399-50	0.38	95	5.6	1.8	4 hrs	

Table 4-12 (cont'd)

4.0 Summary and Recommendations

Figure 4-15 summarizes typical results for polysulfone-supported PVBTAF planar coupons and hollow fiber lab modules. The CO_2 permeance of the coupons and modules agree to within 25-40%. The selectivity of the modules is less than that observed on coupons, probably for the reasons stated above, but is acceptable and significantly higher than that of any conventional polymer membrane.

Thus far, dip coating procedures have been used to fabricate laboratory scale modules. The ATM layer thickness of the lab modules is 2-10 μm. It will be necessary to translate these results into a continuous coating process as part of a scale-up program. In addition, methods to increase the CO_2 permeance of the module, through fundamental improvements to ATM chemistry, advanced coating technology and innovative module design should be explored, particularity the effect of substrate porosity on performance. A follow-on program should include:

- determine module performance and stability at P/Po < 0.2 and P/Po > 0.7.
- examine methods to produce thinner coatings and determine the effect of coating thickness on flux
- scale-up a continuous coating process
- field test ATM substrates and composite membrane modules

Figure 4-15A
Comparison of Polysulfone-Supported PVBTAF Planar Coupons and Hollow Fiber Lab Modules

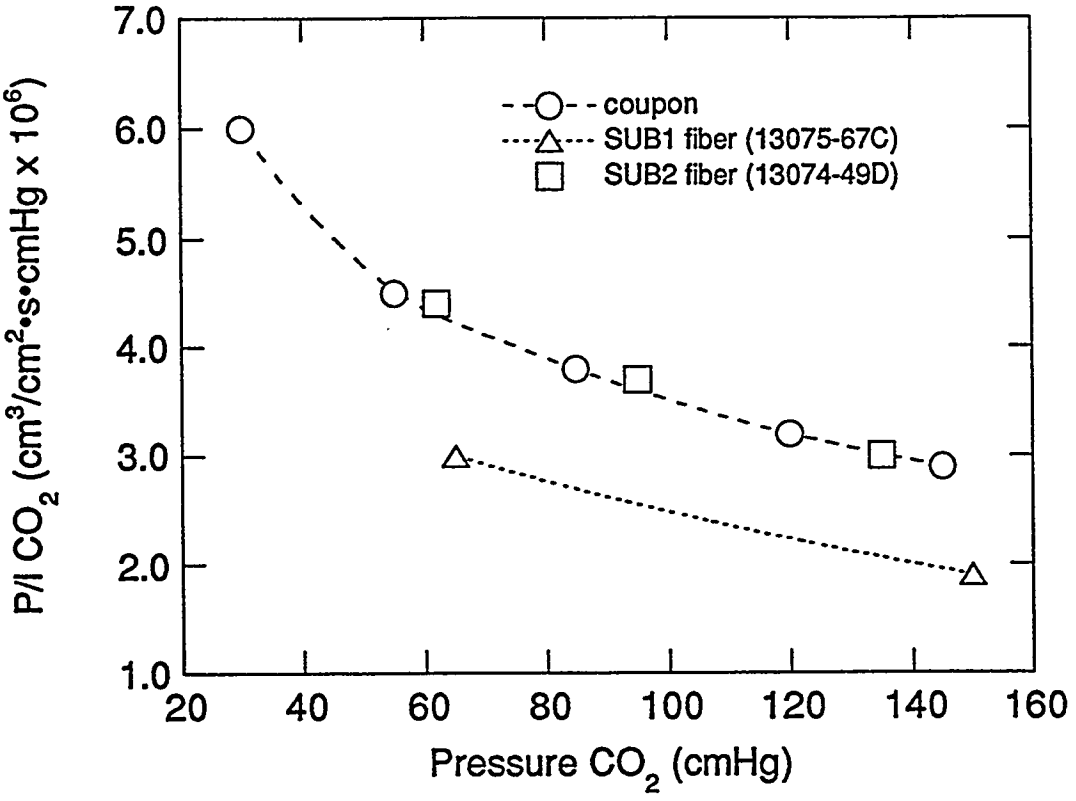

DOE4/F4-15A

Figure 4-15B

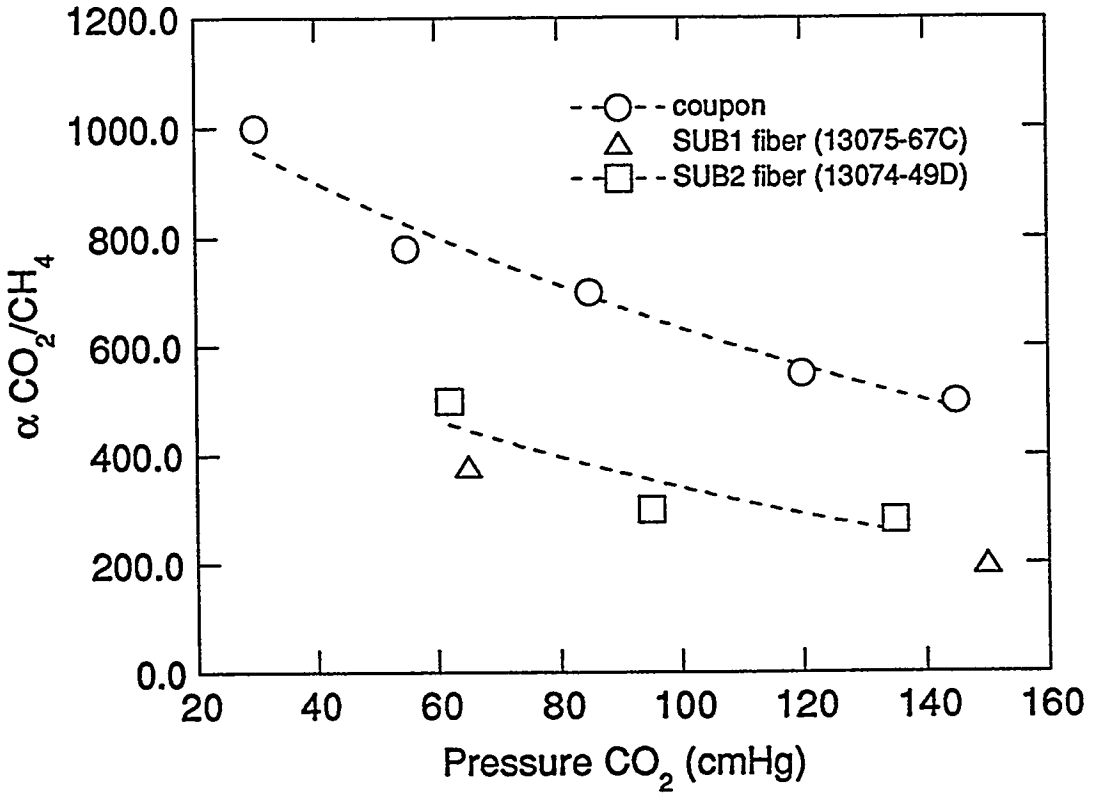

DOE4/F4-15B

Figure 4-15C

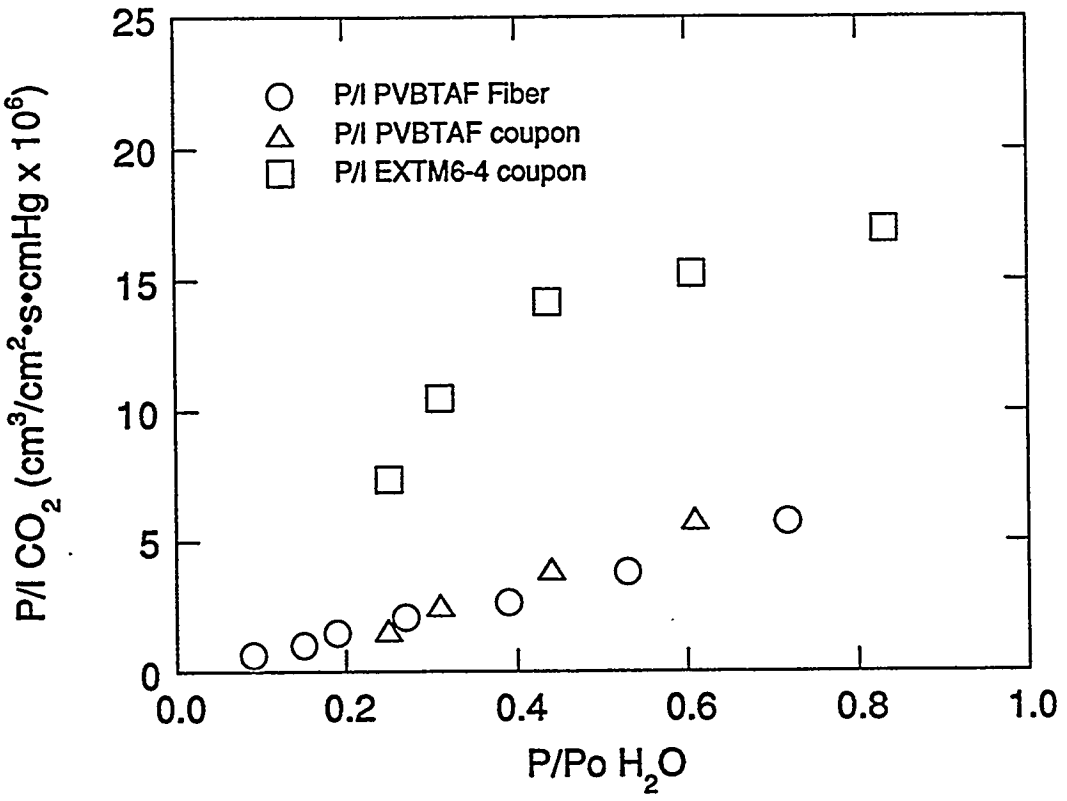

DOE4/F4-15C

V. Recent Advances in the Development of Active Transport Materials

1.0 Influence of H_2O Vapor on ATM Permeation Properties

NMR results[38] support the following acid-base chemistry for the reaction of CO_2 with TMAF and PVBTAF:

$$2F^- + H_2O = HF_2^- + OH^- \quad (1)$$

$$OH^- + CO_2 = HCO_3^- \quad (2)$$

net rxn: $$2F^- + H_2O + CO_2 = HF_2^- + HCO_3^- \quad (3)$$

Water enters directly into CO_2 complexation as one of the reactants. It is believed that the complexation reaction uses water solubilized within the membrane [H_2O]; that is, dissolved water in equilibrium with water vapor in the feed stream. From the above equations, an increase in [H_2O] is expected to drive the reaction forward, however, increasing [H_2O] also increases the solvation sphere of F^- and hence decreases its basicity. Thus, the net effect of increasing [H_2O] at constant temperature is to decrease the equilibrium constant, $K_{eq}CO_2$, for reaction 3; i.e. less CO_2 is dissolved in the membrane as HCO_3^-. This model has been verified experimentally for TMAF and by analogy for PVBTAF (Figure 5-1).

The equilibrium constant for CO_2 complexation is highest for TMAF•$2H_2O$ (n=2)* and decreases as the hydration state is increased. Thus, CO_2 ATMs are expected to have the maximum loading of chemically bound CO_2 at feed stream dew points which produce low hydration state AT material. It is therefore essential to know how the hydration state of the AT material varies with feed stream dew point.

1.1 Measurement of H_2O Absorption Isotherms

Aqueous PVBTAF and EXTM6-4** solutions were prepared as described previously.[29] "Dry" films were prepared by evaporating the solutions to dryness under nitrogen followed by vacuum at 25°C. Before an H_2O absorption isotherm could be measured, the composition of the starting material had to be identified; that is, the hydration state of the "dry"

---

[38] R. Quinn, Air Products internal memorandum, 1991.

* TMAF•$1H_2O$ absorbs CO_2 irreversibly.

** EXTM6-4 is a proprietary blend of AT polymer and AT salt.

Figure 5-1
Chemical Complexation of CO_2 by TMAF • nH_2O

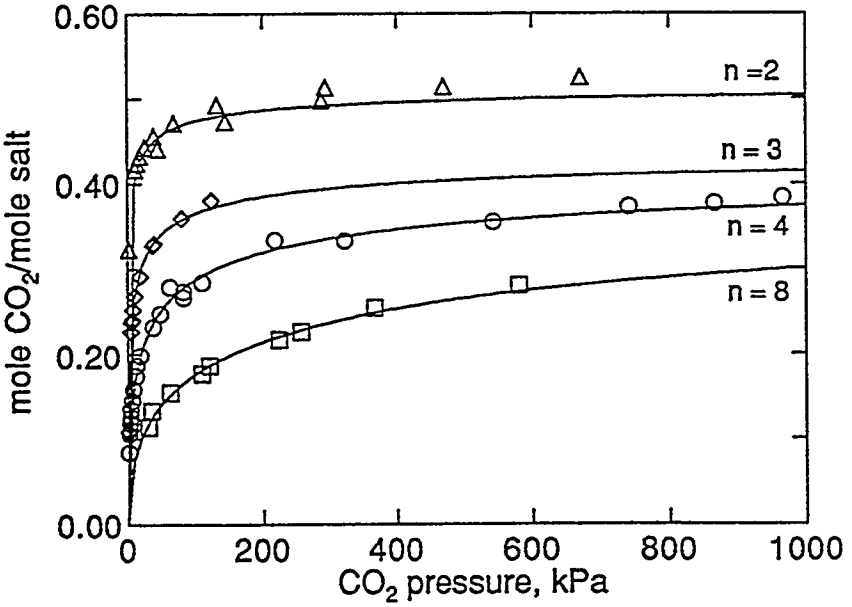

Table 5-1

NMR Peak Assignments

Proton	chemical shift	# of protons PVBTAF	EXTM6-4
a	1.3 ppm	2.6	2.5
b	6.4,6.9 ppm	3.6	3.6
c	4.0 ppm	1.6	1.6
d	2.7 ppm	9.0	6.4
e	4.6 ppm	2.6	3.8

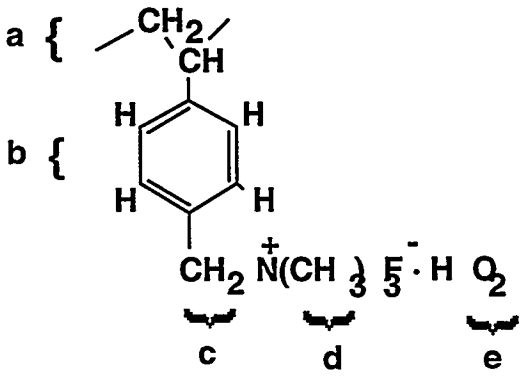

Figure 5-2

Thermal Decomposition of PVBTAF and EXTM6-4

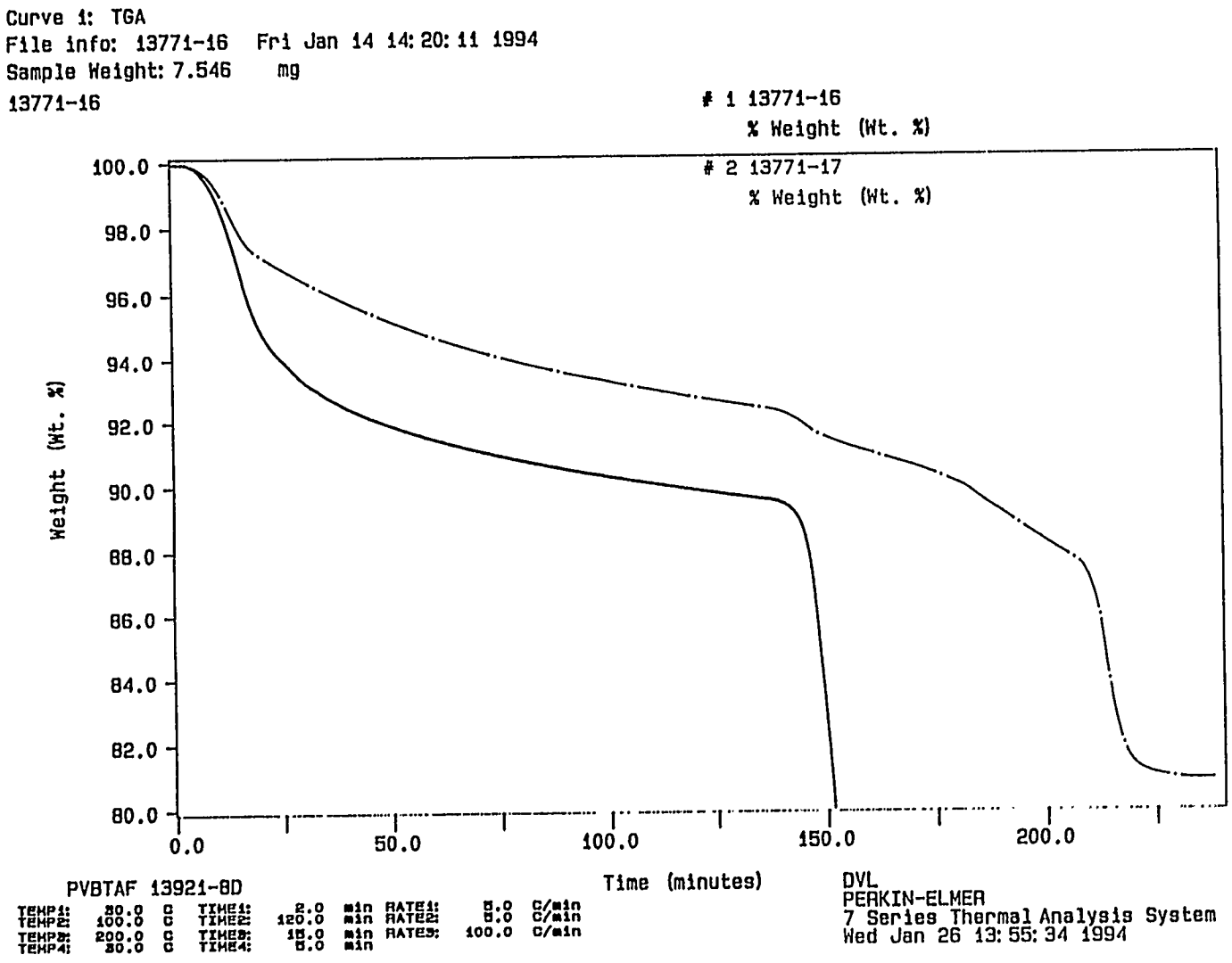

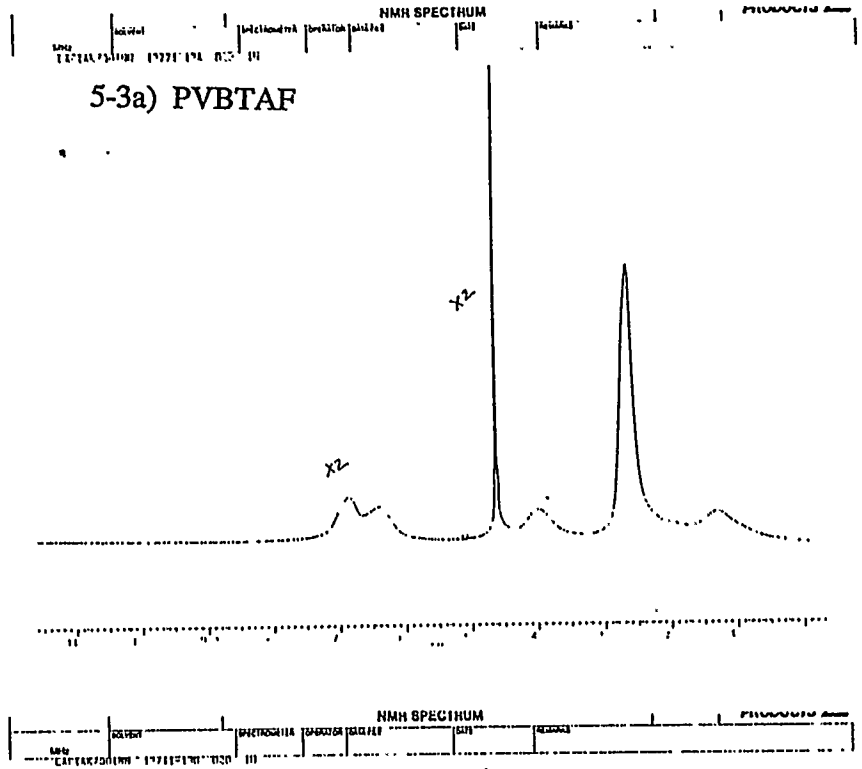

5-3a) PVBTAF

5-3b) EXTM6-4

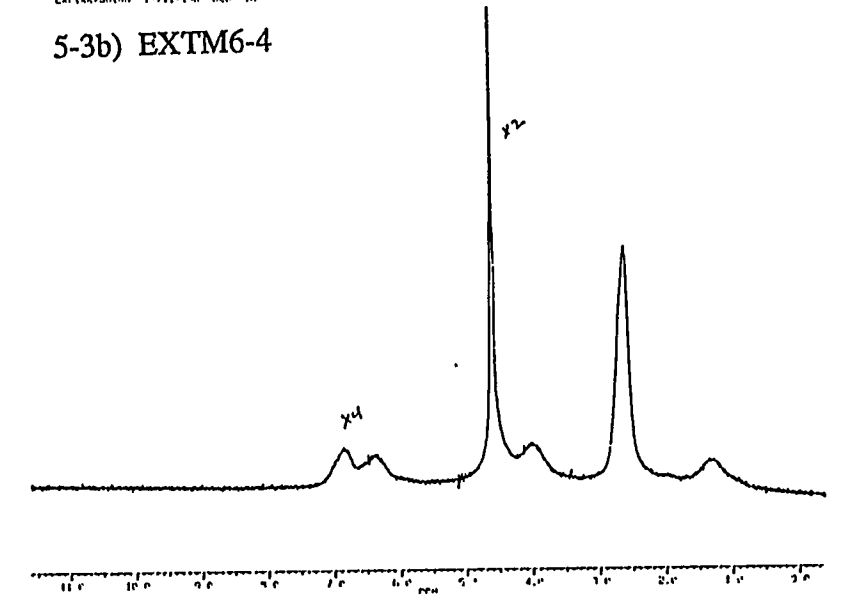

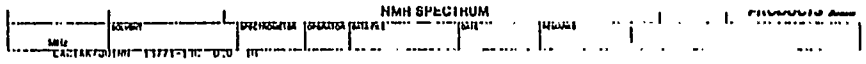

5-3c) D_2O Blank

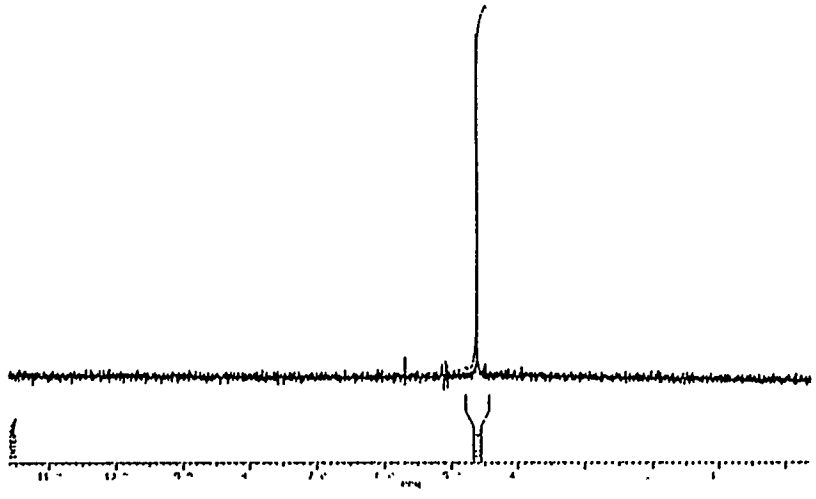

Figure 5-3
^1H nmr of PVBTAF and EXTM6-4

Results of the TGA and NMR experiments are summarized and compared in Table 5-2. Agreement between the methods is excellent. The composition of the "dry" polyelectrolytes can best be expressed as PVBTAF•1H_2O and EXTM6-4• 5H_2O. It is interesting to note that both samples contain 1H_2O/1F^-.

Table 5-2: Water Content of "Dry" PVBTAF and EXTM6-4

			wt% H_2O		
Material	Sample Ref.	Source Ref.	TGA	NMR	Hydrate #
PVBTAF	13771-16	13921-8D	9.7	10.7	0.98
EXTM6-4	13771-17	13921-8E	7.5	6.7	4.88

The H_2O absorption isotherms for PVBTAF and EXTM6-4 were determined using a McBain microbalance. Table 5-3 and Figures 5-4 and 5-5 relate the partial pressure of H_2O in the feed stream to the hydration state of PVBTAF and EXTM6-4. Some interesting points to note about the isotherms include:

1) Consistent with the addition of the AT salt, on a "molar" basis EXTM6-4 absorbs much more H_2O than does PVBTAF (Figure 5-4), however

2) On a fluoride ion basis (Figure 5-5), there is no significant difference in the amount of water absorbed by the two polymers. This suggests that solvating the F^- ion is the driving force behind the water affinity of both these materials.

3) Both isotherms contain an inflection point at P/Po $\approx$ 0.3. At lower values of P/Po, the slope of the isotherm is almost flat. As P/Po passes through $\approx$ 0.3, the slope changes and there is a marked increase in the amount of H_2O absorbed.

Table 5-3

H_2O Absorption by PVBTAF and EXTM6-4 at 25° C

PVBTAF	sample #1			sample #2		
P/Po	mmol H_2O / g sample	mol H_2O / repeat unit	mol H_2O / mol F	mmol H_2O / g sample	mol H_2O / repeat unit	mol H_2O/ mol F
0.000	0	1.17	1.17	0	1.17	1.17
0.123	2.83	1.78	1.78	2.89	1.80	1.80
0.152	6.04	2.47	2.47	5.80	2.42	2.42
0.243	5.98	2.46	2.46	2.91	2.45	2.45
0.345	11.27	3.61	3.61	10.95	3.54	3.54
0.459	14.75	4.36	4.36	14.53	4.31	4.31
0.573	21.35	5.78	5.78	21.05	5.72	5.72
0.741	27.75	7.17	7.17	27.64	7.14	7.14
0.876	37.06	9.18	9.18	36.89	9.14	9.14

EXTM6-4	sampe #1			sample #2		
P/Po	mmolH_2O/g sample	mol H_2O/ repeat unit	mol H_2O / mol F	mmol H_2O/g sample	mol H_2O / repeat unit	mol H_2O / mol F
0.000	0	4.88	0.98	0	4.88	0.98
0.123	1.18	5.92	1.19	0.90	5.68	1.14
0.152	2.83	7.38	1.48	2.41	7.01	1.40
0.243	3.75	8.19	1.64	3.29	7.79	1.56
0.345	10.99	14.59	2.92	10.05	13.76	2.75
0.459	15.52	18.59	3.72	14.37	17.57	3.51
0.573	24.39	26.42	5.28	23.10	25.28	5.06
0.741	32.68	33.74	6.75	31.40	32.62	6.52
0.876	45.66	45.20	9.04	44.13	43.85	8.77

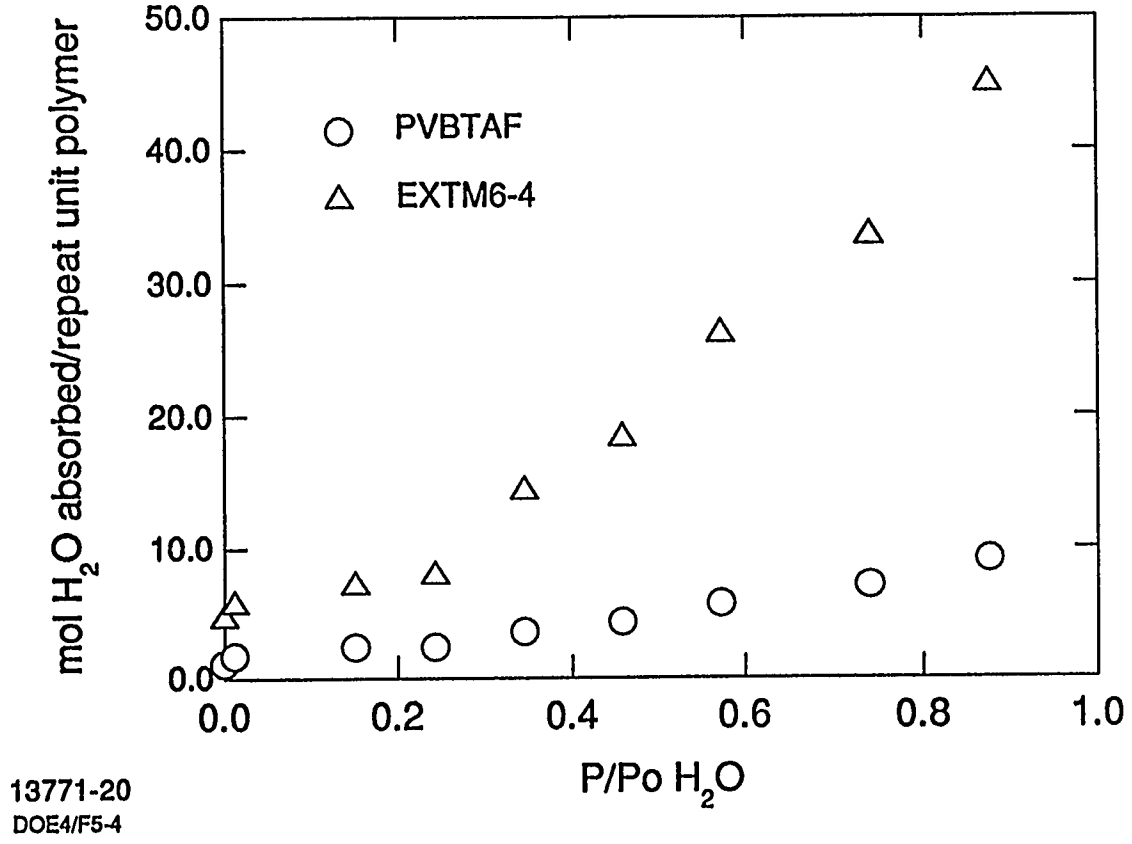

Figure 5-4
H_2O Absorption by PVBTAF and EXTM6-4 at 25°C Repeat Unit Basis

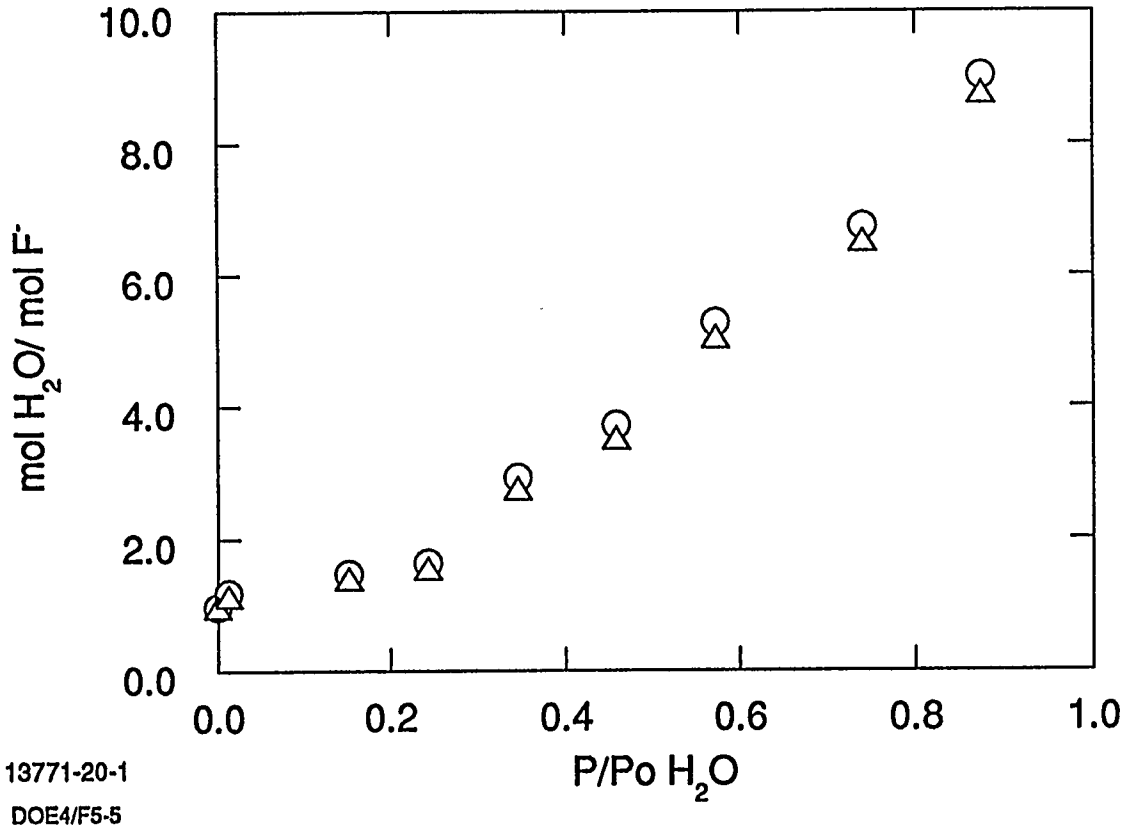

Figure 5-5
H_2O Absorption by PVBTAF and EXTM6-4 at 25°C Fluoride Basis

1.2 Correlation of H_2O Absorption with Permselectivity

This information can be used to rationalize the observed properties of PVBTAF and EXTM6-4 composite membranes. Typical results for a CO_2/CH_4 separation as function of P/Po are plotted in Figure 5-4. The increasing permeance of both gases at higher P/Po suggests that the increasing quantity of water absorbed under these conditions acts to "loosen" the polymer network, making diffusion more facile. Since this is a nonselective process, it stands to reason that the flux of all components increases. This hypothesis is being verified experimentally using PGSE-NMR.

We observe experimentally that while P/l of all gases increases with increasing P/Po, the selectivity passes through a maximum. The curve of $\alpha CO_2/CH_4$ vs P/Po for a PVBTAF/Sub1 polysulfone hollow fiber membrane is, in Figure 5-6, superimposed on a graph of H_2O absorption. Clearly the maximum in the selectivity coincides with the flat portion of the isotherm. At very low P/Po it is likely that diffusion is limited because the polymer network, being ionic and having little absorbed water, is very "tight" and diffusion is slow. At P/Po greater than ≈0.35, there is a substantial decrease in selectivity. The reason for this is two-fold:

1) As described earlier, higher P/Po decreases the concentration of complexed CO_2

2) The ionic strength of the medium is lower at higher values of P/Po thus making the ionic barrier to CH_4 less effective, i.e. a diminishing of the "salting-out" effect.

The CO_2/H_2 selectivity of a EXTM6-4 polysulfone planar membrane is superimposed on the graph of H_2O absorption in Figure 5-8. Here however, the maximum selectivity is shifted to slightly higher P/Po. To rationalize this feature one need only consider the differences in ionic strength of the two polyelectrolyte solutions as shown in Figure 5-9. The curve of the ionic strength is nearly flat until P/Po≈0.3 at which point it decreases rapidly. It is interesting to note that the ionic strength of PVBTAF at it optimum P/Po (≈ 0.25) is equal to that of EXTM6-4 at P/Po≈0.45.

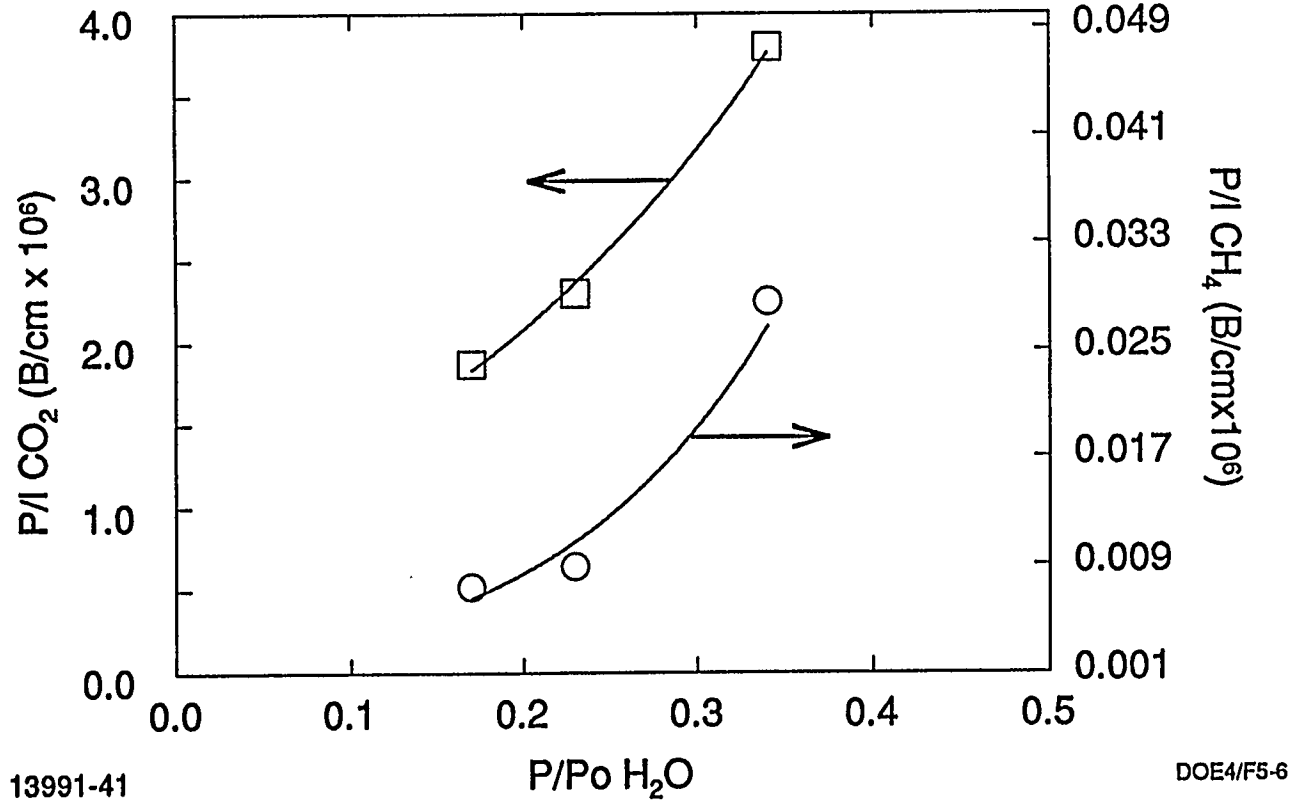

Figure 5-6

Permselectivity of a PVBTAF/Polysulfone Membrane as a Function P/Po

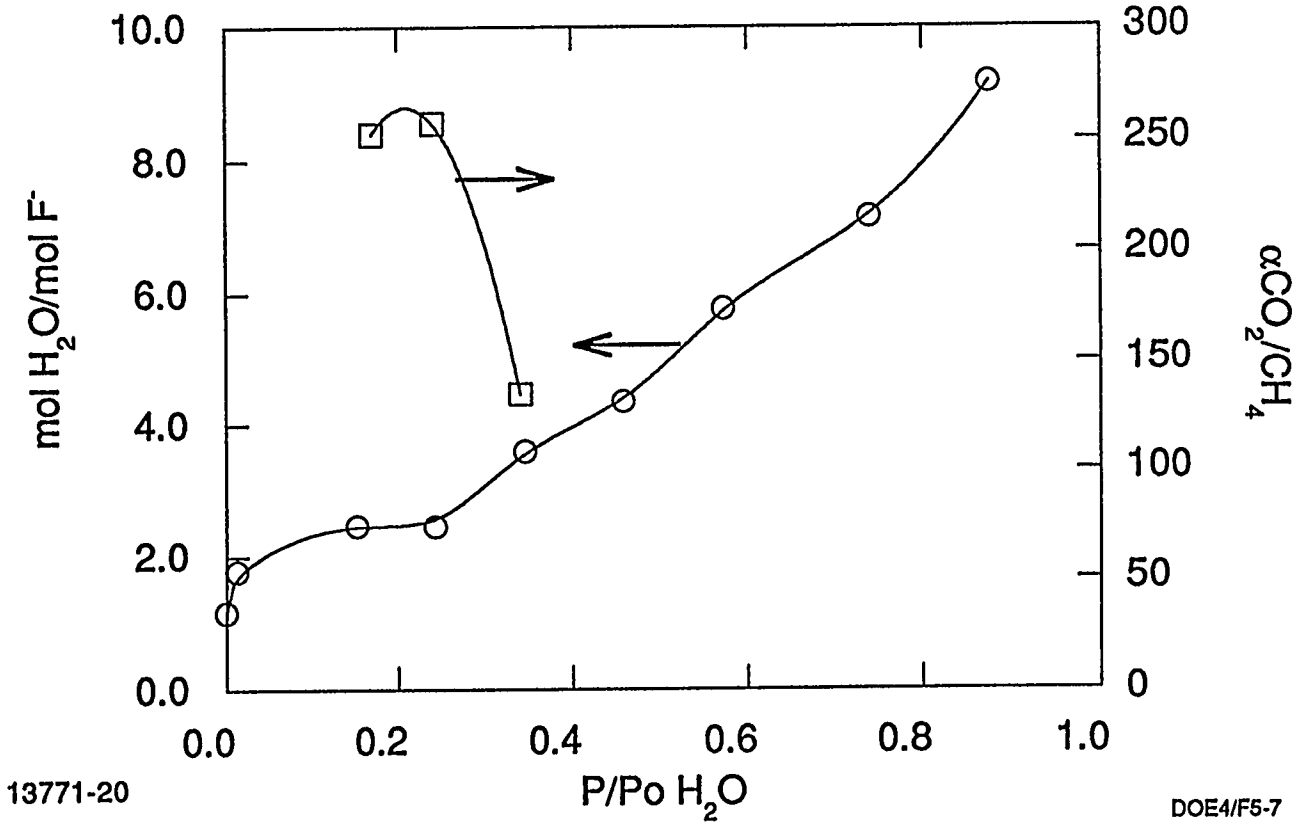

Figure 5-7
Selectivity and H2O Absorption of PVBTAF

Figure 5-8
Selectivity and H_2O Absorption of EXTM6-4

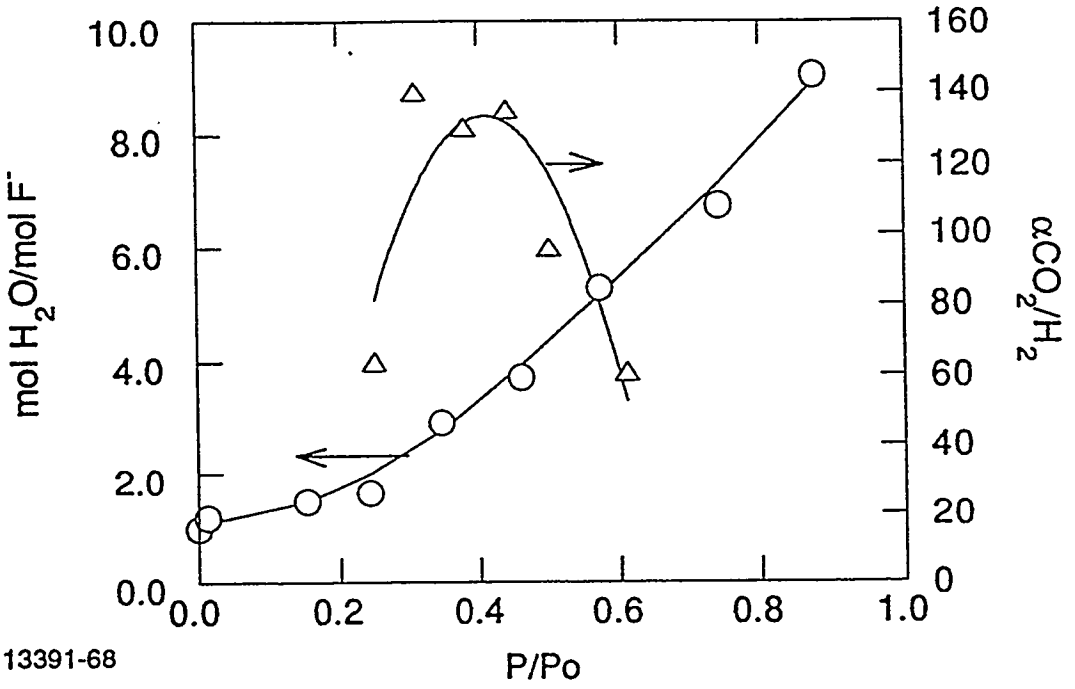

Figure 5-9
Ionic Strength of PVBTAF and EXTM6-4

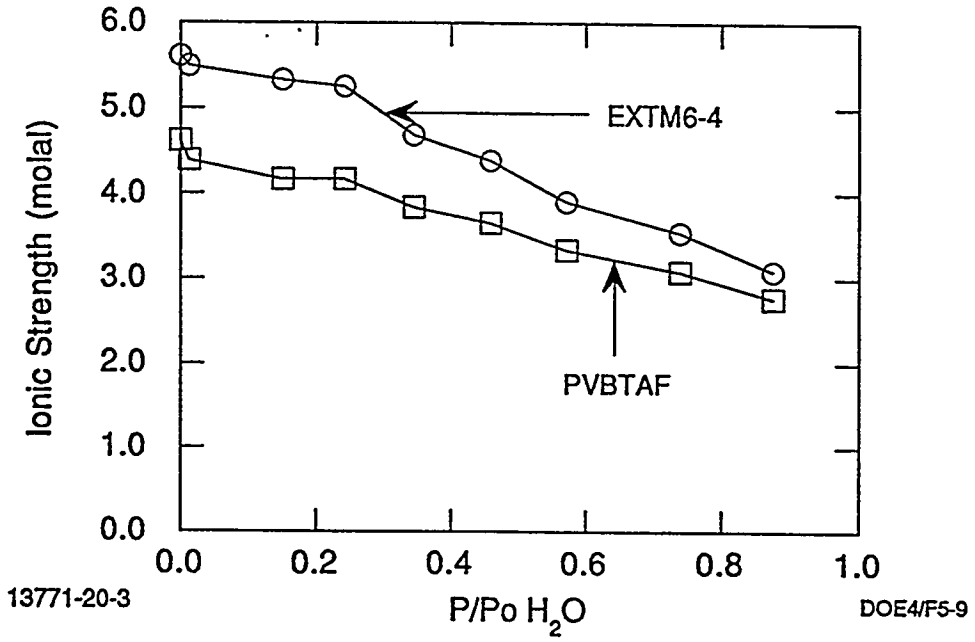

1.3 Conclusions

The dew point-dependent permselectivity of CO_2-selective Active Transport membranes fabricated from poly(vinylbenzyltrimethylammoniumfluoride) [PVBTAF] or blends of polymers with AT salts can be related to the equilibrium water absorption of the materials. An inflection point in the isotherm correlates with the observed decrease in the selectivity of PVBTAF composite membranes. Differences in performance between PVBTAF and EXTM6-4 can be attributed to differences in ionic strength. Because extremes of dew point result in either delamination of the AT layer or loss of permselectivity it will be necessary to control the level of water in the feed stream to Active Transport membranes.

2.0 Assessment of H_2S Reactivity of ATM Membranes

2.1 H_2S Permselectivity

PVBTAF composite membranes also selectively permeate H_2S. Typical gas permeation properties of PVBTAF composite membranes are listed in Table 5-4. The H_2S permeance varies from 28 - 10 x 10^{-6} $cm^3/cm^2 \bullet s \bullet cmHg$ [12582-40B1] over the pressure range studied indicating facilitated transport of that gas. The selectivity of >1000 to CH_4 is impressive.

The H_2S and CO_2 permselective properties of PVBTAF membranes depend on the composition of the feed gas. Both H_2S and CO_2 are acid gases and should compete for the same permeation sites. The H_2S permeance decreased by 15-40% when CO_2 was admitted to the feed gas at an equal partial pressure ([12582-40B2] and Figure 5-10). Similarly, the presence of H_2S in the feed suppress permeation of CO_2. Under comparable experimental conditions, addition of H_2S to the feed decreased the CO_2 permeance by approximately an order of magnitude (Figure 5-11).

H_2S/CO_2 selectivities ranged from 11 to 8. In this regard, PVBTAF membranes are unique and potentially useful for the separation of H_2S from CO_2-containing mixtures. Typical polymer membranes show little selectivity for H_2S over CO_2 with selectivities of 2 or less.

Table 5-4
H_2S Permselective Properties of PVBTAF Membranes at 22°C

membrane	feed P(psig)	H_2S P(cmHg)	CO_2 P(cmHg)	$(P_o/l)\cdot10^6$ cc/cm^2•s•cmHg H_2S	CO_2	CH_4	selectivity H_2S/CO_2	H_2S/CH_4
12582-40-B1*	2.4	9.2	0	27.9	-	nd	-	7000#
	24.1	20.9	0	17.2	-	nd	-	1290#
	44.1	31.6	0	13.2	-	nd	-	990#
	58.4	39.3	0	12.7	-	nd	-	950#
	96.6	59.8	0	9.95	-	0.00388	-	2500
12582-40-B2**	2.1	8.95	8.67	16.1	1.49	nd	10.8	3300#
	21.5	19.3	18.7	12.4	1.33	nd	9.3	2600#
	34.0	25.9	25.1	12.0	1.41	nd	8.5	2500#
	52.7	35.9	34.8	10.4	1.24	nd	8.4	2200#
	70.4	45.3	43.9	9.60	1.18	0.00530	8.1	1920
	90.3	55.9	54.2	8.70	0.953	0.00476	9.1	1730
	110.1	66.7	64.4	8.30	0.949	0.00436	8.7	2100
return to:	41.7	30.0	29.1	12.4	1.11	nd	11.1	n.o.

* Feed Gas: 10.5% H_2S in CH_4; P/Po=0.3
** Feed Gas: 10.3% H_2S, 10% CO_2 in CH_4; P/Po=0.3
# no CH_4 was detected. Selectivity based on observed CH_4 permeance at higher pressures

Figure 5-10
H_2S Permeance of a PVBTAF Composite as a Function of H_2S Pressure

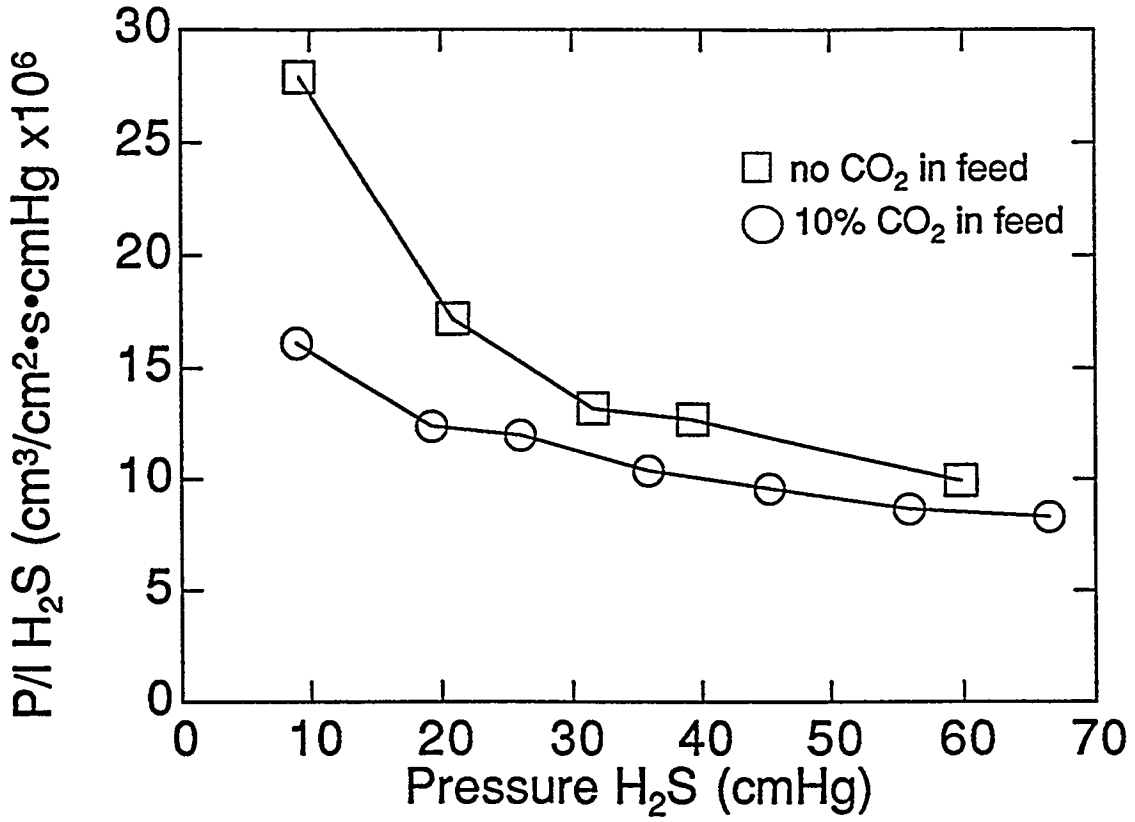

12582-40-B

DOE4/F5-10

Figure 5-11
CO_2 Permeance of a PVBTAF Composite as a Function of CO_2 Pressure

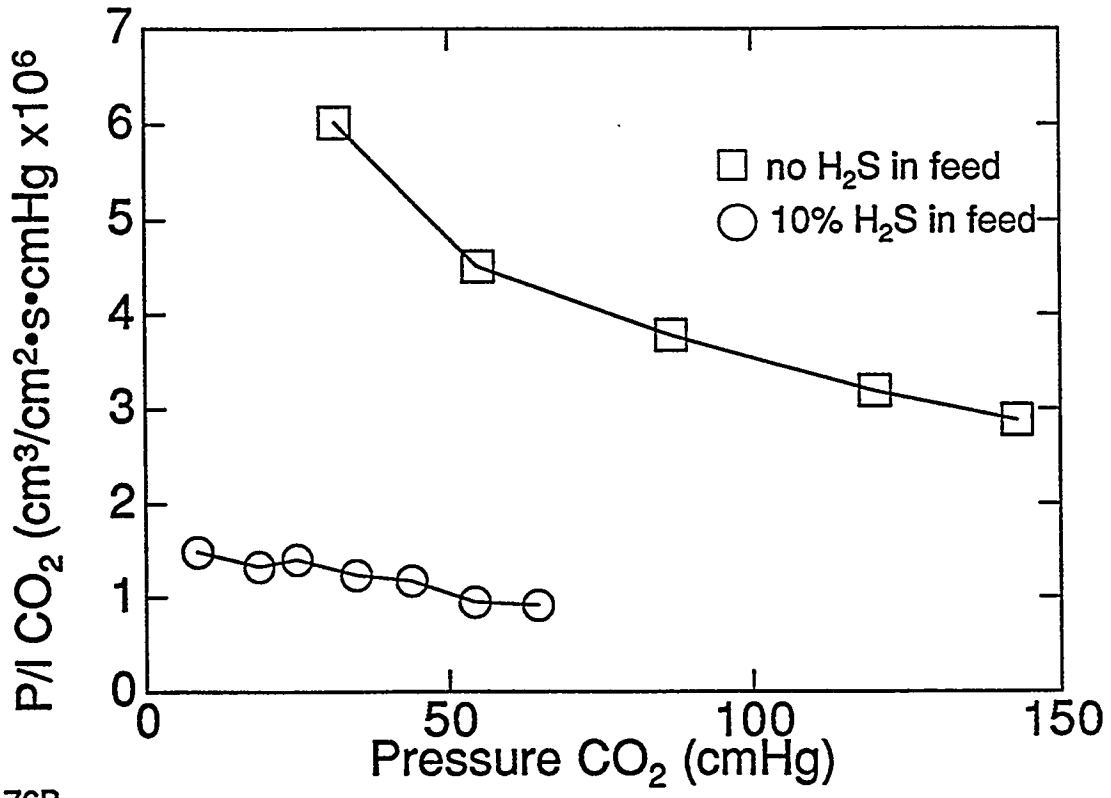

12484-76B
12582-40-B

DOE4/5-11

2.2 Membrane stability

Membrane stability was investigated by measuring the permselectivity of planar PVBTAF composite membranes as a function of time. The data was collected under one of two set of conditions: (1) helium was used to sweep permeating gases from permeate and (2) no sweep gas was used. The latter represents the harsher condition since the permeate pressure of H_2S was significantly greater than zero. Permeance as a function of time is graphed Figure 5-12. A membrane (13095-1-9) operating with a helium sweep exhibited a 34% decline in H_2S permeance over a 19.5 day period (Table 5-5). Near the end of the run, the H_2S permeance appeared to have leveled off. H_2S/CO_2 selectivities remained constant or increased slightly throughout the run. CH_4 was not detected in the permeate but the estimated minimum H_2S/CH_4 selectivities are high - 6500 to 2200. Under harsher conditions, the decline of H_2S permeance with time was more pronounced. For example, a similar membrane (13095-1-3) evaluated without a helium sweep gas and at higher feed partial pressures than above exhibited a 70% H_2S permeance decline over 7 days, at which time a steady state permeance had apparently been reached (Table 5-6).

To evaluate the chemical stability of PVBTAF in the presence of CO_2 and particularly H_2S, samples of solid polymer were exposed to each gas for an extended period and subsequently characterized by NMR. Exposure of solid PVBTAF to CO_2 at 480kPa and 23°C for three weeks resulted in absorption of 0.70 mole CO_2/mole repeat unit. A portion of the sample containing absorbed CO_2 was dissolved in D_2O, resulting in evolution of gas. The ^1H, ^{13}C, and ^{19}F spectra of this sample and of PVBTAF in D_2O were identical (Figure 5-13) implying that PVBTAF is not degraded by CO_2.

An H_2S containing sample was prepared in a similar manner and, after a three week exposure, solid PVBTAF absorbed 2.0 mole H_2S/mole repeat unit at 476 kPa and 23°C. The H_2S-containing sample was brittle and almost insoluble in water and other common solvents (e.g. methanol , acetone, and acetonitrile). The solid was also insoluble in 1M HCl which would appear to eliminate the possibility of an S^{2-} crosslinked structure. Clearly, however, exposure to H_2S caused some chemical change to the polymer.

Solid state NMR spectra of pure PVBTAF and PVBTAF containing absorbed H_2S and CO_2 were obtained (Figure 5-14). The solid state ^{13}C NMR spectra of PVBTAF and PVBTAF exposed to CO_2 or H_2S are identical with the exception of the intensity of the methyl

Table 5-5
H_2S Permselectivity vs. Time for a PVBTAF Composite at 30°C
(13095-1-9)

Feed P (psig)	H_2S P(cmHg)	time, min.	Average P_o/l H_2S	CO_2	CH_4	Average α H_2S/CO_2	H_2S/CH_4
30.4[a]	23.2	5760-6540	38.4	3.71	nd	10.3	6500[c]
		10080-11160	35.6	3.46	nd	10.3	6000[c]
		14400-15480	34.1	3.22	nd	10.6	5800[c]
4.0[b]	29.0	17280-18360	29.4	2.56	nd	11.5	5000[c]
		20640-21720	27.4	2.36	nd	11.6	4600[c]
		24480-25560	25.5	2.15	nd	11.8	4300[c]
30.6[b]	70.4	27000-28080	12.9	1.20	nd	10.7	2200[c]

c. No CH_4 detected; estimated minimum selectivity based on a calculated maximum CH_4 permeance of 0.0059.
Sweep: helium;
feed: (a)9.9% H_2S, 10.0% CO_2 in CH_4 or
(b)30.0% H_2S, 30.0% CO_2 in CH_4;
P/Po=0.3

Table 5-6
H_2S Permselectivity vs. Time for a PVBTAF Composite Membrane at 30°C

membrane	Feed P* (psig)	run time (min)	$(Po/l)\cdot10^6$ cc/cm^2•s•cmHg H_2S	CO_2	CH_4	Selectivity H_2S/CO_2	H_2S/CH_4
13095-1-3[b]	54.4	960-1440	11.5	2.25	0.0352	5.1	326
		2340-2820	9.51	1.90	0.0274	5.0	348
		5700-7140	4.95	0.817	0.0157	6.1	315
		8040-8520	3.55	0.639	0.0145	5.6	245
		9600-10080	3.45	0.564	0.0140	6.1	247

*Feed: 27.4% H_2S, 30.0 % CO_2 in CH_4; P/Po=0.4
permeate pressure, 1.0-1.4 psig;

Figure 5-12
Lifetime of a PVBTAF Composite Membrane

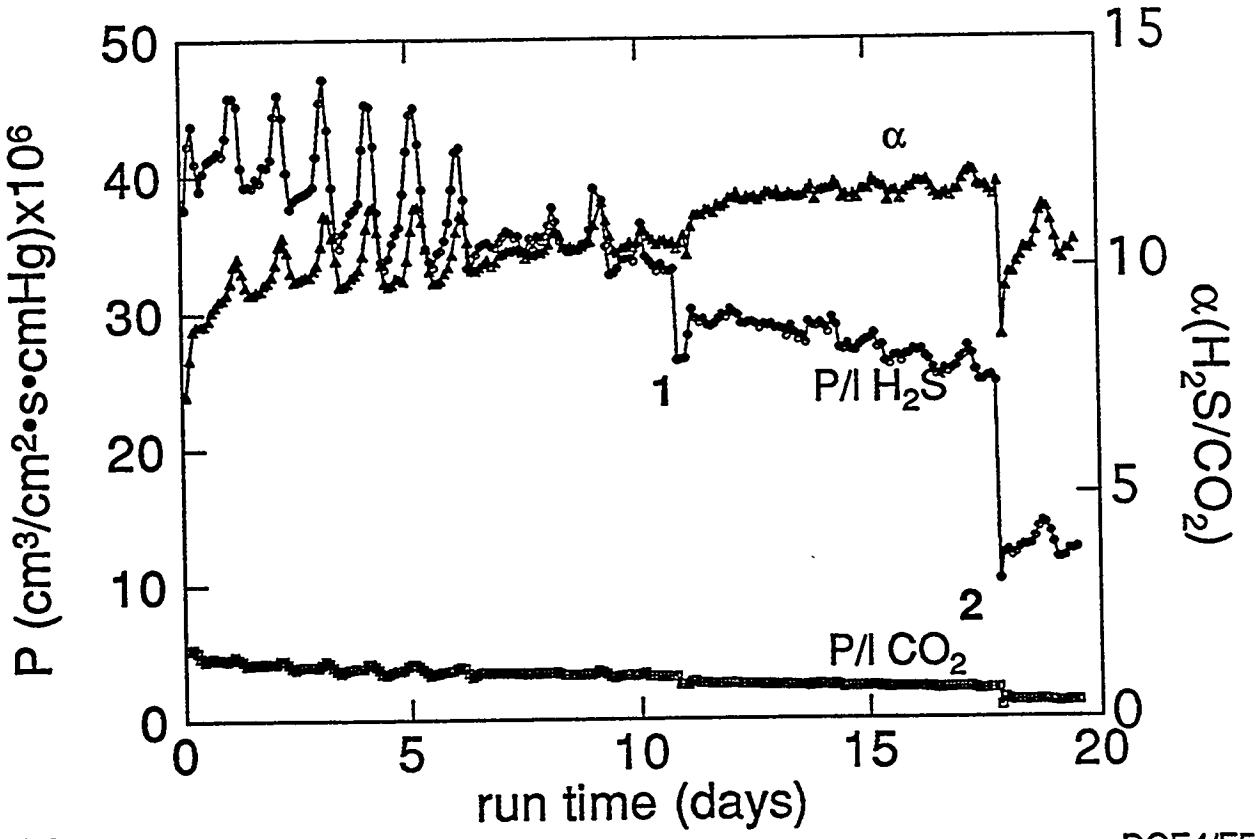

13095-1-9
13230-84

DOE4/F5-12

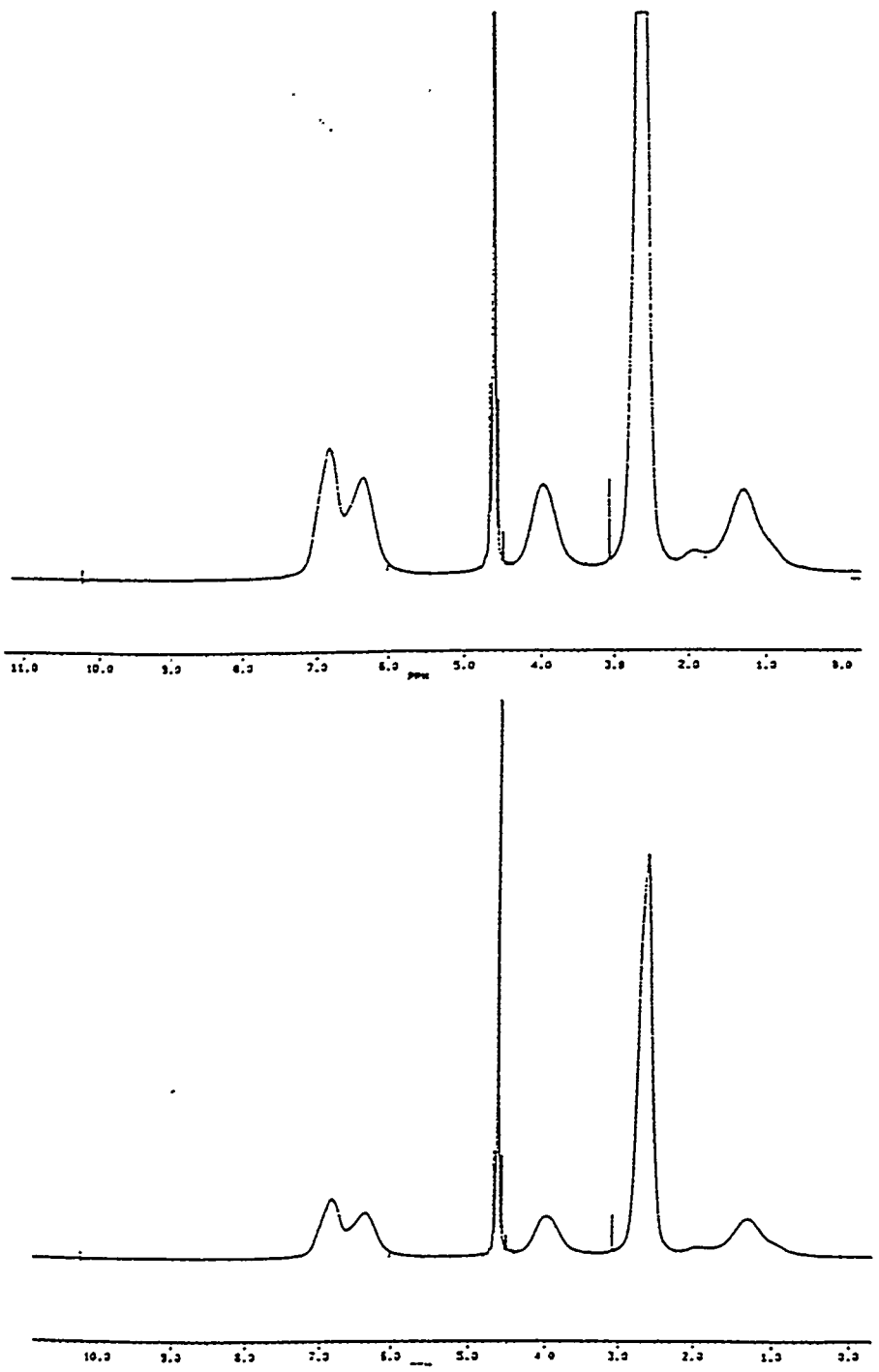

Figure 5-13
^1H NMR spectra of D_2O solutions of PVBTAF before (top) and after (bottom) exposure to CO_2.

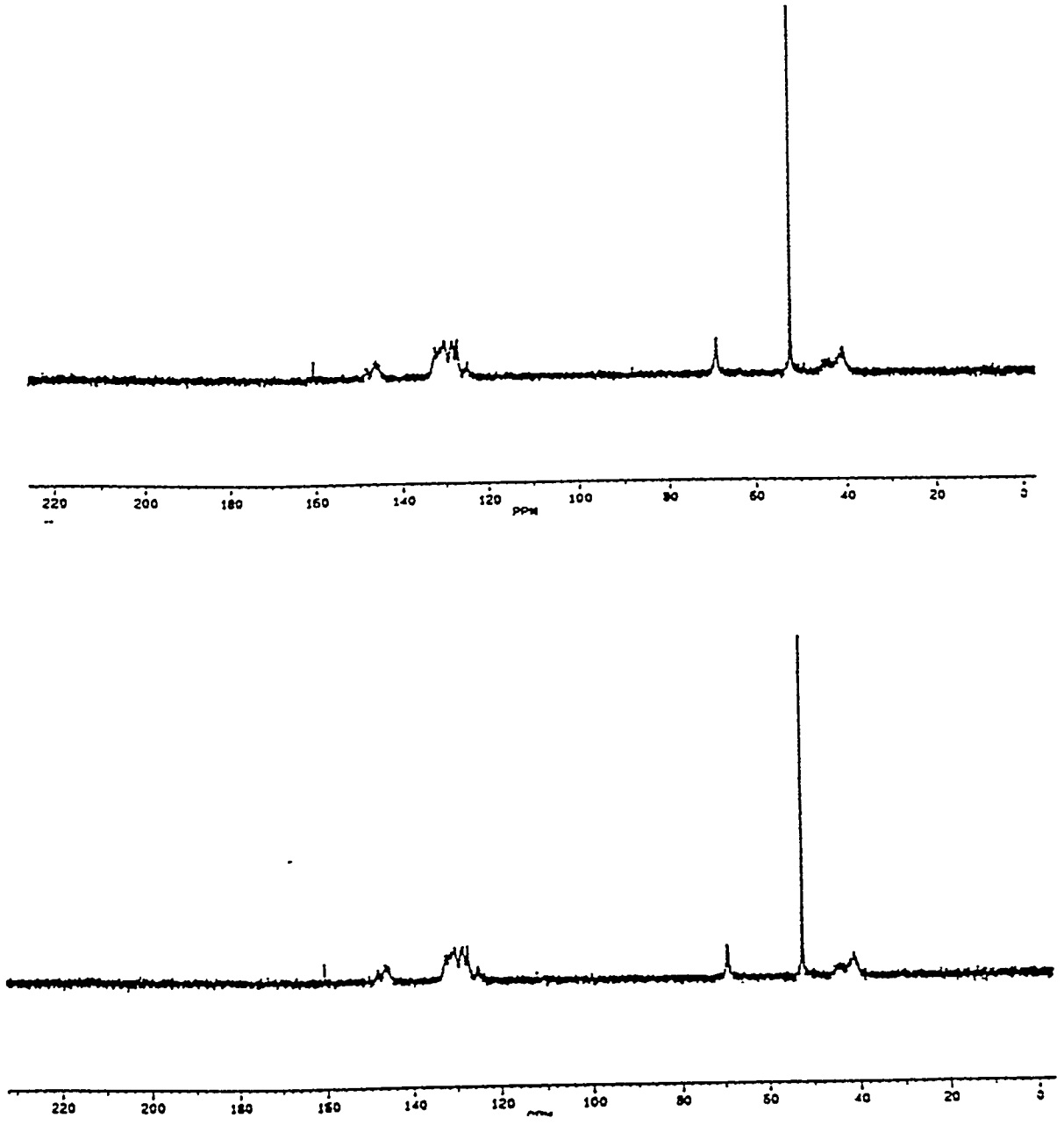

Figure 5-13 (continued)
^{13}C NMR spectra of D_2O solutions of PVBTAF before (top) and after (bottom) exposure to CO_2.

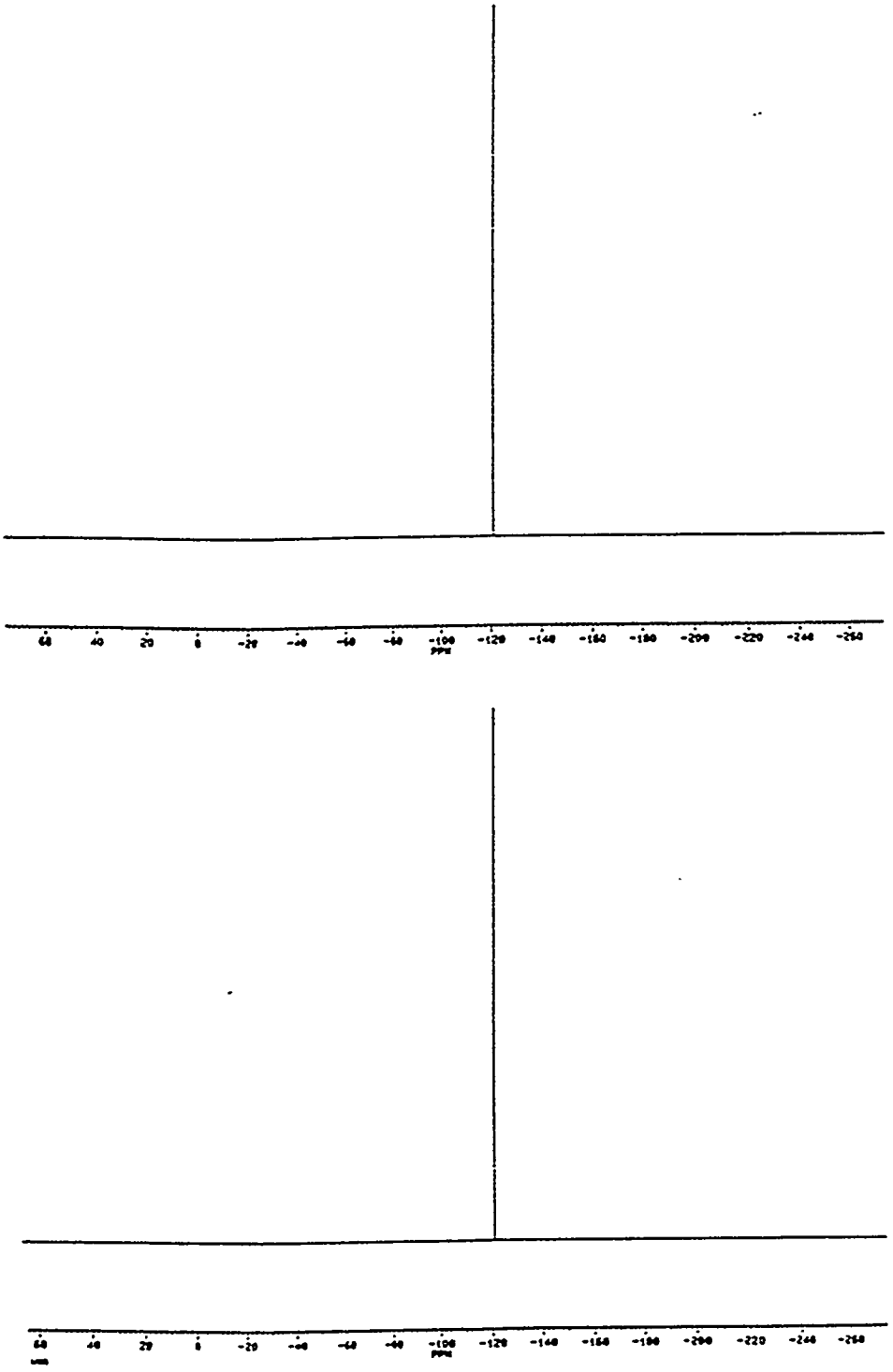

Figure 5-13 (continued)
^{19}F NMR spectra of D_2O solutions of PVBTAF before (top) and after (bottom) exposure to CO_2.

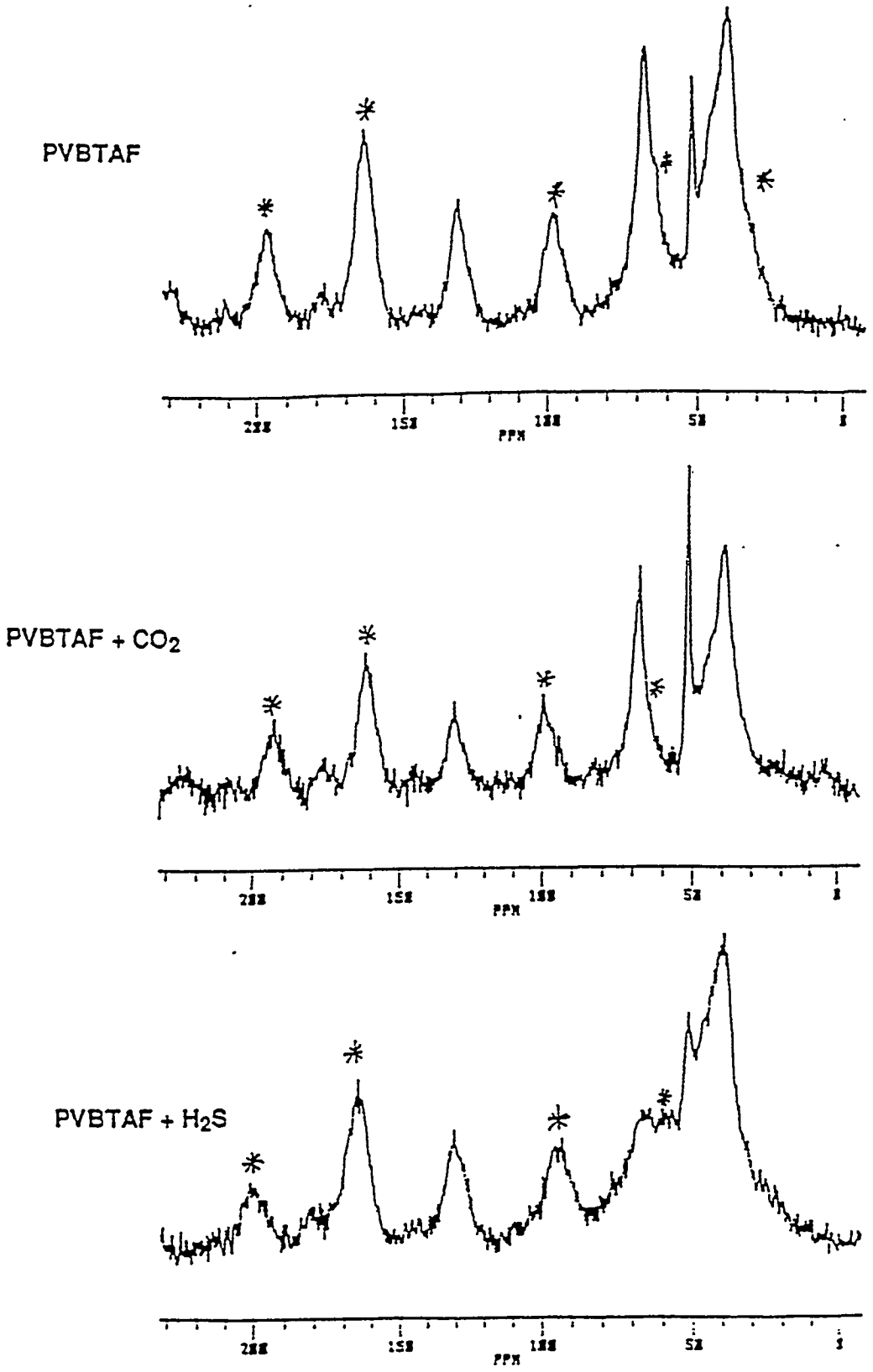

Figure 5-14

Solid state CP MAS ^{13}C NMR spectra of PVBTAF and PVBTAF after exposure to CO_2 or H_2S. Top: PVBTAF. Middle: PVBTAF + CO_2. Bottom: PVBTAF + H_2S. Spinning side bands indicated by *

resonances. The intensity of the methyl resonances can vary with the number of methyl groups in the sample or with its proximity to neighboring H atoms (i.e. the rigidity of the structure about the methyl group). That no resonances different from those of PVBTAF are observed in the spectrum of PVBTAF containing absorbed H_2S or CO_2 implies that no appreciable cleavage and loss of methyl groups occurs upon exposure to either gas. Hence, based on solid state NMR evidence, the organic portion of PVBTAF is inert with respect to degradation by H_2S or CO_2.

Analysis of the H_2S source gas indicated the presence of numerous components in addition to H_2S including COS, several hydrocarbons, methanol, methylformate, CH_3SH, 2-chloropropane, propane-2-thiol, t-butane thiol, propane thiol, CH_3CCl_3, CH_3SSH, H_2S_2, diisopropylthioether, and S_8. The headspace of the absorption reactor contained H_2S, air and only these same contaminants. This implies that exposure of PVBTAF to H_2S does not result in the formation of volatile components. Additional mass spec data provided no positive evidence for the liberation of HF upon exposure of PVBTAF to H_2S. Although this does not rule out the possibility of HF formation, it is thought to be unlikely.

The above GCMS and NMR data implies that PVBTAF is not reacting with H_2S nonetheless something clearly happens when the polymer is exposed to H_2S. Based on the change in solubility of PVBTAF, the above spectroscopic evidence, and the fact that many of the contaminants found in the source gas are more reactive than H_2S, we believe that an impurity in H_2S reacts to crosslink a relatively small portion of the polymer. Efforts are continuing to understand this phenomenon.

3.0 Discovery of New "High Performance" ATMs

Air Products has discovered a new class of proprietary AT materials. They consist of blends of AT polymers and AT salts. Planar composite membranes of these materials met preliminary CO_2 flux and CO_2/CH_4 selectivity targets. Much to our surprise, these blends were clear, apparently homogeneous (by eye) films and could be cast from aqueous or methanlic solutions. Unexpectedly large amounts of the AT salt could be incorporated into the blend, 0.25 to 4 mol per mol of polymer repeat unit. It is rare that equal molar quantities of a salt can be added to a polymer and that apparently homogeneous films can be obtained. Membranes examined visually after permeation testing generally showed no sign of salt crystallization. Two membranes examined by SEM after permeation testing revealed a largely homogeneous surface with some areas of widely scattered crystals and a few regions of crystal clusters.

Permselective properties of one such ATM blend, EXTM6-4, are listed in Table 5-7 in order of increasing AT salt concentration. It can clearly be seen (Figure 5-15) that incorporation of the AT salt significantly increases the CO_2 permeance while maintaining the exceptional selectivity. CO_2 permeances ranged from 25.7×10^{-6} at low pressure to 13.0×10^{-6} at high pressure. Compared with a PVBTAF at similar feed pressures, these represent a 400 to 600% increase in CO_2 permeance. For three different EXTM6-4 compositions, permeance data was collected as a function of feed pressure and this data is plotted in Figure 5-16. As expected, CO_2 permeances increase with decreasing feed pressure.

In much the same way that ATM blends increased CO_2 permeances with no sacrifice of selectivity, increased acid gas permeances were observed when H_2S-containing feeds were used. Membranes containing 0.5, 1, 2, and 4 mole AT salt per mole of AT polymer repeat unit were evaluated with feeds consisting of H_2S, CO_2, and CH_4 and the results are listed in Table 5-8. For each composition, H_2S permeances decrease with increasing pressure. The blend exhibits a 200-700% higher H_2S flux than does PVBTAF (Figure 5-17).

Table 5-7
CO_2 Permselective Properties of EXTM6-4 Composites at 23°C

AT salt (mol/mol)	feed P(psig)	CO_2 P(cmHg)	$(P_o/l)\cdot10^6$ cc/cm^2•s•cmHg CO_2	H_2	CH_4	Selectivity CO_2/H_2	CO_2/CH_4
0.25	2.6*	29.4	8.78	0.0644	nd	136	-
(12836-14-4)	17.8*	55.3	6.58	0.0625	nd	105	-
	29.9*	76.0	5.87	0.0646	nd	91	-
	39.8*	92.8	5.30	0.0647	0.00325	82	1630
	77.7*	157.4	3.75	0.0620	0.00325	60	1150
0.5	2.8	27.7	9.94	0.0296	nd	335	-
(12575-93-2)	14.3	45.9	8.46	0.0290	nd	291	-
	25.0	62.9	7.10	0.0273	0.00413	260	1720
	39.7	86.2	5.92	0.0249	0.00337	238	1760
	85.9	159.4	4.30	0.0329	0.00361	131	1191
	107.0	192.9	3.45	0.0350	0.00399	99	866
1.1	5.5	32.0	13.0	0.107	nd	122	-
(12836-3-3)	21.1	56.7	10.8	0.102	nd	106	-
	39.8	86.4	9.18	0.102	0.00864	90	1060
	53.5	108.7	7.57	0.0888	0.00421	85	1800
	81.0	151.7	6.05	0.0831	0.00524	73	1150
return to	37.4	82.6	8.96	0.0934	0.00626	96	1430
2.0							
(12836-22-3)	39.7*	92.7	10.2	0.0973	0.00764	105	1340
4.0	3.2**	30.6	25.7	0.203	0.0438	127	588
(13100-41-2)	15.9**	52.4	24.1	0.228	0.0535	106	450
	26.0**	69.7	21.9	0.218	0.0469	100	466
	40.0**	93.8	21.5	0.238	0.0511	90	420
	54.9**	119.3	19.1	0.248	0.0425	77	449
	94.6**	187.4	13.0	0.299	0.0350	43	370
return to	40.2**	94.1	15.9	0.306	0.0560	52	284

feed: 30.6% CO_2, 34.4 % CH_4 in H_2 or (x)
* 32.9% CO_2, 32.6% CH_4, in H_2 or
** 33.1% CO_2, 33.1% CH_4 in H_2;
P/Po=0.3

Figure 5-15

Effect of ATM-AT Salt Blends on CO_2 Permeance

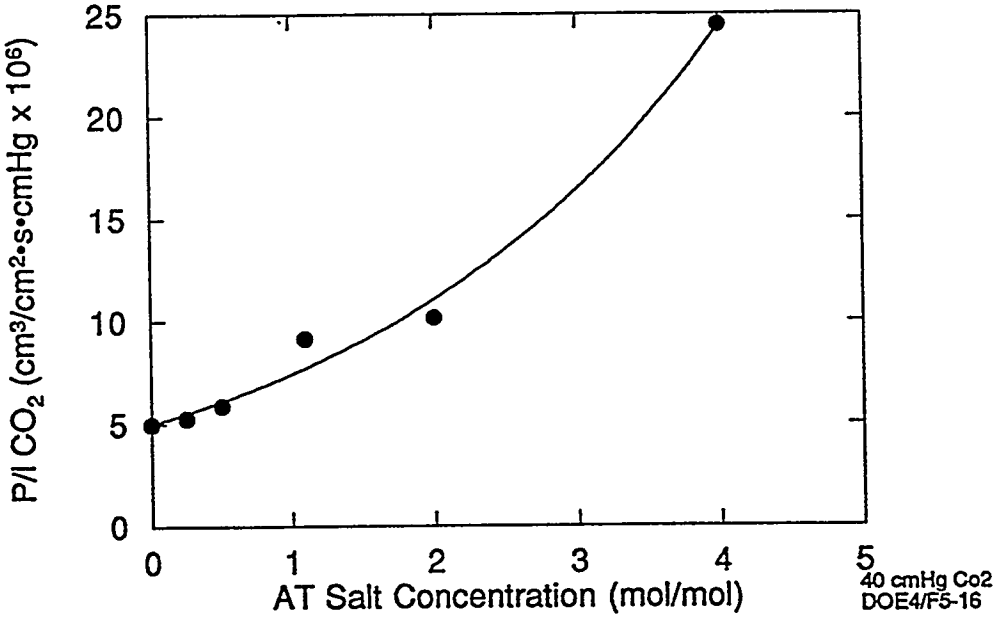

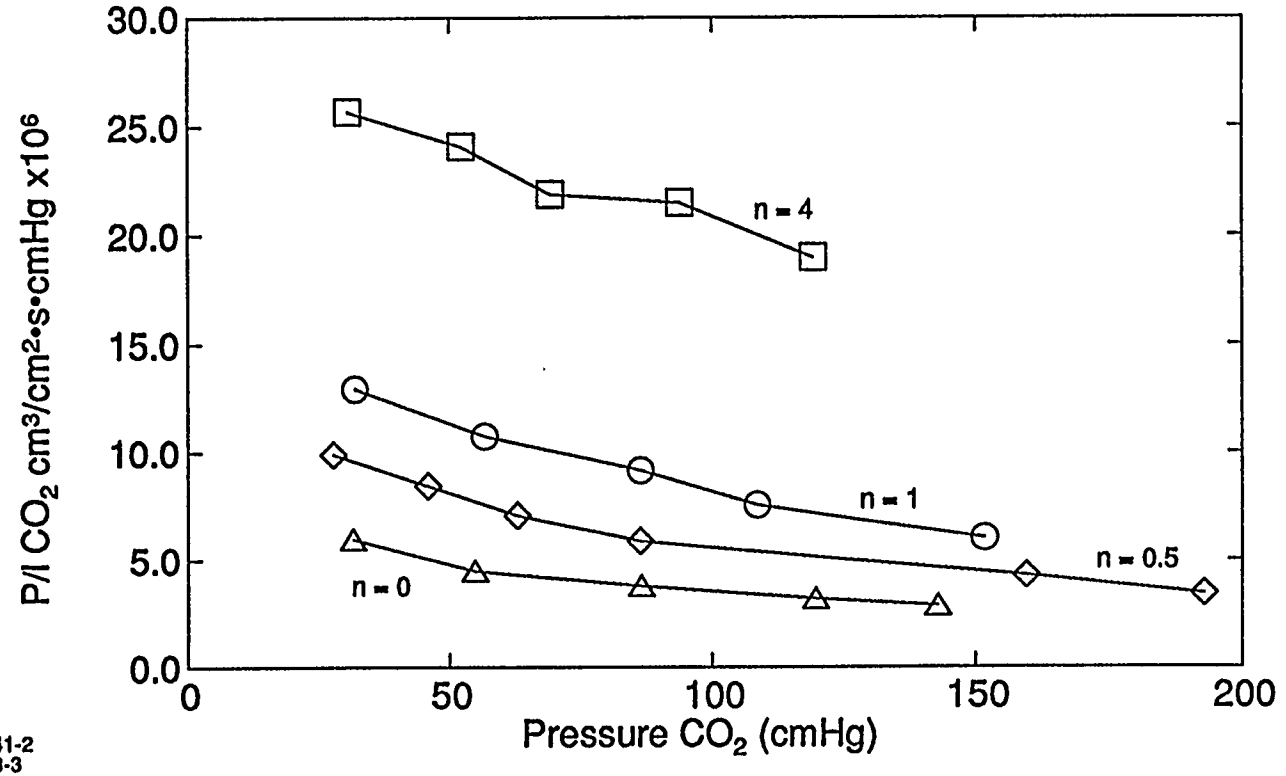

13100-41-2
12836-3-3
12575-93-2
12484-76B

DOE4/F5-16

Figure 5-16
CO_2 Permeance of EXTM6-4 Composite Membranes
as a FunctionΛT Salt Concentration
(n= mol salt/mol polymer)

Table 5-8

H_2S Permselective Properties of EXTM6-4 Membranes at 30°C

membrane	feed P(psig)	H_2S P(cmHg)	CO_2 P(cmHg)	$(P_o/l)\cdot10^6$ cc/cm^2•s•cmHg H_2S	CO_2	CH_4	Selectivity H_2S/CO_2	H_2S/CH_4
0.5	19.6	17.6	17.7	7.06	1.41	nd	5.0	700#
(12836-11-3)	72.3	44.5	45.0	3.50	0.767	nd	4.6	700#
	91.2	54.2	54.8	3.55	0.496	nd	7.2	700#
1.0	20.6	18.1	18.3	33.2	6.77	0.0637	4.9	521
(12836-3-4)	46.8	31.5	31.8	25.3	5.14	0.0550	4.9	460
	70.9	43.8	44.3	23.2	4.06	0.0551	5.7	420
	105.5	61.5	62.1	18.6	3.86	0.0509	4.8	364
2.0	40.7	28.5	28.6	4.44	0.513	nd	8.7	500[a]
(12836-22-3)	48.1	32.3	32.5	4.17	0.260	nd	16.1	500[a]
	39.7*	0	92.7	-	10.2		-	-
4.0	1.1	8.1	8.2	91.6	8.91	nd	10.3	-
(13100-41-2)	25.7	20.8	20.9	73.6	8.83	nd	8.3	-
	35.4	25.7	25.9	57.3	8.30	nd	6.9	-
	50.2	33.3	33.6	42.0	9.03	nd	4.7	4200[a]
(13100-41-4)	1.6	8.4	8.4	155.0	17.8	nd	8.7	nd
	19.6	17.6	17.8	101.0	16.0	0.0457	6.3	222

feed: 9.9% H_2S, 10.0% CO_2 in CH_4 or
* 32.9% CO_2, 32.6% CH_4 in H_2
P/Po=0.2
No CH_4 detected; selectivity based on calculated maximum CH_4 P_o/l of 0.0098

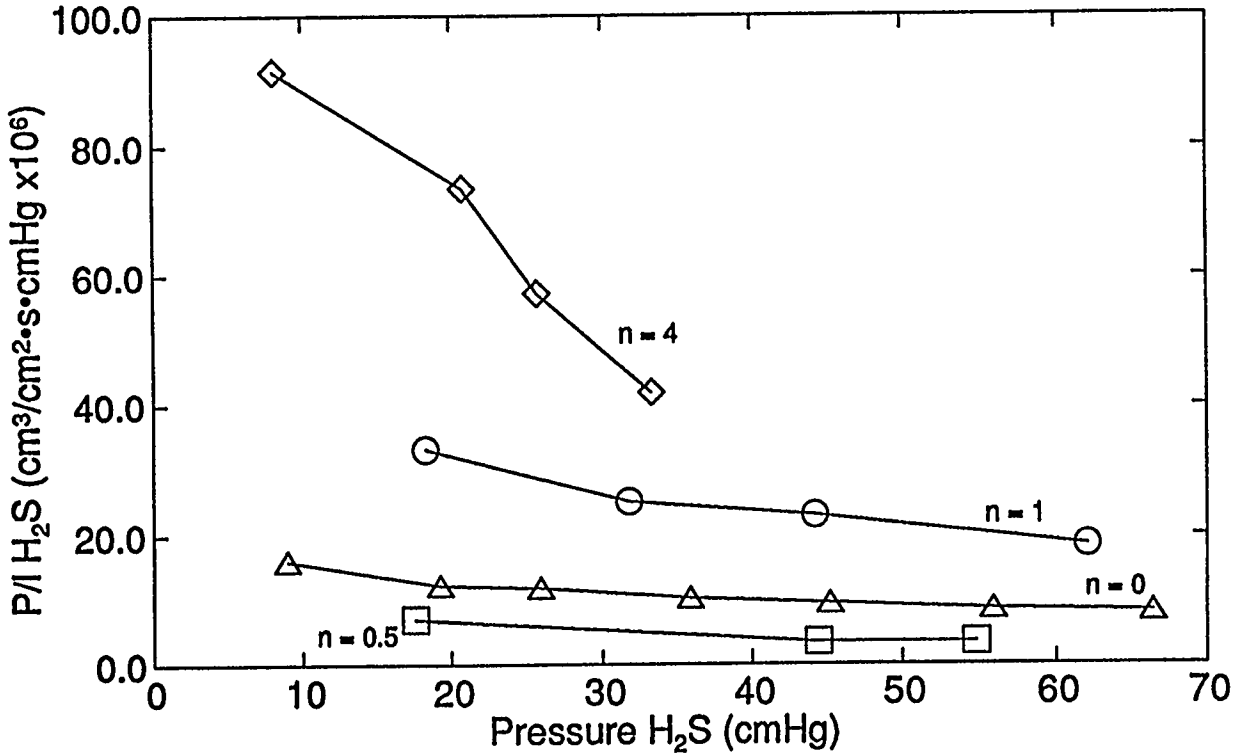

membranes: 12582-40, 12836-11-3, 12836-3-4, 13100-41-2

Figure 5-17
H2S Permeance of EXTM6-4 Composite Membranes as a Function of AT SAlt Concentration
(n=mol salt/mol polymer)

VI. Process Application Development and Technology Benefits - Upgrading Subquality Natural Gas

The objective of this task was to determine the technology benefit that could be derived by applying ATM technology to natural gas processing. This effort comprises the development of a semi-empirical computer model of the gas permeation mechanism and development and evaluation of a process flowsheet.

1.0 Computer Modeling of Active Transport Membranes

The permeation mechanism of ATMs is significantly different from that of conventional (solution-diffusion) polymeric membranes. The mathematical models describing gas permeation through polymeric membranes cannot be applied to AT systems. Like traditional facilitated transport systems, ATM involves coupled chemical reaction and diffusion. However, the current mathematical models of gas transport through facilitated transport systems require detailed knowledge of the chemical complexation products, the kinetics of reaction, and the diffusion coefficients of all chemical species. The fundamental chemistry of ATM has not been developed to the extent necessary to use these models. Therefore, the first element of this task was to develop a semi-empirical computer model of gas permeation in Active Transport membranes. Using laboratory data measured on planar membrane coupons, correlations were derived between the key experimental variables (CO_2 and H_2S partial pressure and gas stream humidity). This model formed the basis for estimating ATM performance, setting preliminary performance targets, calculating the membrane area required for a separation, determining product recovery, and estimating the separation cost. A more rigorous model will eventually have to be developed.

1.1 Model Development

The ATM permeation model assumes reaction equilibria and then correlates permselectivity at various values of P/Po. Details of the model can be found in Appendix A. Briefly, the model is of the form:

$$N = P/\ell \bullet \Delta P \bullet R \bullet F$$

where N = local CO_2 flux
P/ℓ = CO_2 permeance
ΔP = partial pressure driving force
R = semi-empirical P/Po correlation factor
F = facilitation factor (F>1 for CO_2 and H_2S; F<1 for CH_4)

As indicated earlier, R and F were derived from experimental data. It is important to note that when this model was derived only limited information was available on the P/Po dependence of $\alpha(CO_2/CH_4)$ and, thus, the results described below are tentative and, in this respect, need further verification. The model will be updated early in the next phase of this work.

1.2 Results

The model predicted CO_2 permeance is compared to the experimental data in Figure 6-1. The model adequately represents the experimental data as a function of CO_2 partial pressure in the range 100-400 cmHg and P/Po 0.16-0.45. In Figure 6-2 the predicted CO_2 and CH_4 permeance is compared to experimental values as a function of P/Po for a constant CO_2 partial pressure. Again, the fit is good within the range of experimental data. Additional experimental data outside this range is needed to extend the range of operating variables and increase confidence in using the model as a predictive tool.

Figure 6-1

Experimental and Model Predicted CO_2 Permeance of PVBTAF MLC at 34° C

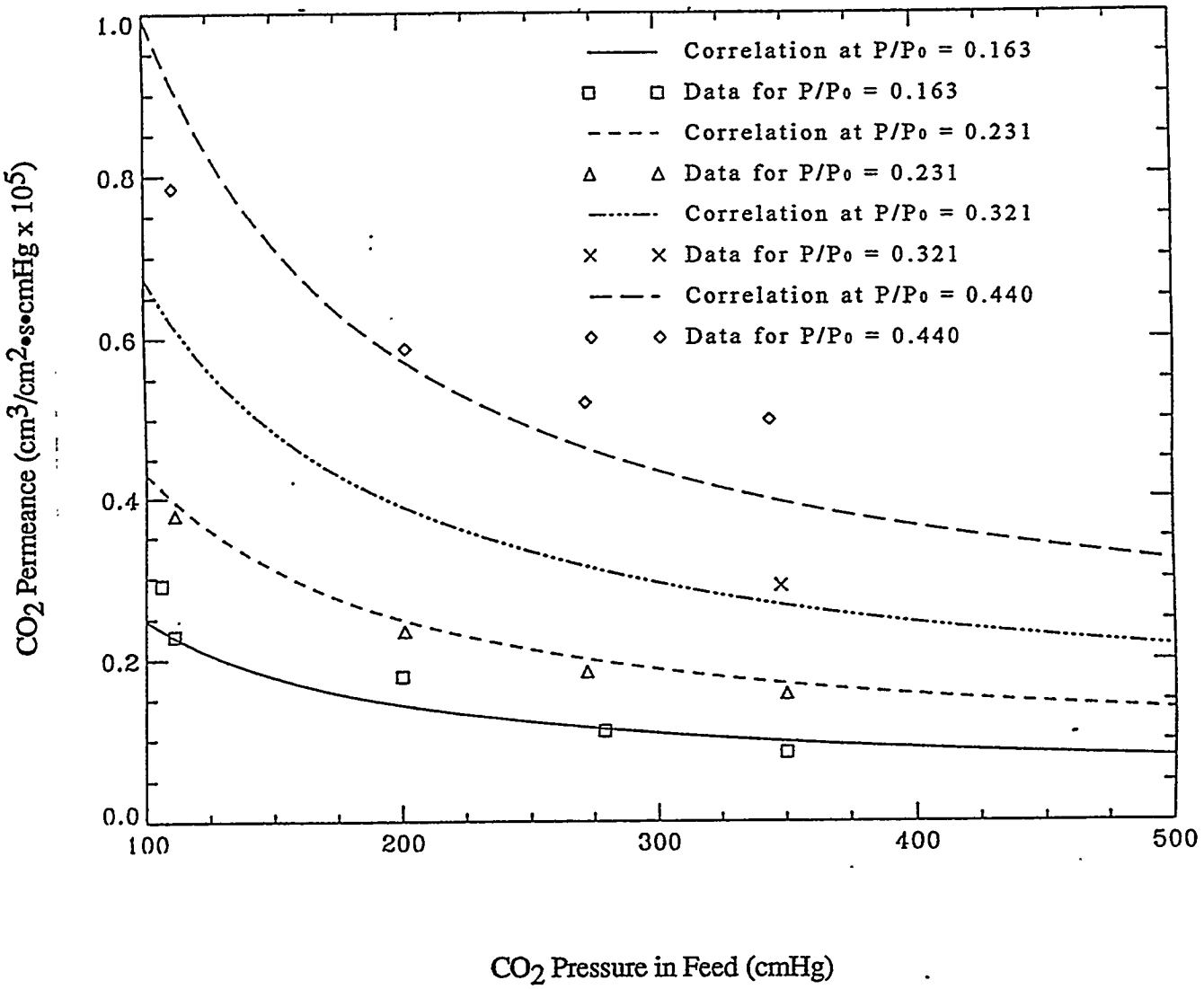

Figure 6-2
Experimental and Model Predicted CO_2 and CH_4 Permeance as a Function of P/Po

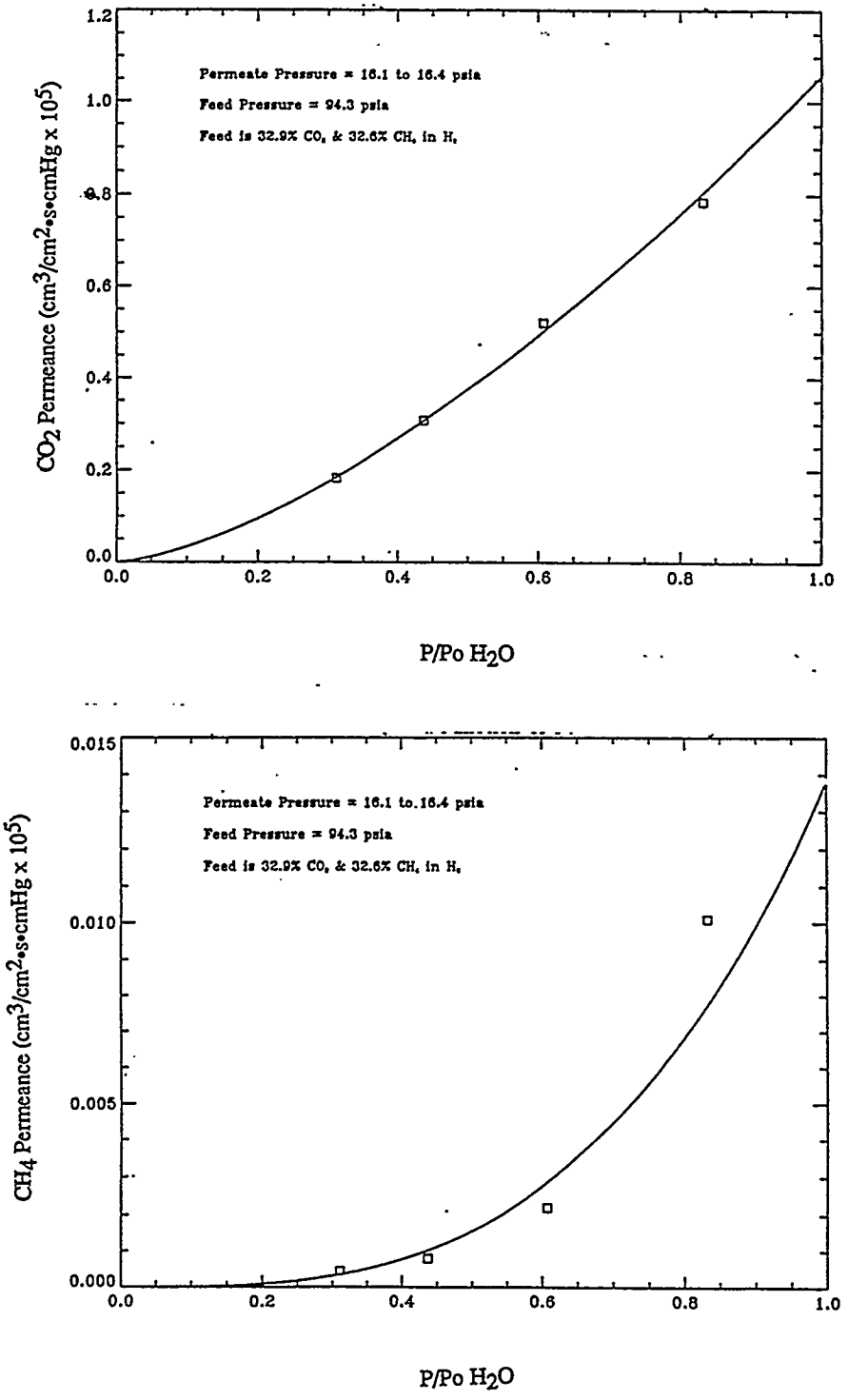

2.0 ATM Process for Upgrading Natural Gas

2.1 Test Case: Upgrading 6.5% CO_2 in CH_4

The simulation used the model described above. Two additions to the model were necessary:

1) The feed gas to the membrane was saturated with H_2O. The H_2O permeability of the ATM was assumed to be 250×10^{-6} $cm^3/cm^2 \cdot s \cdot cmHg$ and independent of pressure.

2) The model was expanded to vary the concentration of CO_2, CH_4 and H_2O in the feed and permeate gas as function of position in the module.

The test case used a natural gas feed containing 6.5% CO_2 at 800-1000 psig at 150 MMSCFD. The goal was to provide at least 20% lower gas processing costs than competing technologies. Additional design specifications were to maintain hydrocarbon losses at less than 1% and power at less than 25 BHP per MMSCFD. The natural gas product specification was 2% CO_2. Module productivity was assumed to be > 0.5 MMSCFD per module.

The process flowsheet is shown in Figure 6-3. After removing condensable components, gas is fed to the ATM at 834 psia. The nonpermeate stream is pipeline quality CH_4 at 822 psia. The membrane permeate is further processed to recover CH_4. It is recompressed from 17 to 864 psia and fed to a second, much smaller, membrane. Permeating CO_2 is vented and the CH_4 - enriched permeate is recycled.

We have found a number of advantages of the idealized ATM-based process:

- **Fewer modules.** Figure 6-4 shows that the optimized ATM requires ≈50% fewer modules than conventional membranes.

- **Less energy**. Figure 6-5 compares the power requirements for the current membrane technology and ATM. An optimized ATM would require about one-half the energy of other membrane systems.

Figure 6-3

Process Flow Diagram: CO_2 Separation from Natural Gas by ATMs

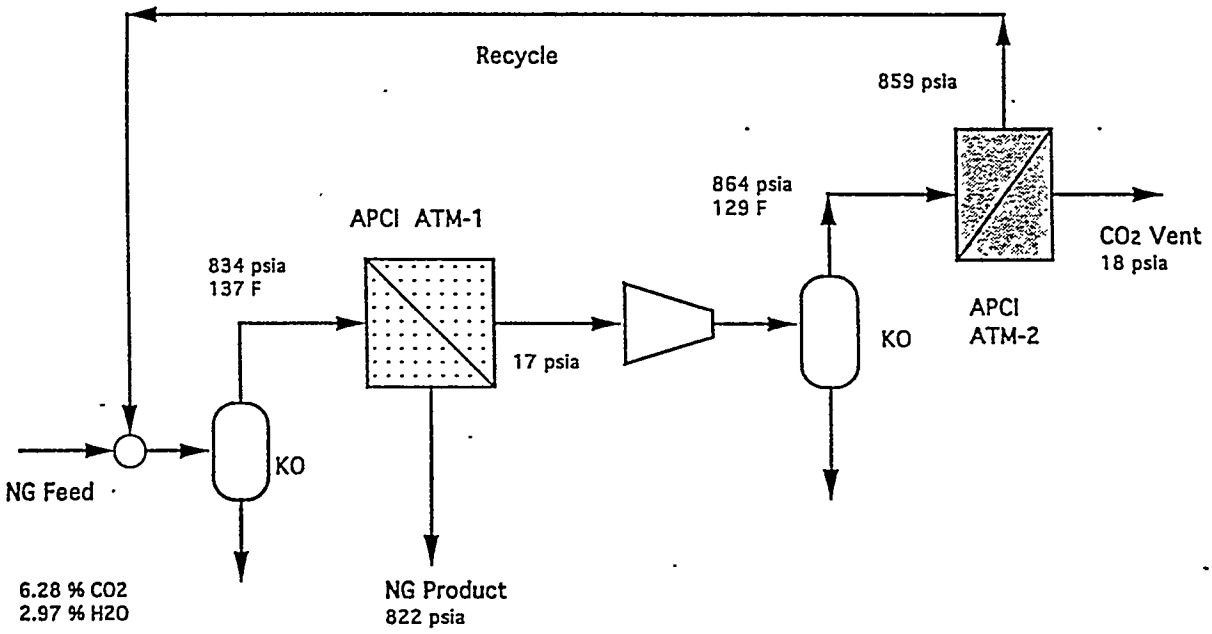

Figure 6-4

Number of Modules

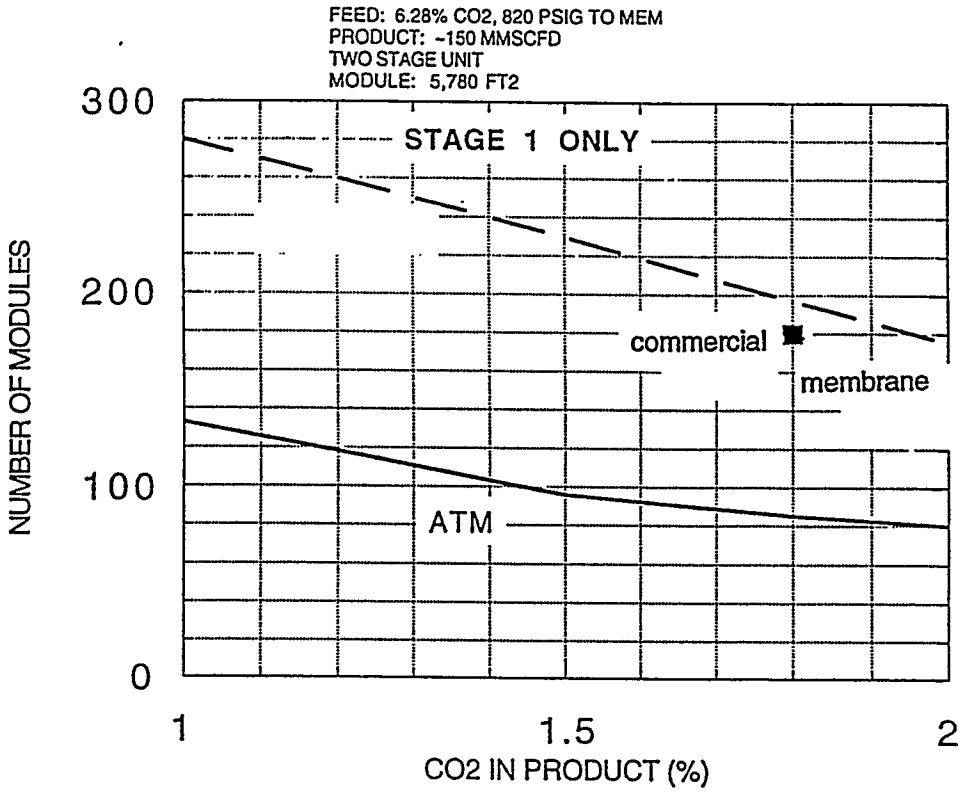

Figure 6-5

Compressor Power

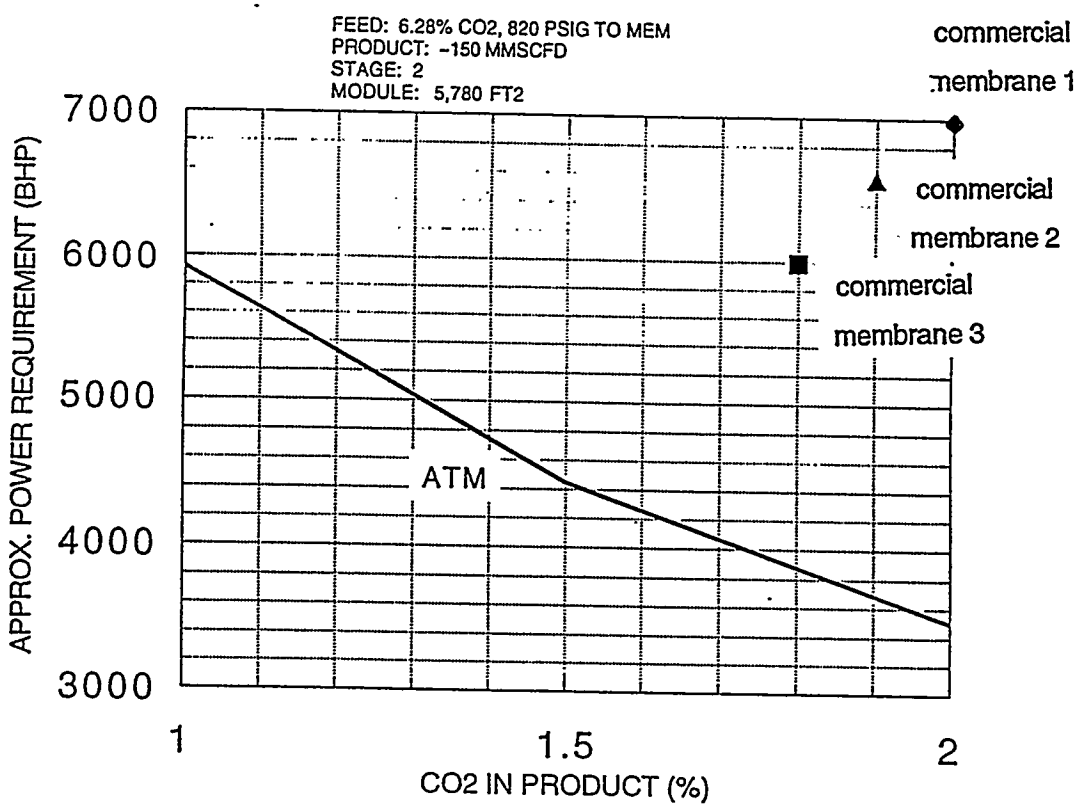

• **Lower product loss.** The inherently high selectivity of the ATM manifests itself as low CH_4 loss (Figure 6-6). Thus, the ATM system has a high CH_4 recovery.

The gas processing costs of the ATM system are compared to diethanolamine (DEA) as a function of capacity in Figure 6-7. An ATM system would be an attractive option for a wide variety of feed rates. By contrast, the market niche for conventional membranes is generally considered to be less than about 10 MMSCFD[39]

2.2 Preliminary ATM Targets

Based on computer modeling to date and the above test case, preliminary permeance targets have been set for the ATM. Since ATM performance is a function of several process variables, this target is not a simple P/ℓ, α combination as it would be for a conventional polymeric membrane. The preliminary ATM permeance target is shown as the solid curve in Figure 6-8. Also shown in Figure 6-8 is the laboratory performance of ATM coupons and hollow fiber modules. Currently, neither PVBTAF planar coupons nor hollow fiber modules meet the performance target, however, it is anticipated that further improvements in membrane fabrication (e.g. thinning the ATM layer) will improve their CO_2 permeance. An attractive ATM material option is the recently discovered EXTM6-4. Planar composite coupons of this ATM do meet the preliminary permeance target. It will interesting to see if hollow fiber modules also exhibit this improved performance.

3.0 Recommendations

The results to date demonstrate the effectiveness of an optimized ATM system. It is important to note that certain assumptions were made in this analysis. It will be critical to verify these assumptions in the next segment of this program. Such a program should address:

[39]R.W. Spillman et.al., "Gas Membrane Process Optimization", presented at the AIChE mtg., New Orleans, LA, March 9, 1988.

Figure 6-6
Hydrocarbon Loss

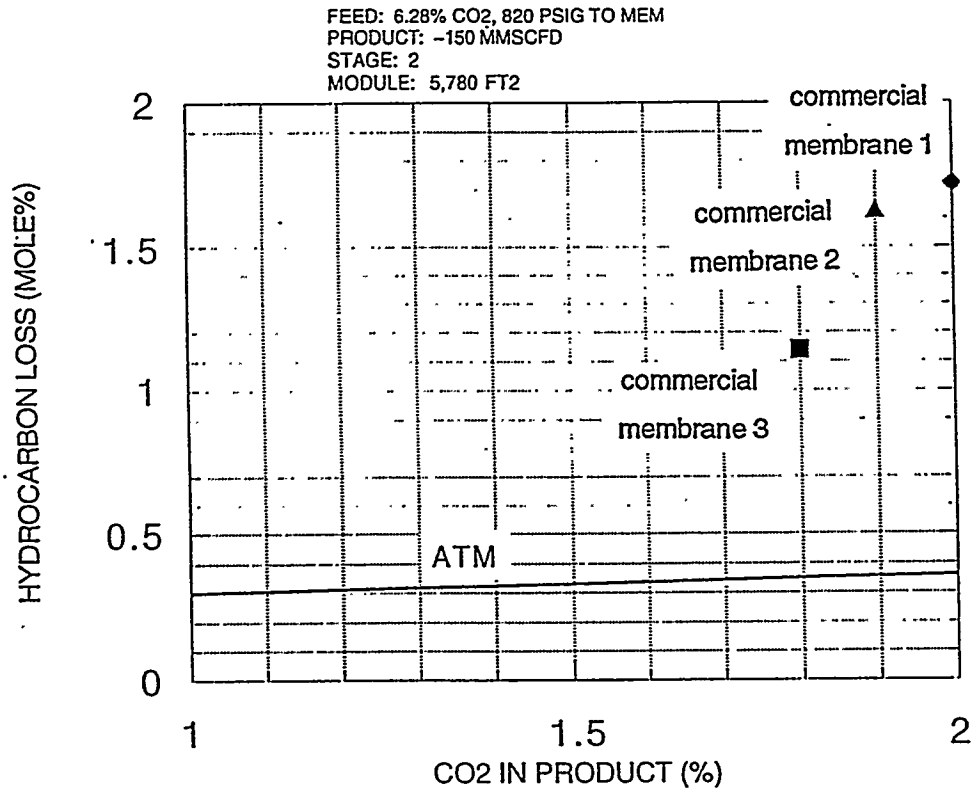

Figure 6-7

Economics of ATM and DEA Systems for CO_2 Separation from Natural Gas

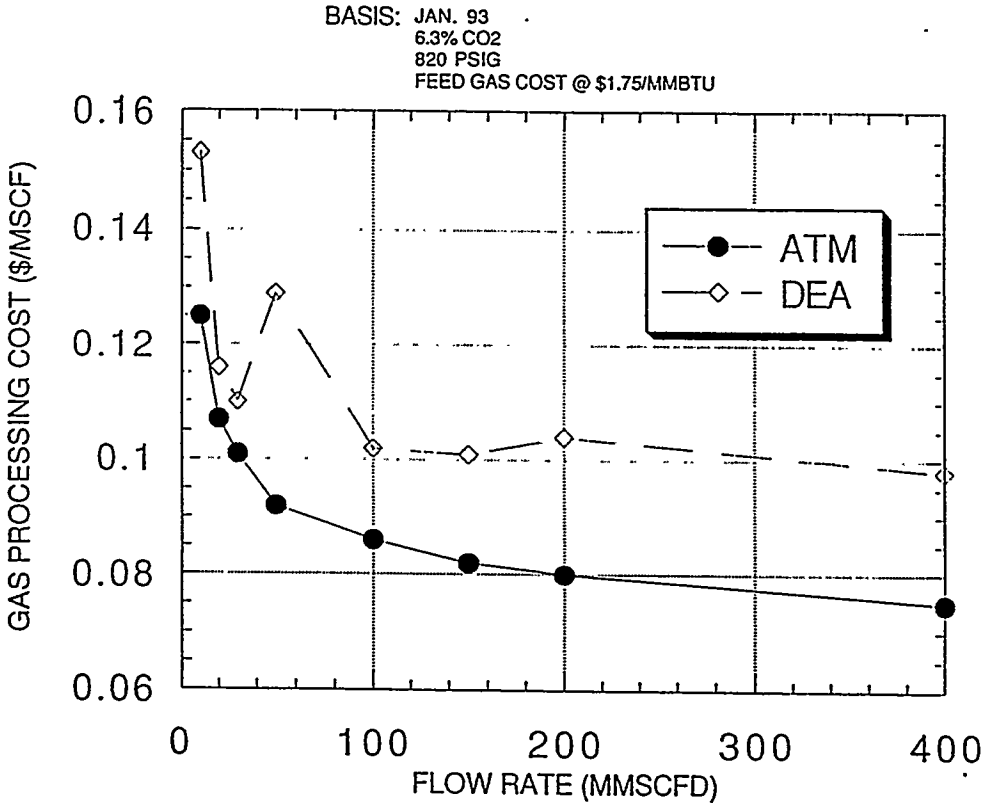

Figure 6-8

Comparison of Laboratory Properties to Targets

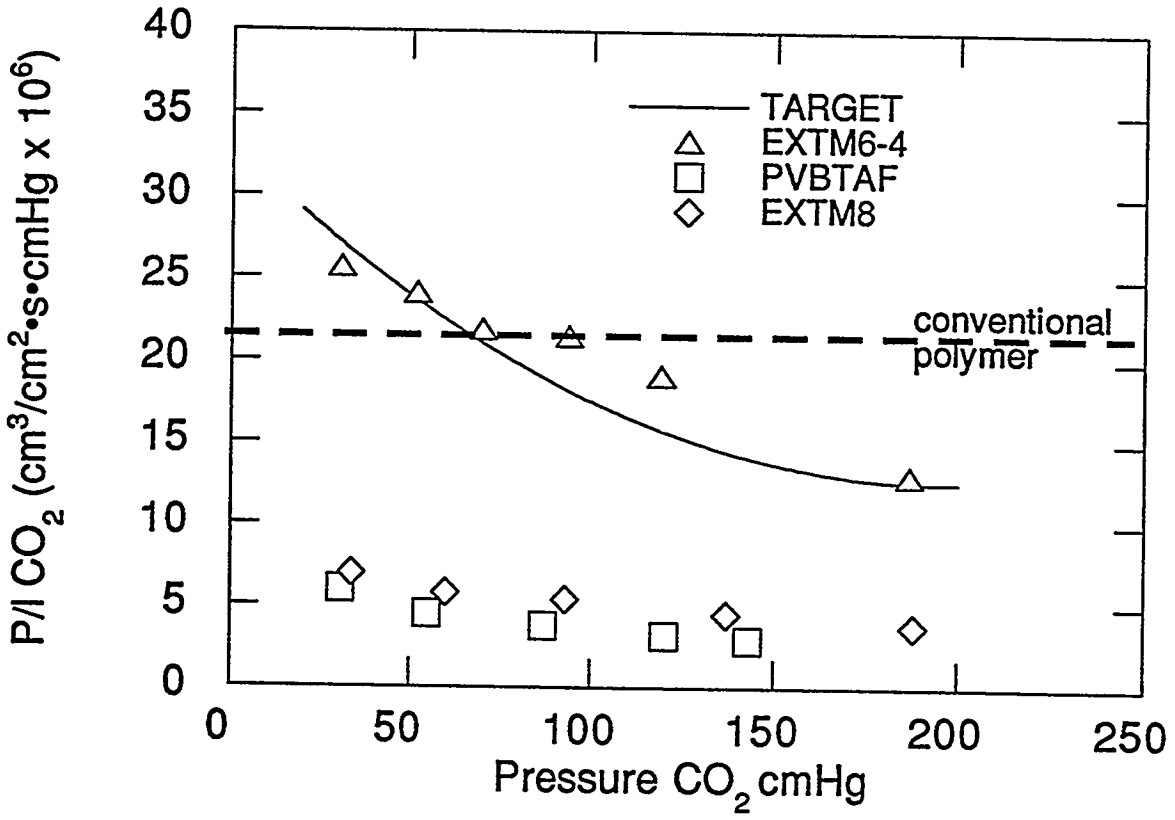

• **Experimentally determine the H_2O permeance of the ATM.** Since water plays a critical role determining ATM permselectivity, it will be essential to have an experimental value for this parameter. The rate at which the ATM permeates water from the gas stream may have a large effect on the membrane area and, hence, gas processing costs.

• **Experimentally determine ATM performance at extremes of P/Po and incorporate into model.** Work to date has focused on ATM performance in the P/Po range 0.2 to 0.6. An ATM module will also have to function outside this range. The current ATM computer model extrapolates into this range from the current dataset. It will therefore be essential to experimentally measure these properties.

• **Examine process variable sensitivity to processing costs.** A follow-on program should address the impact of gas composition, flowrate and membrane selectivity on the natural gas processing cost. Additionally, that analysis should compare the cost of using conventional amine scrubbing and membrane technology.

VII. Commercial Opportunities

Air Products researchers have identified AT membranes which selectively permeate CO_2 from CH_4 and H_2, H_2S from CH_4 and H_2, and NH_3 from N_2 and H_2. Throughout this program commercial development activities have focused on identifying and evaluating industrial applications for ATM, understanding market needs and forces, and setting ATM performance criteria. The following sections describe potential large-scale commercial opportunities for ATM technology.

1.0 Upgrading Subquality Natural Gas

1.1 Recent Market Trends

Background information on the natural gas industry, including size and competition for gas treating, was detailed in a previous report.[29] An update is summarized below.

- *US Consumption and domestic production growing.* Table 7-1 summarizes US natural gas consumption, domestic production and import data since 1987.[40] US consumption is expected to increase nearly 4% in 1994 to 21.1 trillion cubic feet (60,285 MMSCFD). This is the highest consumption level since 1974. Domestic production is expected to increase by 2% in 1994 to 18.8 trillion cubic feet (53,715 MMSCFD). Since 1986, domestic production has been growing at about 2.4% each year, or between 1000 and 1500 MMSCFD. Increased domestic production is expected to meet only about one-half of the increase in demand. The balance will be made up by new imports. Canadian imports will account for roughly 11% of US consumption in 1994.

- *"Gas Bubble" (in capacity) is over.* Figure 7-1 shows US production capacity and utilization rates for the last 8 years. Domestic production capacity surpassed production for this period. The low utilization rate period was commonly termed the

[40]U.S. Chemical Outlook, U.S. Dept. of Energy, Energy Information Administration, 1994.

gas bubble. Recent data estimate utilization rates will near 100%; projected growth in production will require construction of new processing plants.[41]

Table 7-1
U.S. Natural Gas Consumption and Production
(Dry Gas Basis)

	Consumption		Production	
Year	Trillion CFY	MMSCFD	Trillion CFY	MMSCFD
1987	17.21	47,151	16.62	45,534
1988	18.03	49,397	17.10	46,849
1989	18.80	51,507	17.31	47,425
1990	18.72	51,288	17.81	48,795
1991	19.13	52,411	17.75	48,630
1992	19.75	54,110	17.78	48,712
1993*	20.36	55,781	18.41	50,438
1994**	21.10	57,808	18.78	51,452

* estimate
** forecast

1.2 Natural Gas Impurities

Natural gas is obtained from three types of wells: 1) oil wells in which natural gas is associated with oil (associated gas), 2) wet gas wells, which are predominantly natural gas but also produce natural gas liquids (NGLs), and 3) "dry" gas wells which contain low concentrations of heavy hydrocarbons (though the gas is still H_2O saturated). Sources 2 and 3 are collectively termed non-associated gas production. In the US, non-associated gas accounts for 80 to 85% of domestic production. Wellhead gas contains various impurities that must be removed before transmission by pipeline including:

[41] SRI, International, Chemical Economics Handbook, CEH Product Review, Natural Gas, June 1993.

Figure 7.1

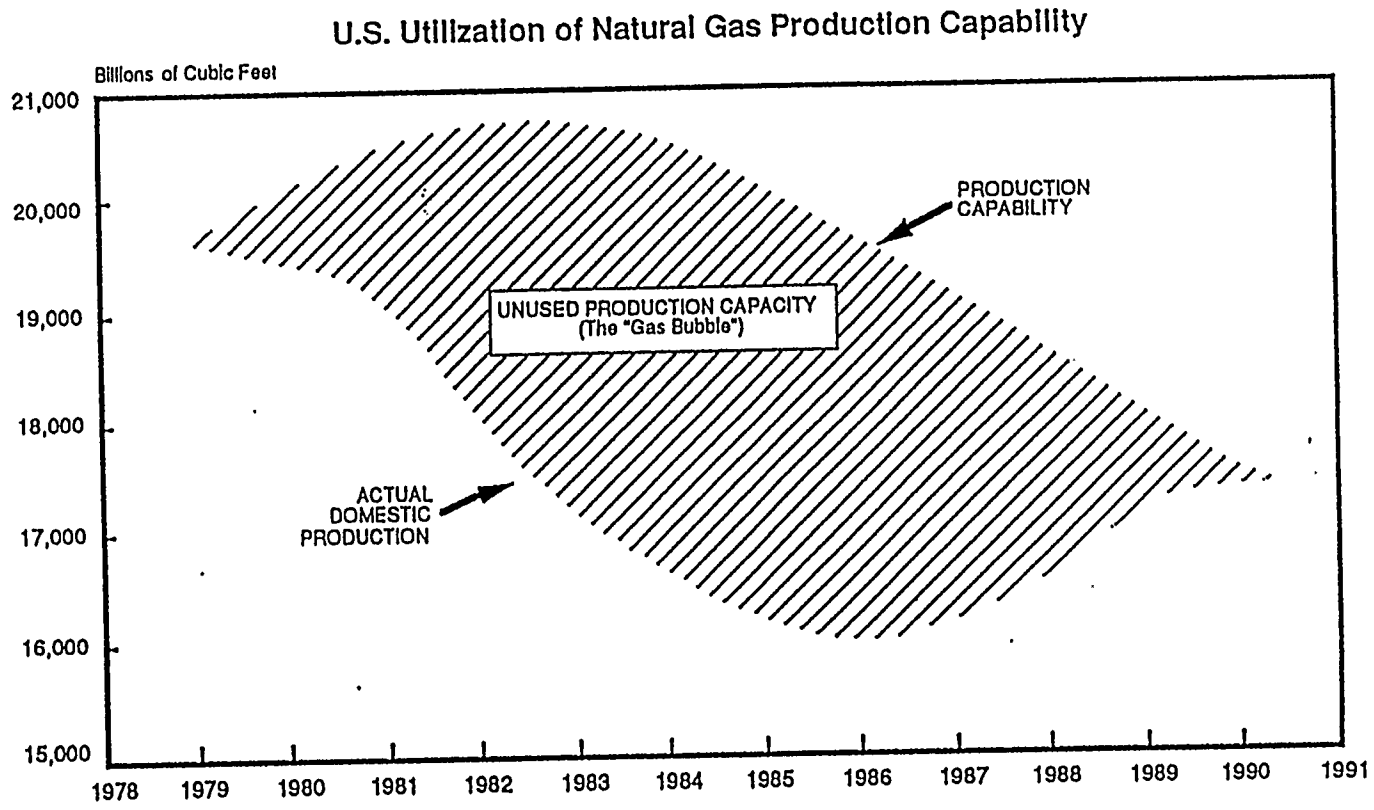

Source: Reference 43

H_2O: Wellhead gas is saturated with water. Gas dehydration is necessary to prevent hydrate formation and corrosion in transmission pipelines. The industry standard is 4 - 7 lbs H_2O per MMSCF of natural gas ($\approx$ 85 - 150 ppm H_2O). The lower specification is typical for northern pipelines due to lower temperatures.

CO_2: The concentration of CO_2 in transmission pipelines is controlled to prevent corrosion and to maintain a high heat value. The most common CO_2 specification is <3 vol%, however, some pipelines limit CO_2 to less than 2 vol%.

H_2S: Most pipeline companies specify a maximum concentration of 4 ppm H_2S. There is also a limit on mercaptans and total sulfur content of the treated gas. Gas treating plants at highly contaminated wells employ a method to convert H_2S to elemental sulfur which can then be sold or disposed.

In 1994, the Gas Research Institute (GRI)[42] estimated gas treating needs for non-associated gas production and reserves using 1988 data (Table 7-2). A large fraction of natural gas (nearly 75% of non-associated 1988 production) required only dehydration. Only 15% of 1988 non-associated gas production needed CO_2 removal. However, by comparing the GRI data for production vs. reserves, it can be seen that the fraction of raw gas needing acid gas removal is expected to increase as the US begins to consume lower quality reserves.

The GRI report did not consider H_2S-containing sources. We met with representatives from GRI to estimate the fraction of gas likely to require H_2S removal. Table 7-3 contains our estimates for the 1988 proven reserves. The data can be summarized as follows:

62% of non-associated gas reserves will require dehydration only.
3% of the gas will require both H_2S treating and dehydration.
10% of the gas will require only CO_2 treating and dehydration.
7% of the gas requires CO_2 and H_2S treating, and dehydration.
18% of the gas is high in N_2 and/or CO_2 and H_2S.

---

42 "Chemical Composition of Discovered and Undiscovered Natural Gas in the Lower-48", Gas Research Institute, 1994.

Table 7.2

US Natural Gas Production and Reserves Data

	1988 Proven Reserves	1988 Production	Undiscovered and Undeveloped Gas Resource	Discovered / Non-Producing Low Quality Gas Resource
		-- All numbers in Trillion SCF --		
High Quality	95.1	10.81	376.9	0
High N2 Only	19.25	1.32	35.2	0
High CO2 Only	24.05	2.18	167.6	1
High N2+High CO2	4.12	0.31	16.6	134
High N2+CO2 Total	1.44	0.09	3.1	0
Totals	**144**	**14.7**	**599.4**	**135**

Definitions:

1. High Quality gas contains less than 2%CO2, and less than 4% N2.
2. High N2 ONLY gas contains more than 4%N2, and less than 2% CO2.
3. High CO2 ONLY gas contains less than 4%N2, and more than 2% CO2.
4. High N2 + High CO2 gas contains more than 4%N2, and more than 2% CO2.
5. For High N2 + CO2 Total gas, % N2 + % CO2 is more than 4.

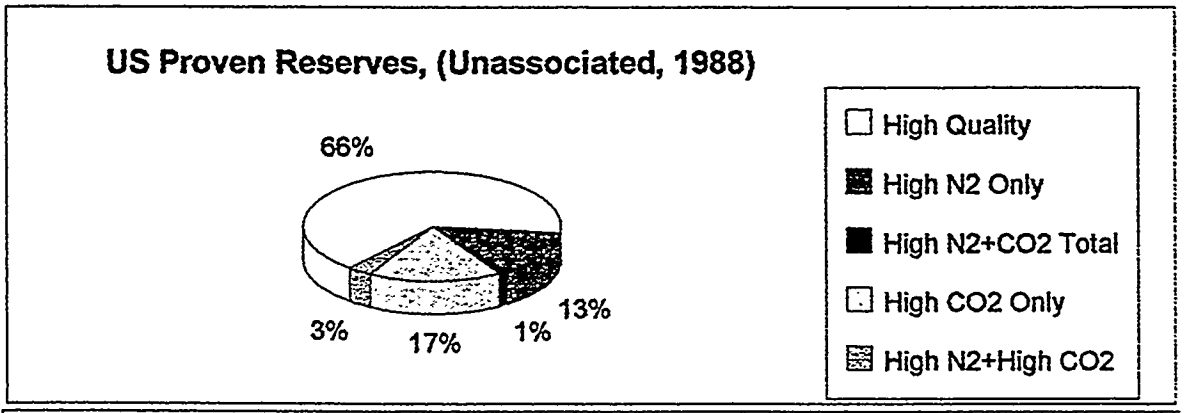

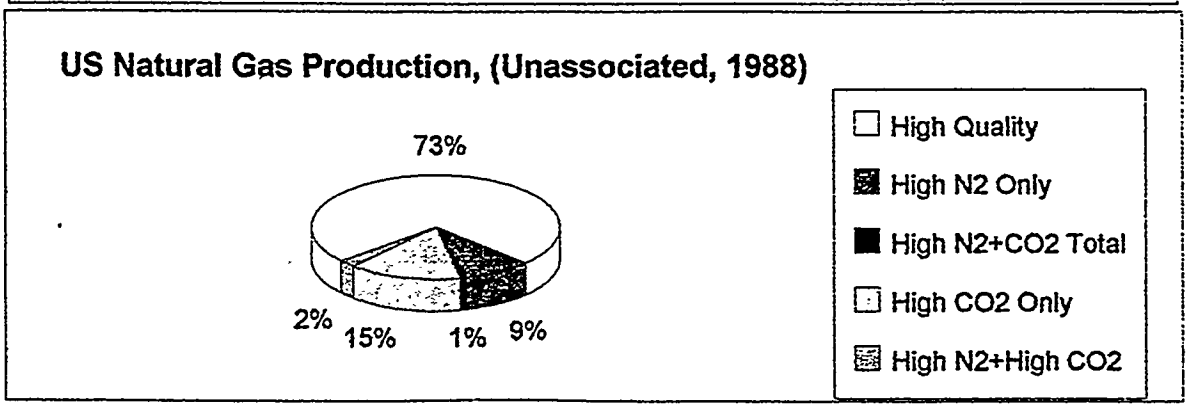

Table 7.3

Non-Hydrocarbon Impurities Estimate for US Natural Gas Reserves

Gas Type	1988 Production	1988 Proven Reserves Total	1988 Reserves H2S Treating Needed	1988 Reserves No H2S Treating
	– All numbers in Trillion SCF –			
High Quality	10.81	95.1	5	90.1
High N2 Only	1.32	19.25	2.4	16.85
High CO2 Only	2.18	24.05	9.6	14.45
High N2+High CO2	0.31	4.12	2.2	1.92
High N2+CO2 Total	0.09	1.44	0.5	0.94
Totals	**14.7**	**144**	**19.7**	**124.3**

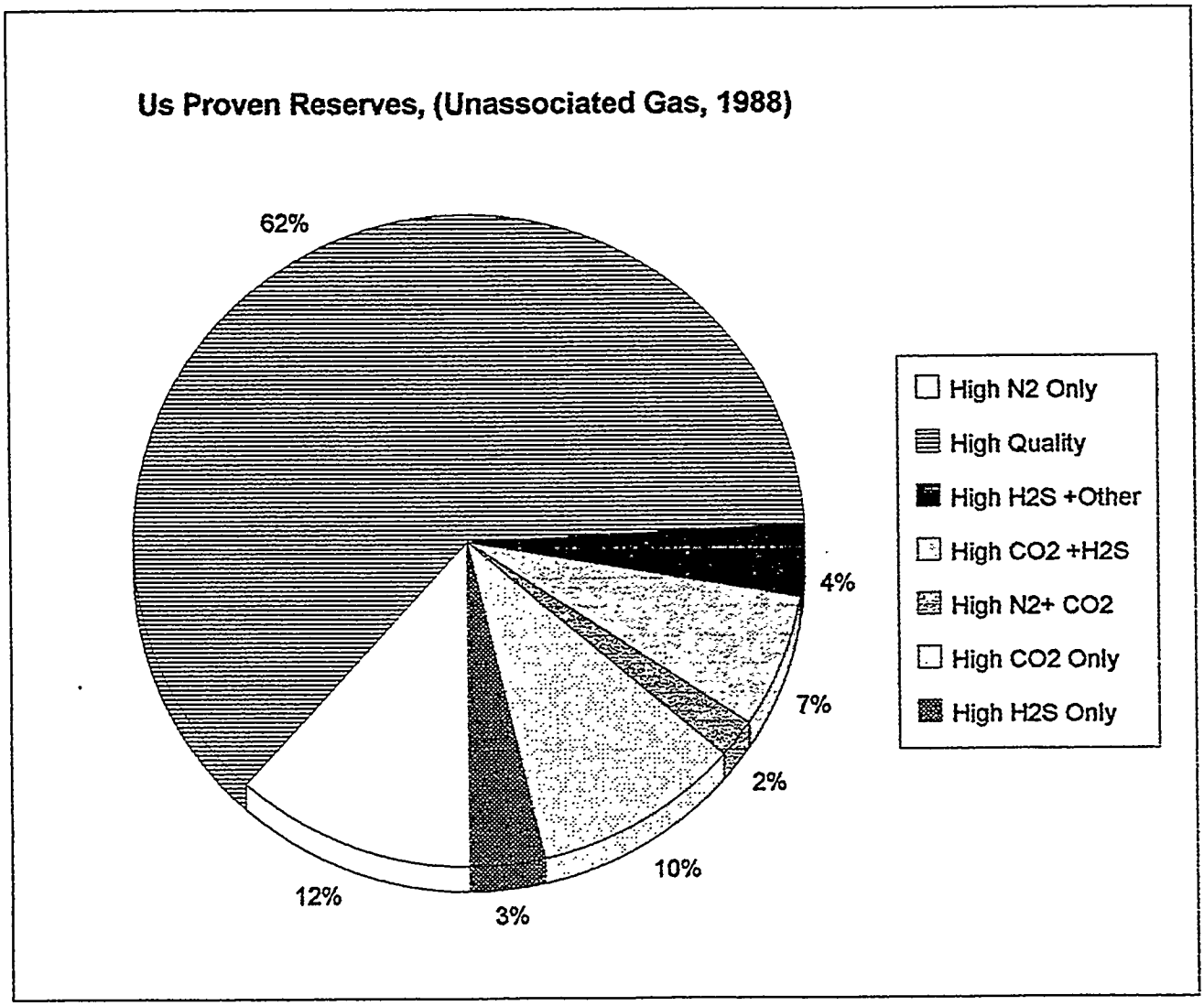

1.3 Natural gas treatment costs

Figure 7-2[43] shows how the price of natural gas increases as it passes from producer to consumer. In 1991, the composite well head price for natural gas was around $1.59 per MSCF. Today it is ≈ $1.65 per MSCF. Some portion of the price is related to the cost of upgrading raw gas to pipeline specifications. A recent presentation at the 73rd Annual Gas Producers Association Conference,[44] estimated gas treating costs for commonly used acid gas treating processes. A summary of the total treatment cost (operating + recovered capital) is provided in Table 7-4.

Table 7-4
Natural Gas Treatment Costs at 10 MMSCFD

Impurity	Treatment Process	Treatment Cost in $/MSCF
H_2O	Glycol Dehydration	0.04 (@ >10 MMSCFD) 0.09 (@ <1 MMSCFD)
CO_2 (2-7%), H_2O	Amine Scrubbing (DEA) + glycol dehydration	0.20 (10 MMSCFD)
CO_2, (6%) H_2S (1%), H_2O	Amine Scrubbing + Liquid Oxidation + Glycol Dehydration	0.50 (10 MMSCFD)
CO_2 (3%), H_2S(3%), H_2O	Amine Scrubbing + Claus Process + Glycol Dehydration	0.47 (10 MMSCFD)
N_2	Cryogenic + Glycol Dehydration	0.85 (10 MMSCFD)

Source: reference no. 44

[43]Natural Gas Monthly, U.S. Department of Energy, Energy Information Administration, March 1992, in "Chemical Economics Handbook", SRI International, (June 1993.)
[44]Tannehill et. al. "Cost of Conditioning your Natural Gas for Market" presented at 73rd Annual GPA Convention, March 1994.

Figure 7.2

Natural Gas Prices In the United States—1991
(national average price per thousand cubic feet)

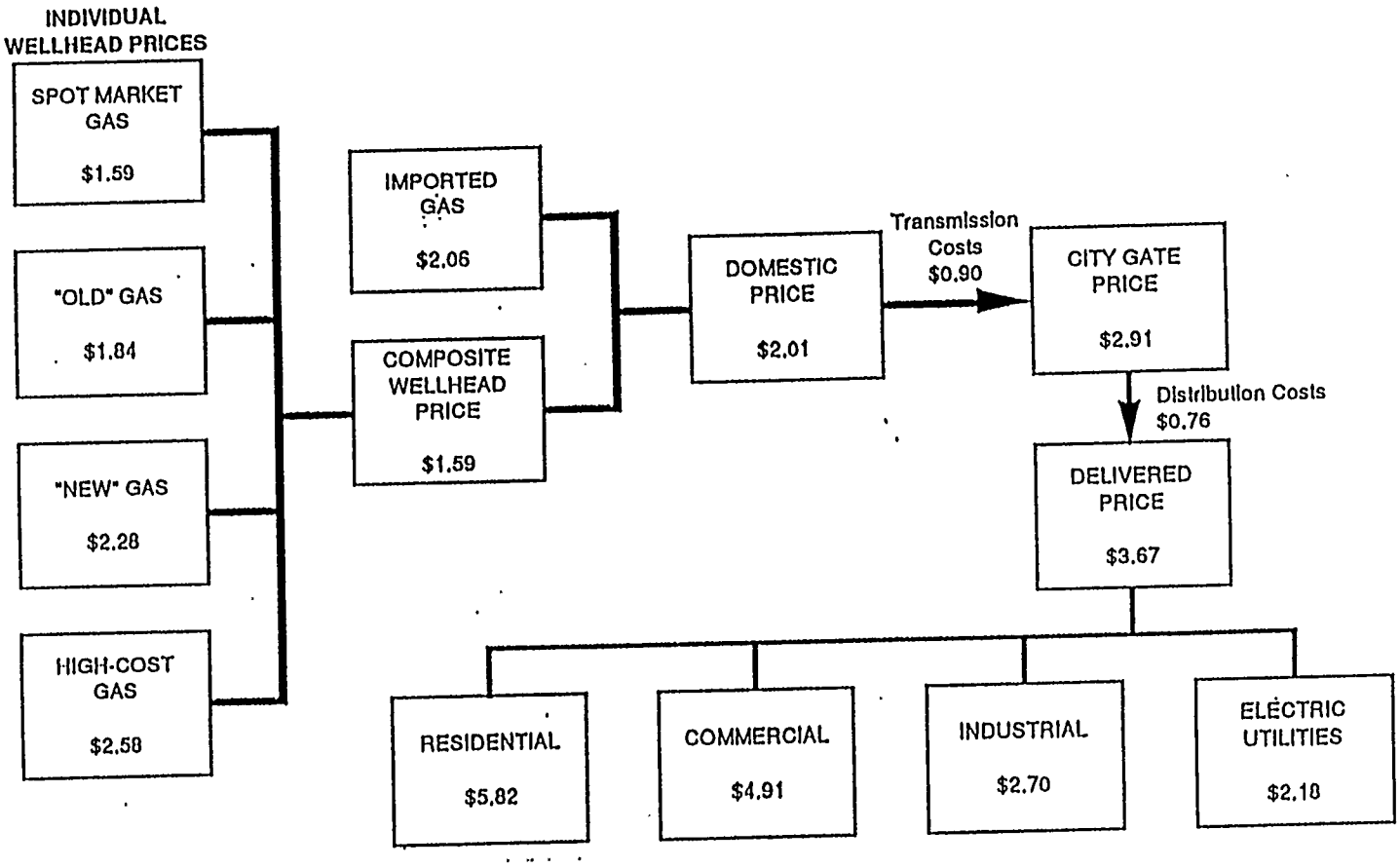

Source: Reference 43

1.4 Amenable U.S. Market

The information in Tables 7-2 and 7-3 was used to estimate the amenable U.S. market segments for the CO_2 ATM. Unassociated production was ~15 trillion ft^3, while the total active reserves are estimated at 144 trillion ft^3. The estimate for the discovered/non-producing low quality resource is comparable to that of the reserves for active wells and the undiscovered/undeveloped resource is estimated to be >4 times that of the current reserves. The portions of low quality gas, as seen, are substantially higher for the latter categories of the resources.

Of the segments identified in the report, two segments are amenable for CO_2 removal technologies: high CO_2 only (>2%), and high CO_2 and high H_2S (>4 ppm). Based on this assumption, the total amenable production and reserve segments (1988) are estimated to be about 2.2 trillion CFY and 24 trillion CF, or 15% and 17% of the total production rate and reserve, respectively. Assuming the ATM technology will capture 5-10% of the amenable production rates, or 0.8-1.7% of the total U.S. production, the market size projected for ATM is 400-800 million CFD/YR. To reiterate, the amenable segment in the discovered/non-producing low quality resource is comparable to the active reserve and the undiscovered/undeveloped resource is about 6 times that of the active reserve.

1.5 ATM Product Differentiation and Technology Benefits

The acid gas removal market is highly competitive as shown by the number of major vendors listed in Table 7-5. As shown in Table 7-6, the most commonly used technologies are absorption systems based on chemical or physical solvents. Major characteristics of amine versus general membrane technologies are compared in Table 7-7. Diethanolamine (DEA) and methyl diethanolamine (MDEA) systems have captured greater than 50% of the AGR market. An increase in market share for membranes and adsorption technologies is forecast if expected improvements to current generation products are realized. Indeed, this is projected to be the fastest growing market segment.

Table 7-5
Acid Gas Removal Market Players

Vendor	Technology Type*	Process Name
Shell	AC, AP	Sulfinol, -M, etc.
	AC	ADIP
Union Carbide	AC	AmineGuard
	AC	HS
	AC	Benfield
	AC	PSA
Dow	AC	GasSpec, ST-1, FT-1
Exxon	AC	Flexsorb -SE, PE, HP, PS
BASF	AC	MDEA
	AC	TEA
	AC	Alkazid
	AC	Sepasolv
Lurgi	AP	Rectisol
	AP	Amisol
Parsons	AP	Purisol
Koch	CR	Ryan-Holmes
Permea	M	Prism
Grace Membrane Systems	M	Grace Membranes
Separex	M	Separex
Delta Engineering	M	DELSEP
Peabody Holmes	DC	Stretford
ARI-Technolgies	DC	LO-CAT

* A=Absorption; C=chemical solvent; P=physical solvent; CR=cryogenic; M=membrane
PSA=pressure swing adsorption; DC=direct conversion

Table 7-6

Acid Gas Removal - Dominant Technologies, U.S. 1984-1995

Technology	Current Market Share	Projected Market Share
DEA (diethanolamine)	29	43
MEA (monoethanolamine)	25	2
Sulfinol (Mixed Solvents)	9	9
DEGA (diethyleneglycolamine)	6	2
Potassium Carbonate	4	0
MDEA (methyl diethanolamine)	4	19
Selexol (glycol derivatives)	2	5
Membranes	<1	3
Ryan-Holmes (cryogenic)	<1	2
Other	20	15
TOTAL	100%	100%

* all existing units
** new units only
from "North American Gas Treating Market Study", Purvin and Gertz, Inc., for Air Products and Chemicals, Inc., May 1984.

Table 7-7
Technology Comparison of Amine and Membrane Technologies

	Amine Technology	Membrane Technology
Pros:	long-term proven technology	active since early 1980s
	know-how in engineering contractors	easier field operation
	H_2S/CO_2 handling*	enhanced flexibility in meeting gas production criteria (flow rate)
	good economy of scale	attractive characteristics for off-shore markets (weight, size, no chemicals, modular design, etc.)
	low hydrocarbon losses*	short start-up time
Cons:	liquid processing/inventory maintenance	limited operating temperatures
		tolerance to trace contaminants (performance & life)
	waste disposal	
	energy consumption increases as CO_2 in feed increases	

* These benefits will diminish in the event of a commercialized ATM technology.

There is some disagreement in the literature concerning the exact fit of membrane technology to this market, however, it is generally held that even currently available membrane systems are preferred over amine systems for production capacity of less than ≈20-30 MMSCFD.[45] In fact, Grace Membrane Systems claims to be competitive up to 60 MMSCFD.[46] It is also generally true that membrane technology is favored as the CO_2 concentration of the gas increases. As shown in Table 7-6, the market share currently held by membrane technology is <1%; but increasing. Membrane technology is becoming more attractive at remote wells, off-shore platforms, etc. Furthermore, the new U.S. energy initiative emphasizing natural gas will encourage future production of discovered but non-producing subquality wells and undeveloped resources.

Key suppliers of polymeric membranes are Grace, Hoechst Celanese (Separex), and Dow Cynara. Dow has been active in EOR application and markets an "own-and-operate" concept. Their overall activities in this application are[47] outlined below.

GRACE:
- o spiral-wound technology originally developed by Bend Research
- o active since 1984
- o large research efforts in CO_2 membranes
- o mainly sale-of equipment
- o ~100 small plants
- o unattended at well head & remote areas
- o <1,500 psia

HOECHST CELANESE/SEPAREX:
- o spiral-wound technology
- o active since early 1980s
- o ~20 plants, generally <3.5 mmscfd
- o <1,400 psia

[45] .K. Changela et. al., "Technical Evaluation of Hybrid Membrane/DEA Modeling", Topical Report, GRI (1990).
[46] R.E. Babcock et. al., "Natural Gas Cleanup: A Comparsion of Membrane and Amine Treatment Processes", presented at the AIChE Spring National Mtg., March 1988.
[47] Torleiv et. al., "CO_2/HC Membrane Separation: A Mature Technology", presented at the AIChE Spring National Meeting, March 1992.

CYNARA/DOW:

- o hollow fiber technology
- o mainly own-and-operate concept
- o primary focus in EOR ($C0_2$ flooding)
- o SACROC operation (80 mmscfd) start-up in 1983, 240 membrane elements
- o a few other small plants

Based on our analyses to date, we believe that a successful ATM technology will be significantly differentiated from current membrane technology and will lead to a number of technology benefits:

DIFFERENTIATION:

- o High selectivity with a CO_2 permeance at least comparable to conventional CO_2 membranes
- o Light gas (CH_4, etc.) recovery at high pressure
- o Outstanding performance characteristics in the low partial pressure region

TECHNOLOGY BENEFITS:

- o Higher product recovery
- o Lower energy consumption
- o Simpler process (number of stages) and less equipment
- o Greater market penetration

2.0 CO_2- Selective ATM: Other Opportunities

In addition to the natural gas application, several large volume markets with good growth opportunities have been identified for ATM materials that will selectively permeate CO_2 from synthesis gas or process gas streams in chemical manufacturing plants. Because the applications and treating specifications vary, we have quantified the size of the amenable market by estimating the gas handling volumes.

As discussed above, roughly, 5100 MMSCFD of natural gas is treated for CO_2 removal in the US. This represents about 10% of current US production. Another 3500 MMSCFD of natural gas is treated for CO_2 and H_2S impurities. This portion of the amenable market

requires AT materials that can withstand some exposure to H_2S. This area is an ongoing part of our Active Transport materials development program.

Chemical manufacturing operations treat large volumes of gas to remove CO_2. They include SYNGAS treating for H_2 and ammonia production; ethylene manufacturing , and selective oxidation processes for ethylene oxide, vinyl acetate monomer, and other chemicals. Since the 1950's, the chemical industry has used selective oxidation routes for key commodity chemicals. Some oxidation processes have evolved from using air to using pure oxygen (> 95% O_2). The oxygen based processes generally remove CO_2 from gases that are recycled to the main reactor. This trend is continuing as evidenced by incorporation of such technology into new processes being developed for maleic anhydride and acrylonitrile. In general, the chemical manufacturing plants require very selective CO_2 removal because they cannot afford to lose high valve feedstocks or products to the permeate.

2.1 Synthesis Gas Treating

Our last interim report provided some background on the use of ATM's for removing CO_2 from synthesis gas in ammonia and hydrogen manufacturing plants. We presented process schemes using hybrid CO_2 removal systems - ATM and MEA combinations for ammonia manufacturing, and ATM-PSA combinations for hydrogen manufacturing.

Ammonia Plants

For ammonia plants, the acid gas treating is for CO_2 removal only. If H_2S is present in the natural gas feed to the plant, it is usually removed by adsorption ahead of the natural gas reformer. The synthesis gas feed to the acid gas removal step contains from 16-19 mole per cent CO_2. It is processed to less than 0.05 mol % CO_2. The tight CO_2 product spec would normally rule out a stand-alone membrane system. The total synthesis gas volumes treated for ammonia manufacturing in the US and the world are 7500 and 30,000 MMSCFD, respectively[29]. The US volume assumes 100% capacity utilization. The world volume assumes 75% capacity utilization.

As discussed earlier,[29] growth in the US ammonia market will occur mainly through retrofits rather than new construction. We concluded from discussion with ammonia producers that the industry is not likely to replace sunk AGR capital with other technologies. In specific

plants, ATMs used ahead of an existing AGR system might be considered for retrofits in connection with capacity increases. At the same time, new inhibitors and additives are being introduced that allow higher MEA concentration solutions be used. This reduces the required solvent recirculation rates (allowing some room for debottlenecking) and the steam needed for solvent regeneration.

Hydrogen Manufacturing

Synthesis gas treating for hydrogen manufacture requires the removal of several impurities - N_2, CO, CO_2, and H_2O. Roughly 3400 MMSCFD of synthesis gas needs to be treated for hydrogen plants serving refineries and chemical plants in the US. (This figure excludes ammonia, methanol, and acetic acid manufacturing.)

The hybrid ATM-MEA combination, discussed above for ammonia plants, can also be used for older hydrogen or carbon monoxide plants using MEA for CO_2 removal. Newer hydrogen plants have adopted PSA technology for synthesis gas purification. The advantages of PSA are 1) the H_2 product is retained at high pressure; 2) the PSA can remove all impurities in one step. (Older methods required MEA (for CO_2 removal), a drier, and then a cold box for high purity H_2 or CO plants; or a MEA -methanator combination for lower purity hydrogen used in refineries and ammonia plants.)

Air Products is the world's largest producer of merchant hydrogen (more than 25 plants) and produces over 400 MMSCFD of hydrogen. We reviewed ATM integration schemes with PSA or MEA systems for CO_2 removal with our HYCO (hydrogen-carbon monoxide) plant process engineering group. If ATMs were commercially available, they could have limited use for older plants using MEA. Some benefits may be derived from ATM-PSA combinations in new plants. At first pass, the HYCO designers estimate there will not be a downsizing significant of the PSA. PSA size is set more by the N_2 and CO removal requirements, rather than CO_2, however, this application is still under review. A perceived drawback to the ATM system is the potential return to multiple process steps for hydrogen clean-up.

2.2 Chemicals Manufacturing by Selective Oxidation Processes

In addition to synthesis gas treating, CO_2 removal is used in chemicals manufacturing for selective oxidation processes. These include ethylene oxide, vinyl acetate monomer, vinyl chloride monomer, and new routes being developed for acrylonitrile and maleic anhydride.

Most of the oxidation processes requiring CO_2 removal use pure O_2 instead of air. They recycle a large volume of gas around a reactor loop to help with reactor temperature control and to avoid flammable conditions since oxygen is being reacted with a hydrocarbon feed. CO_2 is produced in the reactor through nonselective, by-product reactions and must be removed from the recycle gas, usually to optimize catalyst performance. Grouped together, the gases treated for CO_2 removal in the selective oxidation plants represent a large market, comparable to the natural gas treated for CO_2 removal in the US.

Generally, these processes require very selective removal of CO_2 to avoid costly losses of chemical feedstock, e.g., ethylene. The standard technology for the industry is the Benfield process because of its high selectivity and its ability to process gas streams that contain oxygen. Most amine based absorption systems and physical solvents can not be used. Polymer membranes have not been used to remove CO_2 in any of these applications because of their poor selectivity, but they have been used in some plants for purge gas treating.

We met with Scientific Design, a leading licensor for ethylene oxide technology. They expressed interest in an all membrane process to replace the Benfield process in their ethylene oxide plants (Figure 7-4). They stressed high selectivity would be required. Table 7-8 lists typical stream compositions for a CO_2 removal unit in an ethylene oxide plant. The flows are for a 300 MM pound per year plant. Complete CO_2 removal is not required (treated gas CO_2 specification is $\approx$1 mol%). Also, the recycle gas does not need to be dehydrated, as in natural gas treating. On first pass the ethylene oxide process conditions are well suited for an ATM. In addition, because it is an attended plant, humidity control schemes, if required, would be more readily accepted.

3.0 Ammonia-Selective ATM Materials

Marketing activities for ammonia applications were completed in 1992. The details are documented in the latest interim report, "Development of Active Transport Membrane Devices - Interim Report" (issued January 1993). The highlights are presented here.

Table 7-8

Ethylene Oxide Plant - CO2 Removal Service

Component	MWT	Feed to CO2 Removal.		Treated Gas
		mol %		mol %
Ethylene	28	20.50		20.89
Oxygen	32	3.54		3.60
Carbon Dioxide	**44**	**3.94**	(a)	**0.78**
Argon	39.95	9.72		9.91
Methane	16	59.95		61.34
Ethane	30	2.10		2.14
Ethylene Oxide	44	20 - 100 ppm	(b)	20 - 100 ppm
Acetalhyde	44	0.00		0.00
Formaldehyde	30	0.00		0.00
Water	18	0.27		1.34
Ethylene Dichloride	99	2- 3 ppm	(b)	2- 3 ppm
Potassium Carbonate	138	0.00		0.00
TOTAL		100.00		100.00
GAS TREATED, MMSCFD		**140**	(c)	

Notes:

a) Calculated from SRI report. SRI confirms range is from 4 to 7 mole% CO2.
b) Provided by Scientific Design.
c) Gas treated for a 300 MM lb/yr EO Plant (136.1 M MTPA)

Rule of thumb : Gas treated (expressed in MM SCFD) equals about half of EO plant nameplate capacity expressed in MM lb/yr, or equal to nameplate capacity, expressed in M MTPA.

Figure 7-3
Generic Ethylene Oxide Process

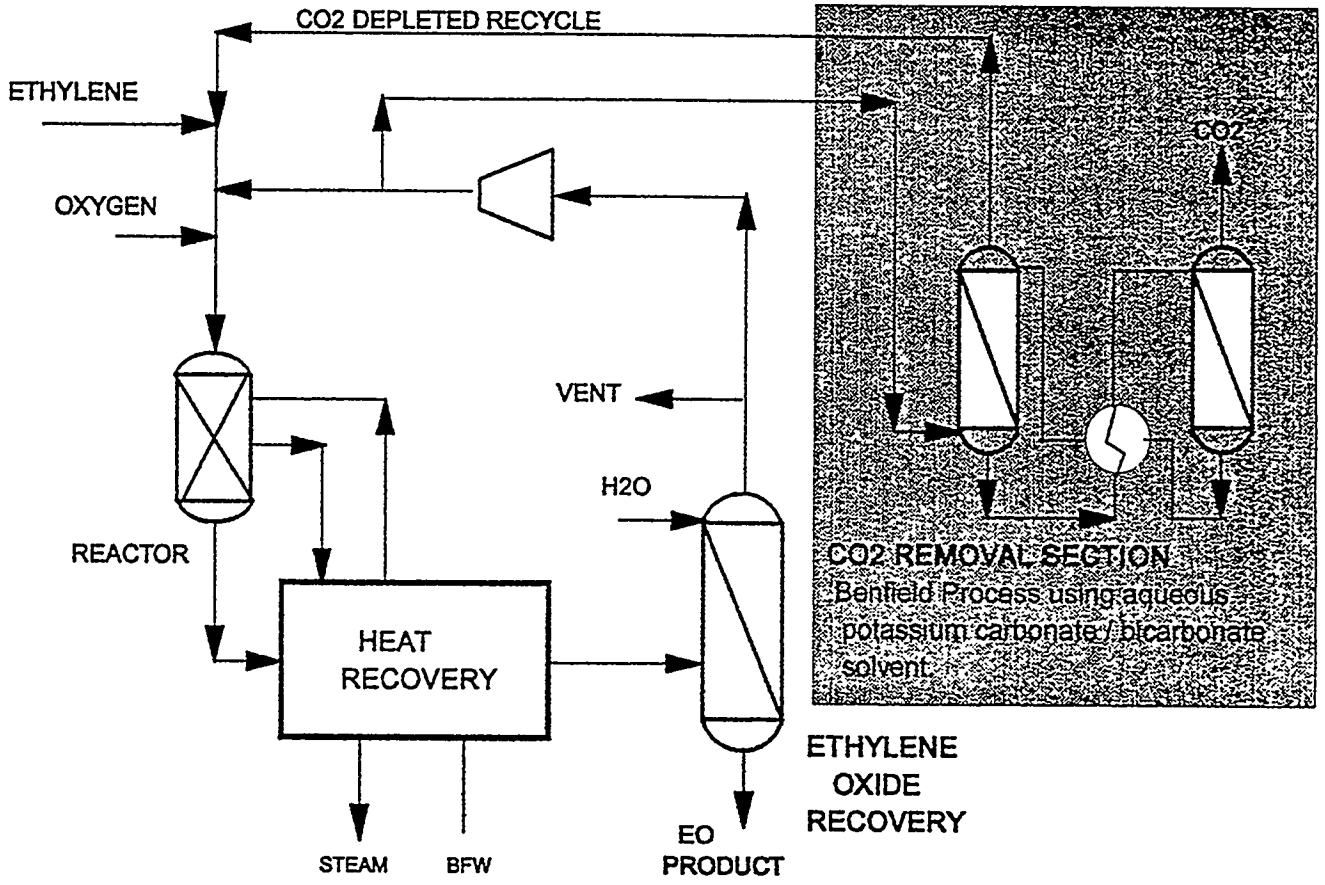

3.1 Technology Status

Air Products researchers fabricated and tested multi-layer composite membranes for NH_3 removal from mixtures of NH_3, H_2 and N_2. These materials exhibited high NH_3 permeance and selectivity over N_2 and H_2. The membranes were stable at pressures up to 1000 psi. The permselectivity at these pressures, while less than at low pressure, was acceptable. Process simulations were completed for several membrane applications in an ammonia synthesis plant. (This analysis assumed that commercial modules could achieve the high permselectivity of laboratory membranes and that concentration polarization effects were not dominant.) The results were encouraging and showed

- Ammonia selective ATMs could be used to increase product recovery and debottleneck existing plant capacity by 25% without major revamps to the refrigeration system.

- For new plants, ammonia selective ATMs could be used with much smaller refrigeration equipment and yield substantial capital and operating savings.

- Ammonia selective ATMs could be used to recover NH_3 product from an existing plant purge gas by sweeping with a low pressure slipstream of syngas. This would compete with water wash systems used in today's operations.

3.2 Marketing

Macro world market conditions were assessed and discussions were held with four major ammonia producers (The producers we contacted account for almost 36% of US production). The findings are summarized below.

World Market Conditions

The world ammonia industry is undergoing a period of restructuring that began in the early 1980's. The industry is recovering from a period of stagnant growth, overcapacity, and relocation of major production facilities to less developed regions with low natural gas feedstock costs. The interim report referenced earlier presents details for ammonia production and consumption by geographic area. The data

includes 1990 actuals and projections for 1995. New plant capacity is anticipated for less developed regions - SW Asia, Africa, South America, and the Middle East.

US Industry

Between 1980 and 1990, US ammonia consumption remained essentially flat, between 14,000 and 15,000 Metric Tons per year. Imports grew 52% and domestic production fell 13%. 34 plants were shutdown. Retrofits for better efficiency and some debottlenecking capacity projects are the only on-going activities. No new capacity is forecast for 1995. Imports are forecast to increase.

3.3 Contacts with Ammonia Producers

Air Products reviewed the potential membrane applications for ammonia manufacturing with four US producers. Most of the producers also manufacture urea; and they discussed membrane uses for both chemical processes.

We presented two process schemes using ATMs for ammonia recovery from the converter effluent gas. One used ATMs to recover bulk NH_3. (This would displace existing equipment.) The second scheme used ATMs before or after the deep level refrigeration stage (last stage) to get higher product recovery. This process would reduce the ammonia content of the gas recycled to the ammonia converter section, and increase conversion per pass.

The producers put a low priority on the bulk removal scheme; however, they thought the second scheme would be useful for their debottlenecking and efficiency improvement programs if we could attain the membrane performance assumed for the process simulation work.

Ammonia recovery from the plant purge gas was also considered. Most existing plants use membranes for H_2 recovery and a water wash operation for ammonia. Producers were interested in an all membrane purge gas treating system. However, it is unlikely that producers would replace existing water wash units with ATM's because operating savings may not be large enough to justify replacement of existing capital.

3.4 Competition

There are no competing membrane technologies for NH_3 removal from N_2 or H_2 containing gases. ATM's would however need to out perform conventional ammonia separation technologies including refrigeration and water wash systems. New catalysts for NH_3 converters that enhance conversion per pass would also compete with the debottlenecking process schemes developed.

4.0 Conclusions

Phase 1 commercial development activities have focused on identifying and evaluating potential ATM applications, understanding market needs and forces, and in setting performance criteria for new gas separation technologies based on active transport membranes.

- Several large volume markets with good growth have identified for AT materials that selectively remove CO_2 from natural gas or process gases in chemical manufacturing plants.

- CO_2 removal from natural gas has been selected as the first target application. Between 15 and 20% of US production and proven gas reserves require treatment to reduce the concentration of CO_2 or CO_2 and H_2S to pipeline specifications. U.S. production is growing at ≈4% per year and capacity utilization rates are high; forecasted growth will require construction of new plants. An H_2S tolerant membrane will be required to capture portions of the market.

- CO_2 removal from natural gas is a highly competitive market. Membrane technology is gaining acceptance, and is now competing with solvent based absorption technologies in small capacity installations. AT materials will need to outperform existing membranes.

- CO_2 removal from process gases in chemical plants represents a potential market as large as natural gas treating (on a volume of gas treating basis). Specific applications include synthesis gas treating for ammonia, hydrogen, and carbon monoxide manufacturing, and CO_2 removal from process gases in chemical plants using oxygen based selective oxidation technologies (e.g. ethylene oxide).

- CO_2 removal services in selective oxidation plants represent an attractive potential market for CO_2 AT materials. Treated gas volumes and projected growth are good, and the service requires very selective CO_2 removal. The competition is limited down to Benfield systems, since the processed gases contained oxygen. On first pass, these applications appear well suited for AT membranes. The treated gas can contain water and some residual CO_2. The operations are attended, so humidity control systems, if required for AT membranes, would be more readily accepted.

- Ammonia manufacturing offers limited market opportunities for new ammonia selective AT materials (especially in the U.S.). Membrane performance targets were established.

We have assigned a low priority to the ammonia selective AT materials, and stopped R&D efforts in order to pursue better opportunities for CO_2 selective membranes in natural gas applications.

VIII. Technology Development Status and Overall Recommendations

ATM developmental efforts have thus far focused on identifying ATM and substrate materials, spinning support fiber, and fabricating and evaluating thin film composite hollow fiber lab modules for the natural gas application. Other work focused on developing a computer model of the permeation mechanism in ATMs.

A number of ATM materials have been identified as candidates for the CO_2 separating layer. These materials are based on polyelectrolytes and have been tested in flatsheet or hollow fiber forms. In general, they exhibited a high selectivity (>>100) but a relatively low permeance rate (<30 X 10^{-6} scc/cm^2•sec•cm-Hg). EXTM6-4 is the leading candidate ATM material. The CO_2 flux of planar EXTM6-4 composite membranes meets the preliminary flux target. Since the economics (and competitiveness) of the ATM system in large natural gas applications are determined mainly by membrane investment (area / permeance), it would be highly desirable to maximize the CO_2 flux.

In addition to the attractiveness of obtaining an optimized permeance, it is also highly desirable to minimize the impact of H_2O vapor on polyelectrolyte ATMs. If the permeance rate of H_2O is very high, the H_2O level in the latter half of the ATM module may become very low and consequently the ATM performance and stability may become issues.

The best support material is PAI, which shows a high tolerance to hydrocarbon solvents and is processable into a microporous hollow fiber substrate. However, the ultimate compatibility and coatability of this support material to the ATM remain to be determined.

Future efforts in ATM should address following development issues:

- Maximizing the CO_2 permeance
- Maintaining high $\alpha(CO_2/CH_4)$, $\alpha(H_2S/CO_2)$ and $\alpha(CO_2/H_2)$ over the range of process conditions
- Establishing the relationship of CO_2 permeance and selectivity to ATM thickness

- Verifying reproducibility and reversibility of the CO_2 permeance versus CO_2 partial pressure and relative humidity

- Further investigate the effect of temperature on performance

- Measuring the H_2O permeance and assessing the impact of feed H_2O level on ATM performance

- Assess the impact of sulfur impurities on process economics and seek material modifications if required

- Extending lifetime and stability studies to real process streams

As these issues are addressed, two key objectives must be accomplished:

1) Achieve the flatsheet EXTM6-4 permeation characteristics (selectivity and intrinsic CO_2 permeability) in a thin hollow fiber membrane form using a substrate material that meets our selection criteria (hydrocarbon tolerance, etc.) such as PAI.

2) Develop a ATM-based thin film composite membrane and its continuous fabrication technologies that require minimal modifications to Air Products' commercial fabrication facilities.

Finally, in addition to developing the ATM technology, one should continue to monitor and assess new conventional polymeric membranes being developed and determine if any of these new polymeric membranes may offer an attractive interim product or overall superior system.

Appendix A - Derivation of ATM Computer Model

A semi-empirical model is proposed for estimating the acid gas flux through active-transport membranes. The flux equation is similar to standard facilitated transport expressions with the exception that the effective permeance is corrected for relative humidity and, if applicable, for carrier facilitation:

$$N_i = P/\ell_i \bullet (p_{if} - p_{iL}) \bullet R_i \bullet F_i \qquad (1)$$

where, N_i = flux of component **i**

p_{if} = partial pressure of component **i** on feed side

p_{iL} = partial pressure of component **i** on permeate side

P/ℓ_i = permeance of component **i** as dissolved free gas at reference humidity $\Re^*$

R_i = relative humidity correction factor for permeance of component **i**:

$$R_i = 1 + \frac{\delta_i (\Re_f - \Re^*)}{\Pi_{i^*}} \qquad (2)$$

δ_i = change in permeance of component **i** per unit change in humidity

$\Re_f$ = relative humidity of vapor on feed side

$\Re^*$ = reference relative humidity

F_i = facilitation factor, which is unity for non-reactive components

For an acid gas, the facilitation factor is given by the following expression, which is based on the assumption of reaction equilibrium throughout the membrane.

$$F_i = 1 + \frac{\alpha_i \beta_i}{\Pi_i^*} \left\{ \frac{\frac{p_{if}}{(p_{if} - p_{iL})}}{1 + \beta_i p_{if} + \beta_j p_{jf}} - \frac{\frac{p_{iL}}{(p_{if} - p_{iL})}}{1 + \beta_i p_{iL} + \beta_j p_{jL}} \right\} \quad (3)$$

where, α_i = product of diffusivity of carrier-solute complex and total carrier concentration divided by the effective thickness of the membrane. This parameter is factor a_4 if the solute is CO_2 or factor a_6 if the solute is H_2S. They are determined by curve-fitting performance data as discussed below.

β_i = product of equilibrium constant of carrier-solute reaction and Henry's Law solubility constant for the solute; factor a_1 or a_2. These parameters are also based on curve-fitting performance data.

The subscript 'j' refers to the second acid gas if present.

The following reactions are assumed to occur within the polyelectrolyte membrane:

$$H_2O + 2F^- \leftrightarrow HF_2^- + OH^- \quad (R1)$$

$$CO_2 + OH^- \leftrightarrow HCO_3^- \quad (R2)$$

$$H_2S + OH^- \leftrightarrow HS^- + H_2O\uparrow \quad (R3)$$

For simplicity, we will use the following symbols to denote the various species:

$A = CO_2$	$E = H_2S$	$F = F^-$
$B = OH^-$	$S = HS^-$	$G = HF_2^-$
$AB = HCO_3^-$	$W = H_2O$	

At equilibrium, the flux of any volatile component through the membrane is simply[#] :

$$N_j = \frac{1}{L} \sum_{i=1}^{M} v_{ij} D_i (C_{io} - C_{iL}) \quad (4)$$

[#] J.S. Schultz et.al.,"Facilitated Transport via Carrier Mediated Diffusion in Membranes," ***AIChE Journal*** **20** (1974).

where, N_j = flux of volatile species **j** through membrane of thickness **L**

D_i = diffusion coefficient of species **i**

v_{ij} = number of molecules of species **j** contained in species **i**

C_{io} = concentration of species **i** in membrane at feed interface

C_{iL} = concentration of species **i** in membrane at permeate interface

M = total number of species

We are assuming that mass transfer resistance between the bulk gas and the membrane interface is negligible and the PDMS coating and microporous support contribute no mass transfer resistance.

Thus for carbon dioxide,

$$N_A = \frac{D_A(C_{Ao} - C_{AL})}{L} + \frac{D_{AB}(C_{ABo} - C_{ABL})}{L} \tag{5}$$

Likewise for hydrogen sulfide,

$$N_E = \frac{D_E(C_{Eo} - C_{EL})}{L} + \frac{D_S(C_{So} - C_{SL})}{L} \tag{6}$$

Assuming that the solubility of the dissolved acid gases can be described adequately by Henry's Law, we have

$$C_A = H_{AP}A \tag{8}$$

$$C_E = H_{EP}E \tag{9}$$

where, p_i = partial pressure of species **i**

H_i = Henry constant for species **i**, assumed to be a function of temperature only

The concentrations of the non-volatile species are derived from the reaction equilibrium relationships:

$$K_1 = \frac{C_B C_G}{C_W C_F^2} \tag{10}$$

$$K_2 = \frac{C_{AB}}{C_A C_B} \tag{11}$$

and $$K_3 = \frac{C_S}{C_E C_B} \tag{12}$$

where, K_i = equilibrium constant for reaction **i**, which is assumed to be a function of temperature only.

For HCO_3^- we have,

$$C_{AB} = K_2 C_A C_B = \frac{K_2 C_A C_T}{1 + K_2 C_A + K_3 C_E} \tag{13}$$

where, C_T = total concentration of carrier, the hydroxyl ion, given by

$$C_T = C_B + C_{AB} + C_S = C_B (1 + K_2 C_A + K_3 C_E) \tag{14}$$

Since the fluoride loading is fixed, then C_T is fixed if the water loading is also fixed. Thus most experiments can be analyzed without the need to incorporate the total fluoride concentration, given by

$$C_{TF} = 2C_G + C_F$$

which is a true system invariant.

Likewise for HS^- we have

$$C_S = \frac{K_3 C_E C_T}{1 + K_2 C_A + K_3 C_E} \tag{15}$$

$$N_A = \frac{D_A H_A (p_{Ao} - p_{AL})}{L} +$$

$$\frac{D_{AB} C_T K_2 H_A}{L} \left\{ \frac{p_{Ao}}{1 + K_2 H_A p_{Ao} + K_3 H_E p_{Eo}} \right.$$

$$\left. - \frac{p_{AL}}{1 + K_2 H_A p_{AL} + K_3 H_E p_{EL}} \right\} \tag{16}$$

$$N_E = \frac{D_E H_E (p_{Eo} - p_{EL})}{L} +$$

$$\frac{D_S C_T K3 H_E}{L} \left\{ \frac{p_{Eo}}{1 + K_2 H_A p_{AL} + K_3 H_E p_{EL}} \right.$$

$$\left. - \frac{p_{EL}}{1 + K_2 H_A p_{AL} + K_3 H_E p_{EL}} \right\} \tag{17}$$

With a sweep stream, the permeate pressures become negligible,

$$N_A = \left\{ D_A + \frac{D_{AB} C_T K_2}{1 + K_2 H_A p_{Ao} + K_3 H_E p_{Eo}} \right\} \frac{H_A p_{Ao}}{L} \tag{18}$$

$$N_E = \left\{ D_E + \frac{D_S C_T K_3}{1 + K_2 H_A p_{Ao} + K_3 H_E p_{Eo}} \right\} \frac{H_E p_{Eo}}{L} \tag{20}$$

In terms of permeance

Table A-1

CO_2 Partial Press (cmHg)	CO_2 Permeance scc/(cm^2-s-cmHg)	H_2S Partial Press (cmHg)	H_2S Permeance scc/(cm^2-s-cmHg)
4.2	0.140	4.2	0.98
5.3	0.11	5.4	0.84
9.5	0.10	9.6	0.76
13.6	0.09	13.8	0.64
17.7	0.08	17.9	0.59
21.2	0.06	21.5	0.49
29.1	0.05	29.5	0.36
34.5	0.04	36.1	0.33
46.9	0.06	49.2	0.39
54.5	0.05	57.1	0.33
29.82	0.183		
48.74	0.155		
66.58	0.145		
99.05	0.12		
146.74	0.087		

Values obtained for the six parameters were:

Parameter index - i	Value of Parameter - a(i)
1	0.0166308
2	0.245230
3	0.0289735
4	13.6300
5	0.218506
6	6.80230

The sum-square relative error was 0.3334. The overall quality of the curve-fits is quite good as may be seen in Figures A-1 and A-2.

For this example, the selectivity of H_2S over CO_2 is shown in Figure A-3. The amount of scatter in the data is typical. In Figure A-4, the predicted facilitation factors are presented as functions of the feed partial pressures for an equimolar mixture of H_2S and CO_2. As expected, the best enhancement in mass transfer occurs at the lowest compositions.

The effect of relative humidity on the permeance of CO_2 for the same membrane was also investigated. In this series of tests, the objective was to measure the permeance of water so a dry sweep gas was used. Thus the CO_2 permeances are not directly comparable to those

above where the sweep gas was humidified. Nonetheless, the CO_2 permeance is a linear function of the relative humidity as shown in Figure A-5.

Data for a PDMS/PVBTAF membrane also indicated that the permeance of CO_2 is linearly dependent upon the relative humidity.

The data were fit to the following function:

Table A-2

CO_2 Partial Press (cmHg)	CO_2 Permeance scc/(cm^2-s-cmHg)	Relative Humidity
111.0	0.229	0.163
106.0	0.291	0.163
200.0	0.179	0.163
279.0	0.111	0.163
350.0	0.085	0.163
111.0	0.378	0.231
201.0	0.235	0.231
272.0	0.185	0.231
350.0	0.158	0.231
348.0	0.291	0.321
111.0	0.785	0.440
202.0	0.587	0.440
272.0	0.520	0.440
344.0	0.499	0.440

$$P/\ell_{CO_2} = [a_3 + a_4 (\Re_f - \Re^*)]\left\{1 + \frac{a_2}{a_3 PCO_2}\right\} \qquad (23)$$

Note that the term in brackets is the facilitation factor when the term $a_1 PCO_2 >> 1$, which is true in this case. In order to accurately determine a_1, data at lower partial pressures of CO_2 are required.

Using a reference humidity of 0.163, values obtained for the 3 parameters were:

$a_2 = 20.99$

$a_3 = 0.03838$

$a_4 = 0.4165$

and the sum-square relative error was 0.2053. As shown in Figure A-6, the data correlate fairly well, with the worst deviation between data and model occurring at the highest relative humidity tested.

Figure A-1

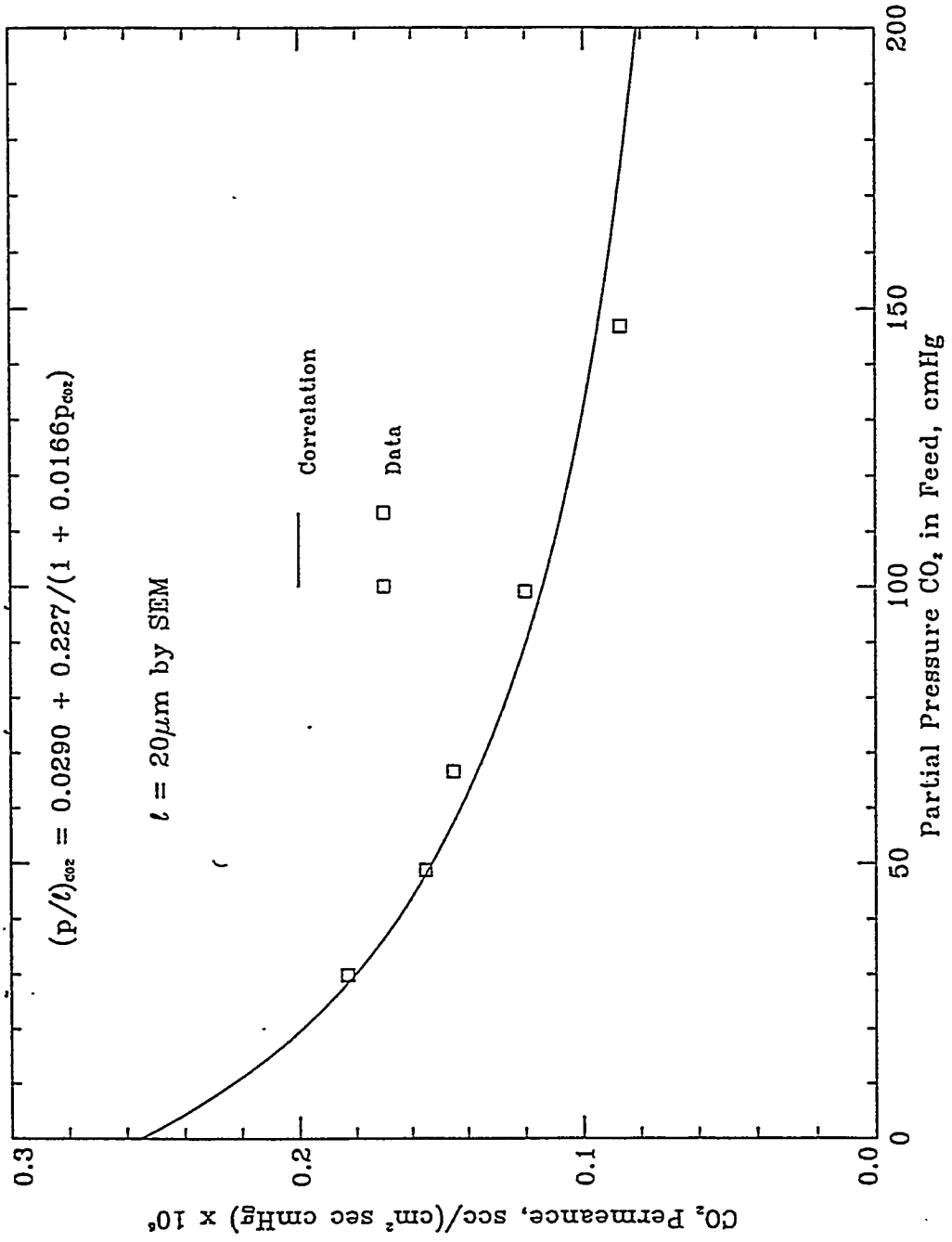
$(p/\ell)_{co_2} = 0.0290 + 0.227/(1 + 0.0166p_{co_2})$
$\ell = 20\mu m$ by SEM
Correlation
Data
CO_2 Permeance, scc/(cm² sec cmHg) x 10^6
Partial Pressure CO_2 in Feed, cmHg
0.0
0.1
0.2
0.3
0
50
100
150
200

Figure A-2

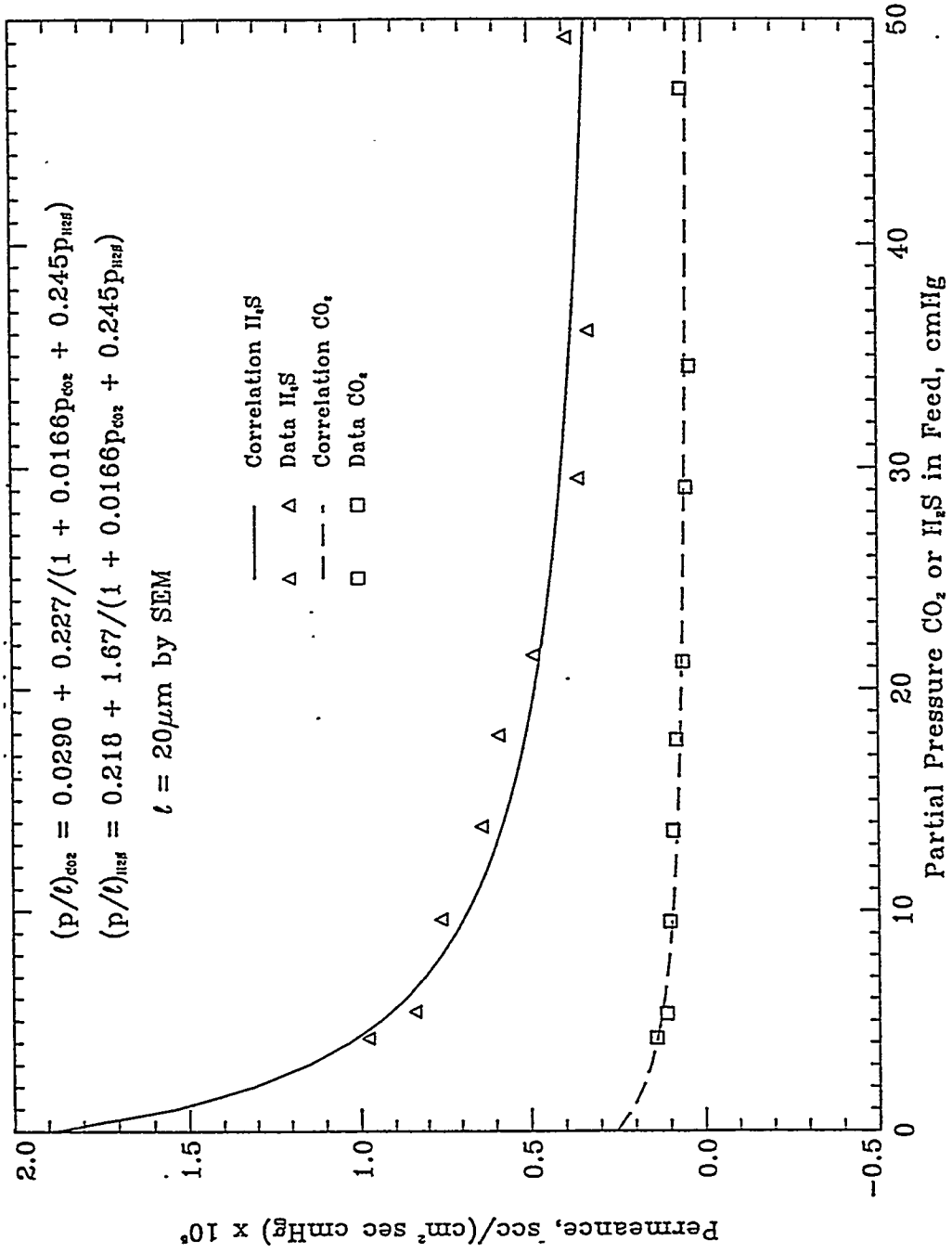
$(p/\ell)_{CO_2} = 0.0290 + 0.227/(1 + 0.0166p_{CO_2} + 0.245p_{H_2S})$
$(p/\ell)_{H_2S} = 0.218 + 1.67/(1 + 0.0166p_{CO_2} + 0.245p_{H_2S})$
$\ell = 20\mu m$ by SEM
Correlation H_2S
Data H_2S
Correlation CO_2
Data CO_2
Permeance, scc/(cm² sec cmHg) x 10^6
Partial Pressure CO_2 or H_2S in Feed, cmHg
2.0
1.5
1.0
0.5
0.0
-0.5
0
10
20
30
40
50

Figure A-3

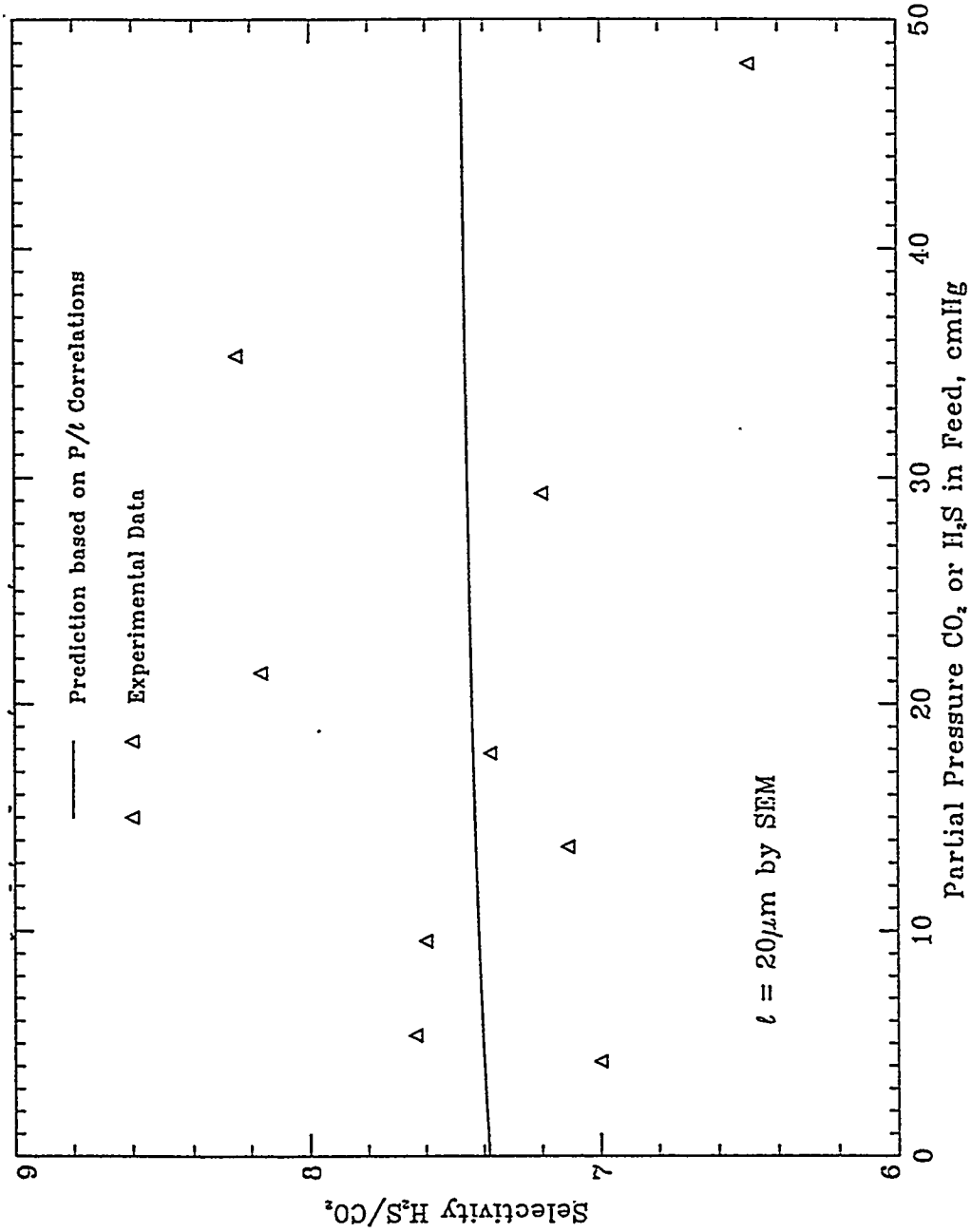
Prediction based on P/ℓ Correlations
Experimental Data
ℓ = 20μm by SEM
Selectivity H₂S/CO₂
Partial Pressure CO₂ or H₂S in Feed, cmHg
6
7
8
9
0
10
20
30
40
50

Figure A-4

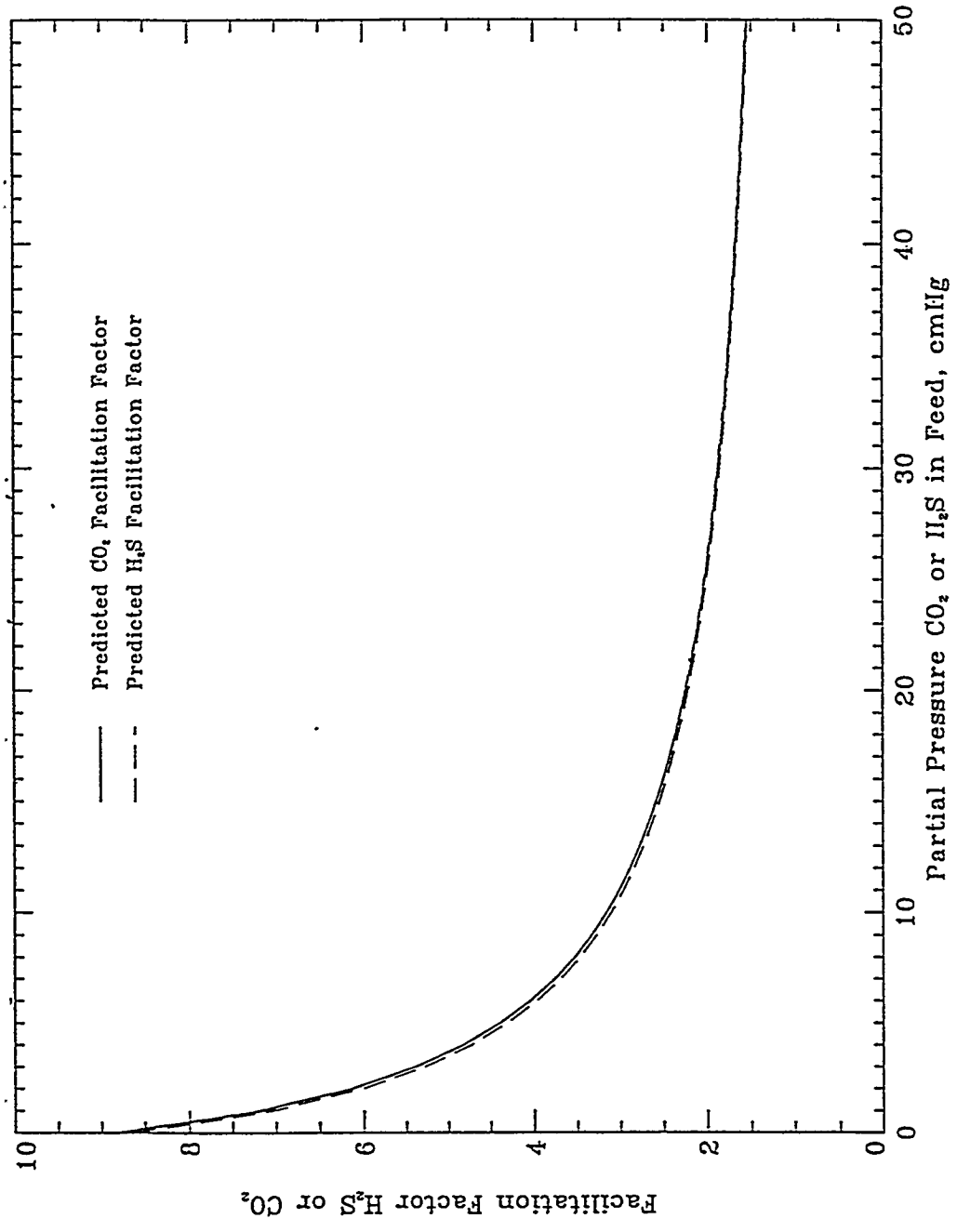
Predicted CO_2 Facilitation Factor
Predicted H_2S Facilitation Factor
Facilitation Factor H_2S or CO_2
Partial Pressure CO_2 or H_2S in Feed, cmHg
0
2
4
6
8
10
0
10
20
30
40
50

Figure A-5

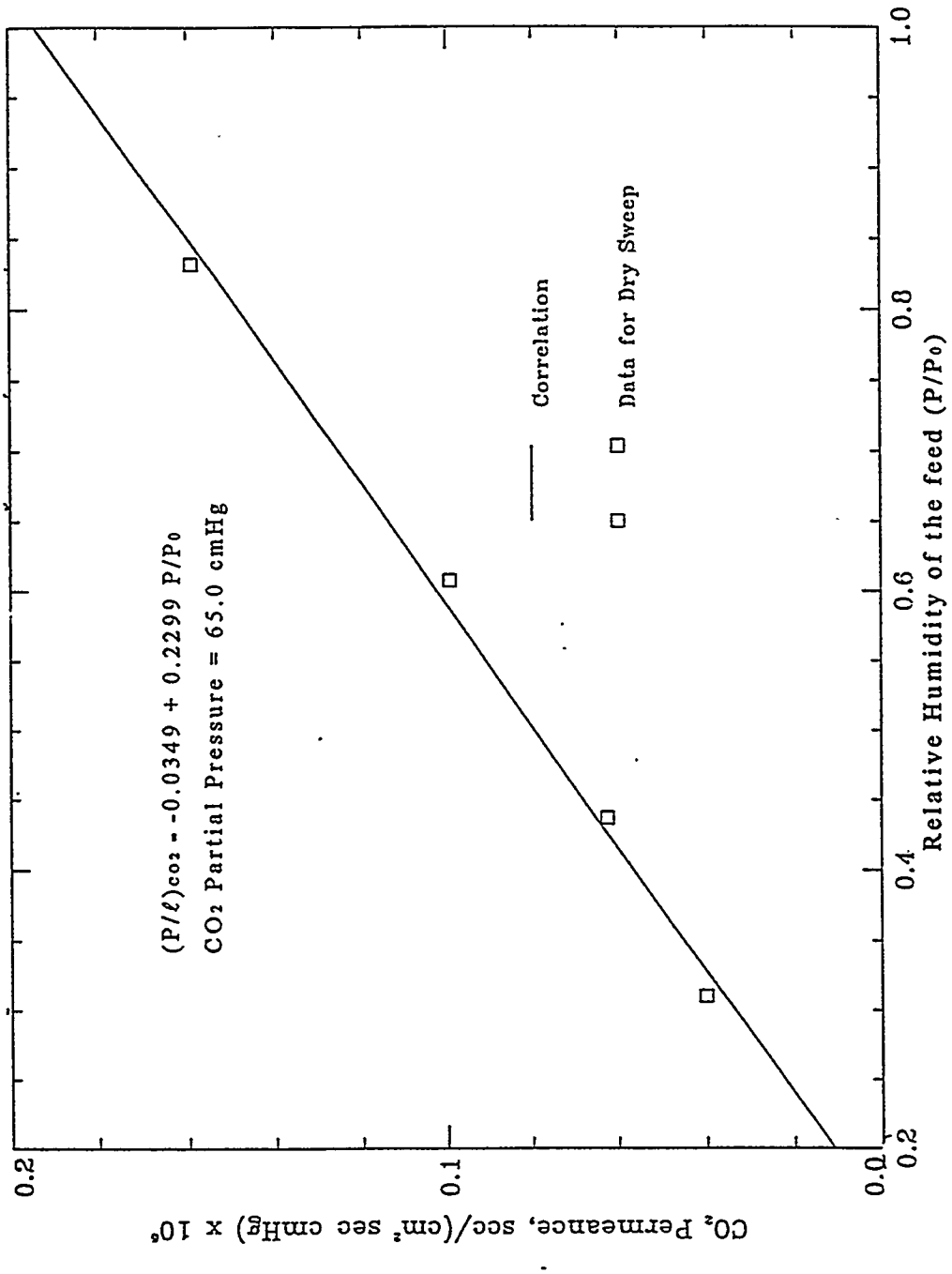
CO₂ Permeance, scc/(cm² sec cmHg) x 10⁶
0.0
0.1
0.2
0.2
0.4
0.6
0.8
1.0
Relative Humidity of the feed (P/P₀)
Correlation
Data for Dry Sweep
(P/ℓ)CO₂ = -0.0349 + 0.2299 P/P₀
CO₂ Partial Pressure = 65.0 cmHg

Figure A-6

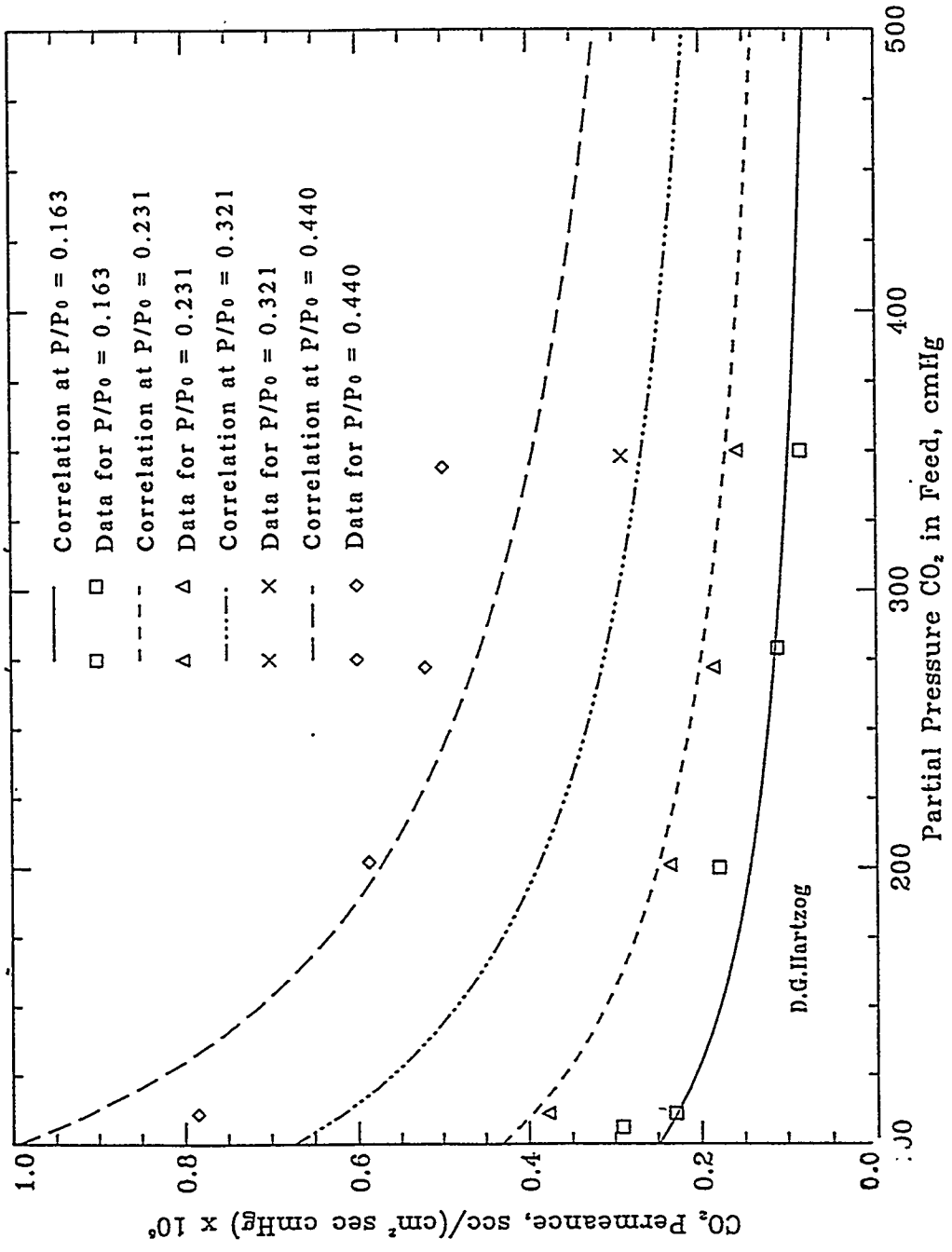
Correlation at P/Po = 0.163
Data for P/Po = 0.163
Correlation at P/Po = 0.231
Data for P/Po = 0.231
Correlation at P/Po = 0.321
Data for P/Po = 0.321
Correlation at P/Po = 0.440
Data for P/Po = 0.440
D.G.Hartzog
CO2 Permeance, scc/(cm² sec cmHg) x 10⁶
Partial Pressure CO2 in Feed, cmHg
0.0
0.2
0.4
0.6
0.8
1.0
100
200
300
400
500